



저작자표시-비영리-동일조건변경허락 2.0 대한민국

이용자는 아래의 조건을 따르는 경우에 한하여 자유롭게

- 이 저작물을 복제, 배포, 전송, 전시, 공연 및 방송할 수 있습니다.
- 이차적 저작물을 작성할 수 있습니다.

다음과 같은 조건을 따라야 합니다:



저작자표시. 귀하는 원저작자를 표시하여야 합니다.



비영리. 귀하는 이 저작물을 영리 목적으로 이용할 수 없습니다.



동일조건변경허락. 귀하가 이 저작물을 개작, 변형 또는 가공했을 경우에는, 이 저작물과 동일한 이용허락조건하에서만 배포할 수 있습니다.

- 귀하는, 이 저작물의 재이용이나 배포의 경우, 이 저작물에 적용된 이용허락조건을 명확하게 나타내어야 합니다.
- 저작권자로부터 별도의 허가를 받으면 이러한 조건들은 적용되지 않습니다.

저작권법에 따른 이용자의 권리는 위의 내용에 의하여 영향을 받지 않습니다.

이것은 [이용허락규약\(Legal Code\)](#)을 이해하기 쉽게 요약한 것입니다.

[Disclaimer](#) 

공학박사학위논문

THEORETICAL ANALYSIS OF  
DISTURBANCE OBSERVER:  
STABILITY AND PERFORMANCE  
외란 관측기의 이론적 해석 : 안정성 및 성능

2014 년 8 월

서울대학교 대학원

전기컴퓨터공학부

주 영 준



THEORETICAL ANALYSIS OF  
DISTURBANCE OBSERVER:  
STABILITY AND PERFORMANCE

외란 관측기의 이론적 해석 : 안정성 및 성능

지도교수 심 형 보

이 논문을 공학박사 학위논문으로 제출함.

2014년 05월





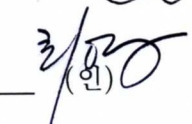
서울대학교 대학원

전기컴퓨터공학부

주 영 준

주 영 준의 공학박사 학위논문을 인준함.

2014년 06월

위원장	하인경	
부위원장	심형보	
위원	서권환	
위원	김경수	
위원	최영진	

# ABSTRACT

## THEORETICAL ANALYSIS OF DISTURBANCE OBSERVER: STABILITY AND PERFORMANCE

BY  
YOUNGJUN JOO

SCHOOL OF ELECTRICAL ENGINEERING  
AND COMPUTER SCIENCE  
COLLEGE OF ENGINEERING  
SEOUL NATIONAL UNIVERSITY

AUGUST 2014

This dissertation provides the stability and performance analysis of the disturbance observer and proposes several design methods for guaranteeing the robust stability and for enhancing the disturbance rejection performance. Compared to many success stories in industry, theoretic analysis on the disturbance observer itself has attracted relatively little attention. In order to enlarge the horizon of its applications, we provide some rigorous analysis both in the frequency and time domain.

In the frequency domain, we focus on two main issues: disturbance rejection performance and robust stability. In spite of its powerful ability for disturbance rejection, the conventional disturbance observer rejects the disturbance approximately rather than asymptotically. To enhance the disturbance rejection performance, based on the well-known internal model principle, we propose a design

method to embed an internal model into the disturbance observer structure for achieving the asymptotic disturbance rejection and derive a condition for robust stability. Thus, the proposed disturbance observer can reject not only approximately the unmodeled disturbances but also asymptotically the disturbances of sinusoidal or polynomial-in-time type. In addition, a constructive design procedure to satisfy the proposed stability condition is presented. The other issue is to design of the disturbance observer based control system for guaranteeing robust stability under plant uncertainties. We study the robust stability for the case that the relative degree of the plant is not exactly known and so it happens to be different from that of nominal model. Based on the above results, we propose a universal design method for the disturbance observer when the relative degree of the plant is less than or equal to 4. Moreover, from the observation about the role of each block, we generalize the design of disturbance observer and propose a reduced order type-k disturbance observer to improve the disturbance rejection performance and to reduce the design complexity simultaneously.

As a counterpart of the frequency domain analysis, we analyze the disturbance observer in the state space for the purpose of extending the horizon of the disturbance observer applications and obtaining the deeper understanding of the role of each block. Based on the singular perturbation theory, it reveals not only well-known properties but also interesting facts such as the peaking in the transient response. Moreover, we investigate robust stability of the disturbance observer based control systems with and without unmodeled dynamics and derive an explicit relation between the nominal performance recovery and the time constant of Q-filter. Since the classical linear disturbance observer does not ensure the recovery of transient response, a nonlinear disturbance observer, in which all the benefits of the classical one are still preserved, is presented for guaranteeing the recovery of transient as well as steady-state response.

**Keywords:** disturbance observer, robust stability, disturbance rejection performance, internal model principle, unmodeled dynamics, nominal performance recovery

**Student Number:** 2008–30244



# Contents

<b>ABSTRACT</b>	<b>i</b>
<b>List of Figures</b>	<b>ix</b>
<b>Symbols and Acronyms</b>	<b>xiv</b>
<b>1 Introduction</b>	<b>1</b>
1.1 Motivation . . . . .	1
1.2 Contributions and Outline of the Dissertation . . . . .	5
<b>2 Robust Stability for Closed-loop System with Disturbance Observer</b>	<b>9</b>
2.1 Structure of Disturbance Observer . . . . .	9
2.2 Robust Stability Condition for Closed-loop System with Disturbance Observer . . . . .	12
2.3 Illustrative Example . . . . .	16
<b>3 Embedding Internal Model in Disturbance Observer with Robust Stability</b>	<b>19</b>
3.1 Design Method for Embedding Internal Model of Disturbance . . . . .	21
3.2 Design of Q-filter for Guranteeing Robust Stability . . . . .	27
3.2.1 Robust Stability Condition of Closed-loop System . . . . .	27
3.2.2 Selecting $a_i$ 's for Robust Stability . . . . .	30
3.3 Illustrative Example . . . . .	32
3.4 Discussions on Robustness . . . . .	36



3.4.1	Pros and Cons of Proposed Design Procedure . . . . .	36
3.4.2	Bode Diagram Approach . . . . .	38
<b>4</b>	<b>Disturbance Observer with Unknown Relative Degree of the Plant</b>	<b>45</b>
4.1	Robust Stability . . . . .	46
4.2	A Guideline for Selecting $Q$ and $P_n$ . . . . .	53
4.2.1	A Universal Robust Controller . . . . .	54
4.3	Technical Proofs . . . . .	54
4.4	Illustrative Examples . . . . .	60
<b>5</b>	<b>Reduced Order Type-k Disturbance Observer under Generalized Q-filter</b>	<b>65</b>
5.1	Concept of Disturbance Observer with Generalized Q-filter Structure	66
5.2	Robust Stability . . . . .	68
5.3	Reduced Order Type-k Disturbance Observer . . . . .	71
5.4	Illustrative Examples . . . . .	75
<b>6</b>	<b>State Space Analysis of Disturbance Observer</b>	<b>81</b>
6.1	State Space realization of Disturbance Observer . . . . .	82
6.2	Analysis of Disturbance Observer based on Singular Perturbation Theory . . . . .	88
6.3	Discussion on Disturbance Observer Approach . . . . .	91
6.3.1	Relation of Robust Stability Condition between State Space and Frequency Domain Analysis . . . . .	91
6.3.2	Effect of Zero Dynamics . . . . .	91
6.3.3	Stability of Nominal Closed-loop System . . . . .	92
6.3.4	Infinite Gain Property with $p$ -dynamics . . . . .	92
6.3.5	Peaking in Fast Transient . . . . .	94
6.4	Nominal Performance Recovery with respect to Time Constant of Q-filter . . . . .	95
<b>7</b>	<b>Nominal Performance Recovery and Stability Analysis for Disturbance Observer under Unmodeled Dynamics</b>	<b>99</b>
7.1	Problem Formulation . . . . .	100

7.2	Stability and Performance Analysis based on Singular Perturbation Theory . . . . .	104
7.2.1	Nominal Performance Recovery . . . . .	105
7.2.2	Multi-time-scale Singular Perturbation Analysis . . . . .	106
7.3	Nominal Performance Recovery by Disturbance Observer under Unmodeled Dynamics . . . . .	108
<b>8</b>	<b>Extensions of Disturbance Observer for Guaranteeing Robust Transient Performance</b>	<b>115</b>
8.1	Extensions to MIMO Nonlinear Systems . . . . .	116
8.1.1	SISO Nonlinear Disturbance Observer with Nonlinear Nominal Model . . . . .	118
8.1.2	MIMO Nonlinear Disturbance Observer with Linear Nominal Model . . . . .	121
<b>9</b>	<b>Conclusions</b>	<b>125</b>
	<b>APPENDIX</b>	<b>127</b>
	<b>BIBLIOGRAPHY</b>	<b>131</b>
	국문초록	141
	감사의 글	143



# List of Figures

1.1	(a) The nominal closed-loop system with $P_n(s)$ and (b) The actual closed-loop system with $Pf(s)$ . . . . .	2
1.2	The closed-loop system with the disturbance observer structure (shaded block). . . . .	3
2.1	The closed-loop system with the disturbance observer structure (shaded block). . . . .	10
2.2	Step responses of the nominal closed-loop system in the absence of disturbance ('Nominal response'), the nominal closed-loop system in the presence of the disturbance $d(t) = 5 \sin(2\pi t)$ ('W/O DOB'), and the nominal closed-loop system with the disturbance observer with $Q_b(s)$ in the presence of the disturbance ('W/ DOB') when $\tau = 0.01$ . . . . .	17
2.3	The error between the step response of the nominal closed-loop system and that of the actual closed-loop system with the disturbance observer with $Q_b(s)$ for the time constant $\tau = 0.01$ ('Time constant $\tau = 0.01$ ') and $\tau = 0.001$ ('Time constant $\tau = 0.001$ ') when $J = 1$ and $B = 8$ . . . . .	17
2.4	The error between the step response of the nominal closed-loop system and that of the actual closed-loop system with the disturbance observer with $Q_b(s)$ ('DOB with $Q_b(s)$ ') and $Q_p(s)$ ('DOB with $Q_p(s)$ ') when $J = 0.1$ and $B = 11.3$ . . . . .	18
3.1	The closed-loop system with the disturbance observer structure (dotted-line block). . . . .	22

3.2	Equivalent block diagram of the DOB structure in Fig. 3.1. . . . .	23
3.3	The error between the step response of the nominal closed-loop system and that of the actual closed-loop system with the disturbance observer with $Q_b(s)$ ('DOB with $Q_b(s)$ ') and $Q_p(s)$ ('DOB with $Q_p(s)$ ') when $J = 1$ . . . . .	34
3.4	The error between the step response of the nominal closed-loop system and that of the actual closed-loop system with the disturbance observer with $Q_b(s)$ ('DOB with $Q_b(s)$ ') and $Q_p(s)$ ('DOB with $Q_p(s)$ ') when $J = 4.2$ . . . . .	35
3.5	Bode diagrams of sensitivity functions without the disturbance observer ('W/O DOB') and with the disturbance observer with $Q_b(s)$ ('DOB with $Q_b(s)$ ') and $Q_p(s)$ ('DOB with $Q_p(s)$ ') when $J = 1$ . . .	35
3.6	The value sets of the four extreme polynomials of $p_1(s; g)$ ('blue solid line') and $p_1(s; g)$ ('red plus signs') for each $\omega \geq 0$ . . . . .	37
3.7	Bode diagrams of sensitivity functions without the disturbance observer ('W/O DOB') and with the disturbance observer with $Q_{type-1}^b(s)$ ('DOB with $Q_{type-1}^b(s)$ '), $Q_{type-2}^b(s)$ ('DOB with $Q_{type-2}^b(s)$ '), $Q_{type-3}^b(s)$ ('DOB with $Q_{type-3}^b(s)$ '), $Q_{IM}^b(s)$ ('DOB with $Q_{IM}^b(s)$ '), and $Q_{type-4}^b(s)$ ('DOB with $Q_{type-4}^b(s)$ ') when $\tau = 0.001$ and $\omega_1 = 8 \times 2\pi$ . . . . .	40
3.8	Bode diagrams of loop transfer functions without the disturbance observer ('W/O DOB') and with the disturbance observer with $Q_{type-1}^b(s)$ ('DOB with $Q_{type-1}^b(s)$ '), $Q_{type-2}^b(s)$ ('DOB with $Q_{type-2}^b(s)$ '), $Q_{type-3}^b(s)$ ('DOB with $Q_{type-3}^b(s)$ '), $Q_{IM}^b(s)$ ('DOB with $Q_{IM}^b(s)$ '), and $Q_{type-4}^b(s)$ ('DOB with $Q_{type-4}^b(s)$ ') when $\tau = 0.001$ and $\omega_1 = 8 \times 2\pi$ . . . . .	40
3.9	Bode diagrams of sensitivity functions without the disturbance observer ('W/O DOB') and with the disturbance observer with $Q_{type-1}^p(s)$ ('DOB with $Q_{type-1}^p(s)$ '), $Q_{type-2}^p(s)$ ('DOB with $Q_{type-2}^p(s)$ '), $Q_{type-3}^p(s)$ ('DOB with $Q_{type-3}^p(s)$ '), $Q_{IM}^p(s)$ ('DOB with $Q_{IM}^p(s)$ '), and $Q_{type-4}^p(s)$ ('DOB with $Q_{type-4}^p(s)$ ') when $\tau = 0.001$ and $\omega_1 = 8 \times 2\pi$ . . . . .	41

3.10	Bode diagrams of loop transfer functions without the disturbance observer ('W/O DOB') and with the disturbance observer with $Q_{type-1}^p(s)$ ('DOB with $Q_{type-1}^p(s)$ '), $Q_{type-2}^p(s)$ ('DOB with $Q_{type-2}^p(s)$ '), $Q_{type-3}^p(s)$ ('DOB with $Q_{type-3}^p(s)$ '), $Q_{IM}^p(s)$ ('DOB with $Q_{IM}^p(s)$ '), and $Q_{type-4}^p(s)$ ('DOB with $Q_{type-4}^p(s)$ ') when $\tau = 0.001$ and $\omega_1 = 8 \times 2\pi$ . . . . .	41
3.11	Bode diagrams of sensitivity functions without the disturbance observer ('W/O DOB') and with the disturbance observer with $Q_{type-1}^p(s)$ ('DOB with $Q_{type-1}^p(s)$ '), $Q_{type-2}^p(s)$ ('DOB with $Q_{type-2}^p(s)$ '), $Q_{type-3}^p(s)$ ('DOB with $Q_{type-3}^p(s)$ '), $Q_{IM}^p(s)$ ('DOB with $Q_{IM}^p(s)$ '), and $Q_{type-4}^p(s)$ ('DOB with $Q_{type-4}^p(s)$ ') when $\tau = 0.1$ and $\omega_1 = 2\pi$ . . . . .	42
3.12	Bode diagrams of loop transfer functions without the disturbance observer ('W/O DOB') and with the disturbance observer with $Q_{type-1}^p(s)$ ('DOB with $Q_{type-1}^p(s)$ '), $Q_{type-2}^p(s)$ ('DOB with $Q_{type-2}^p(s)$ '), $Q_{type-3}^p(s)$ ('DOB with $Q_{type-3}^p(s)$ '), $Q_{IM}^p(s)$ ('DOB with $Q_{IM}^p(s)$ '), and $Q_{type-4}^p(s)$ ('DOB with $Q_{type-4}^p(s)$ ') when $\tau = 0.1$ and $\omega_1 = 2\pi$ . . . . .	42
3.13	Bode diagrams of $Q_{type-1}^b(s)$ , $Q_{type-2}^b(s)$ , $Q_{type-3}^b(s)$ , $Q_{IM}^b(s)$ , and $Q_{type-4}^b(s)$ when $\tau = 0.1$ and $\omega_1 = 2\pi$ . . . . .	43
3.14	Bode diagrams of $Q_{type-1}^p(s)$ , $Q_{type-2}^p(s)$ , $Q_{type-3}^p(s)$ , $Q_{IM}^p(s)$ , and $Q_{type-4}^p(s)$ when $\tau = 0.1$ and $\omega_1 = 2\pi$ . . . . .	43
4.1	Structure of the disturbance observer control system. The shaded region represents the real plant $P(s)$ augmented with the disturbance observer . . . . .	47
4.2	Newton diagram for $\bar{\delta}(s; \tau)$ in (4.1.6) when $r.deg(P) > r.deg(P_n)$ ( <i>i.e.</i> , $m_\beta > m_\alpha$ ). . . . .	55
4.3	Newton diagram for $\hat{\delta}(\hat{s}; \hat{\tau})/\hat{\tau}^{l+1}$ . . . . .	57
4.4	Newton diagram for the case $r.deg(P) < r.deg(P_n)$ . . . . .	58
4.5	Newton diagram for $\hat{\delta}(\hat{s}; \hat{\tau})/\hat{\tau}^{2l}$ under the condition $r.deg(P) < r.deg(P_n)$ . . . . .	59
4.6	Simulation results for $P_{1,a}$ , $P_{1,b}$ , and $P_{1,c}$ (plants having relative degree 1) in the presence of disturbance $d(t) = \sin(2\pi t)$ . . . . .	62

4.7	Simulation results for $P_{2,a}$ , $P_{2,b}$ , and $P_{2,c}$ (plants having relative degree 2) in the presence of disturbance $d(t) = \sin(2\pi t)$ . . . . .	62
4.8	Simulation results for $P_{3,a}$ , $P_{3,b}$ , and $P_{3,c}$ (plants having relative degree 3) in the presence of disturbance $d(t) = \sin(2\pi t)$ . . . . .	63
4.9	Simulation results for $P_{4,a}$ , $P_{4,b}$ , and $P_{4,c}$ (plants having relative degree 4) in the presence of disturbance $d(t) = \sin(2\pi t)$ . . . . .	63
5.1	Structure of the disturbance observer control system. The shaded region represents the real plant $P(s)$ augmented with the disturbance observer . . . . .	66
5.2	The equivalent block diagram of the disturbance observer structure in Fig. 5.1. . . . .	72
5.3	The output $y$ of the overall system with $Q_{D,p,type-2}(s)$ (solid) and $Q_{D,b}(s)$ (dashed) when $d(t) = -2.5t^2 + 10t + 1$ . . . . .	78
5.4	The output $y$ of the overall system with $Q_{D,p,type-0}(s)$ (dot-dashed), $Q_{D,p,type-1}(s)$ (dashed), and $Q_{D,p,type-2}(s)$ (solid) when $d(t) = -2.5t^2 + 10t + 1$ . . . . .	78
5.5	The output $y$ of the overall system with $Q_{D,p,type-0}(s)$ (dot-dashed), $Q_{D,p,type-1}(s)$ (dashed), and $Q_{D,p,type-2}(s)$ (solid) when $d(t) = 2\sin(2\pi t)$ . . . . .	79
5.6	Bode plot of sensitivity function of the overall system with $Q_{D,p,type-0}(s)$ (dot-dashed), $Q_{D,p,type-1}(s)$ (dashed), and $Q_{D,p,type-2}(s)$ (solid) . . . . .	79
5.7	Bode plot of Q-filters $Q_{D,p,type-0}(s)$ (dot-dashed), $Q_{D,p,type-1}(s)$ (dashed), and $Q_{D,p,type-2}(s)$ (solid) . . . . .	80
6.1	Conventional linear disturbance observer structure with the outer-loop controller. Here, $Q_A(s) = Q_B(s) = Q(s)$ , but unique names are given for convenience. . . . .	83
6.2	Since both systems $Q_A$ and $P_n^{-1}$ are linear, two configurations in this figure are equivalent in the steady-state. For implementation the configuration of the bottom is used while the upper one is employed for the stability analysis in this paper. . . . .	86
6.3	Equivalent configuration of the shaded block of Fig. 6.1 . . . . .	93

8.1	Proposed SISO nonlinear disturbance observer structure. $P$ , $Q_q(s)$ , and $Q_p(s)$ correspond to (8.1.1) and (8.1.10), respectively. . . . .	119
8.2	Proposed MIMO nonlinear disturbance observer structure. $P$ cor- responds to (8.1.1). . . . .	123





# Symbols and Acronyms

## Symbols

$\mathbb{R}$	field of real numbers
$\mathbb{C}$	field of complex numbers
$\mathbb{C}^-$	open left-half complex plane; i.e., $\{s \in \mathbb{C} : \text{Re}(s) < 0\}$
$\mathbb{C}^+$	open right-half complex plane; i.e., $\{s \in \mathbb{C} : \text{Re}(s) > 0\}$
$\mathbb{R}^n$	real Euclidean space of dimension $n$
$\mathbb{R}^{m \times n}$	space of $m \times n$ matrices with real entries
$\text{deg}(D)$	the degree of the polynomial or transfer function $D(s)$
$\text{r.deg}(D)$	the relative degree of the transfer function $D(s)$
$\text{h.gain}(D)$	the high frequency gain of the transfer function $D(s)$
$I_n$	$n \times n$ identity matrix (subscript $n$ is omitted when there is no confusion.)
$0_n$	$n \times 1$ column vector having all elements equal to 0
$0_{m \times n}$	$m \times n$ matrix having all elements equal to 0
$\text{diag}(A_1, \dots, A_k)$	block diagonal matrix with its $i$ th block diagonal $A_i \in \mathbb{R}^{m_i \times n_i}$ , $i = 1, \dots, k$
$\det(A)$	the determinant of the matrix $A$
$\lambda_{\max}(A)$	the maximum eigenvalue of the matrix $A \in \mathbb{R}^{n \times n}$
$\lambda_{\min}(A)$	the minimum eigenvalue of the matrix $A \in \mathbb{R}^{n \times n}$

$[a; b]$	$[a; b] := [a^T, b^T]^T$ for two column vectors $a$ and $b$
$\ a\ $	$\ a\  := \sqrt{a^T a}$ for a vector $a \in \mathbb{R}^n$
$\ A\ $	$\ A\  := \sqrt{\lambda_{\max}(A^T A)}$ for a matrix $A \in \mathbb{R}^{n \times n}$
$\mathfrak{C}^i$	$i$ -th times continuously differentiable
$:=$	defined as
$\square$	end of proof, definition, theorem, remark, and so on

## Acronyms

LTI	Linear time-invariant
SISO	Single-input single-output
MIMO	Multi-input multi-output

# Chapter 1

## Introduction

### 1.1 Motivation

The primary objective of control may be to make a system response satisfy a given specification such as the overshoot, settling time, steady-state error between the reference input and system output, and so on [DFT92, Che99, SSJH02, FPEN06]. When there is no modeling error (*i.e.*, information about an actual plant is completely known *a priori*), it is easy to achieve the given specification by a simple unity feedback control system shown by Fig. 1.1 (a). In this figure<sup>1</sup>,  $P_n(s)$  and  $C(s)$  denote a nominal model obtained from information about the plant and controller, respectively, and the signals  $r$  and  $y$  represent the reference input and plant output, respectively. The controller  $C(s)$  is designed based on the nominal model  $P_n(s)$  to achieve the given specification. Then, the plant output is simply computed as, for all  $\omega \in [0, \infty)$ ,

$$y(j\omega) = \frac{P_n(j\omega)C(j\omega)}{1 + P_n(j\omega)C(j\omega)} r(j\omega) \quad (1.1.1)$$

since  $P_n(s)$  equals to the actual plant. Thus, one can obtain the desired system response merely by selecting appropriate  $C(s)$ .

However, it is impossible to obtain a precise mathematical model from the actual plant because there are some limitations<sup>2</sup> to obtain exact information about

---

<sup>1</sup>For simplicity, we assume that an actual plant is a single-input single-output (SISO) linear time-invariant system. More general class of systems will be discussed in Chapter 8.

<sup>2</sup>In general, when the nominal model is derived from the system identification method, the

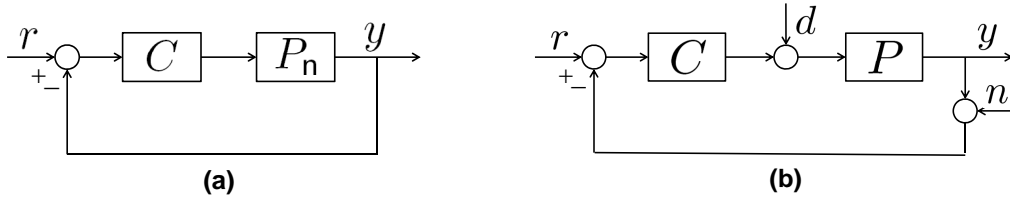


Figure 1.1: (a) The nominal closed-loop system with  $P_n(s)$  and (b) The actual closed-loop system with  $P_f(s)$

the actual plant. Moreover, in real control situation, the existence of the disturbance<sup>3</sup> and measurement noise is also inevitable. Here, an actual closed-loop system under such situation is described as Fig. 1.1 (b). The actual plant is denoted by  $P(s)$  and the input signals  $d$  and  $n$  denote the disturbance and measurement noise, respectively.

If there exists a modeling error, then  $P(s)$  is no longer equal to  $P_n(s)$ . Hence, it is not easy to accomplish the primary control objective and the situation becomes much worse because of the existence of the disturbance and sensor noise as well as the modeling error. Therefore, the secondary control objective may be to compensate the effect of plant uncertainties, disturbance, and noise as much as possible so that the control system behaves approximately like the nominal one depicted in Fig. 1.1 (a).

Designing controllers to compensate the effect of plant uncertainties and disturbances have been one of the major issues in control fields, and many useful solutions such as robust output regulation [Dav76, FW76, Isi95, Hua04],  $H_2/H_\infty$  control [DGKF89, ZD98], sliding mode control [Utk92], adaptive control [NA89, IS96, YAMT97], disturbance accommodation controller [Joh71, Joh86], proportional integral observer [JWS00, KRK10, SK10], disturbance observer [Ohn87], and so on, are available in the literature.

---

obtained data is contaminated by the measurement error, parameter variations, and unexpected unmodeled dynamics. Therefore, the modeling error, the difference between the actual plant and its nominal model, is an unavoidable element in the controller design task.

<sup>3</sup>The disturbance is defined as external signals caused by unexpected environment. In general, there are two main sources of the disturbance: 1) unknown or unpredictable external inputs such as friction, load torque, nonlinearity, and so on, [AHDW94, OÅdW<sup>+</sup>98, MÖ05, MGÖ08], 2) unknown exogenous input generated by an exosystem [Joh71, MGB06, CLP06]. Sometimes, the modeling error is also considered as the disturbance.

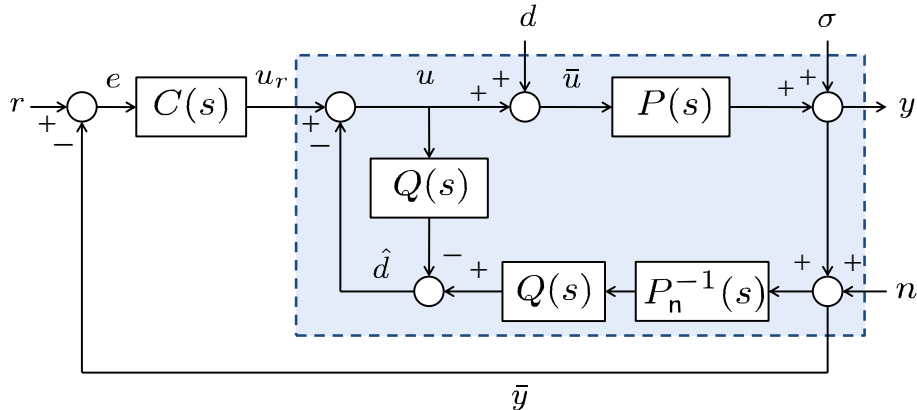


Figure 1.2: The closed-loop system with the disturbance observer structure (shaded block).

Among various robust control schemes, in mechatronics (see, *e.g.*, [Tom96a, Tom96b]), the disturbance observer has been recognized as a powerful tool for robust control due to its simple structure and ability for disturbance rejection. In addition, it is flexible because it constitutes an inner-loop, that is, merely by adding disturbance observer feedback in the inner-loop, the conventional (outer-loop) feedback design is enabled without taking into account the effects from disturbances and uncertainties. Since its introduction in 1987 [Ohn87], the disturbance observer has been widely applied to industrial applications such as motor control [UH91, YCS09, KT13], robot manipulator [UH93, OC99, KMH00, ESC01, SD02, KIO08, BSPS10], positioning table [LT96, EKK<sup>+</sup>96, KK99, TLT00, KC03b], optical disk drive [CYC<sup>+</sup>03, KC03a, WT04], hard disk drive [IT98, HM98, YT99, WTS00, YCC05], automotive vehicle [GG02, GGK09], power-assisted wheelchair [OHH08, OOH10], to name only a few. In this dissertation, we focus our attention on the disturbance observer to analyze and extend its properties.

Fig. 1.2 describes a basic configuration of disturbance observer based control system. Roughly speaking, the disturbance observer compares the control input we apply to the plant with an estimate of the actual input which refers to the control input together with the disturbance, and we estimate it by passing the system output to an inverse model of the plant. The difference between the control input and the estimate we obtain will be similar to the disturbance, and we can

use this signal to estimate the disturbance and generate a compensating signal if needed. In practice, a low pass filter called Q-filter is added in the loop to make the idea implementable, and the coefficients of Q-filter are design parameters. It is noted that the external disturbance and plant uncertainties are lumped into the disturbance, which means that the disturbance observer can provide robustness against plant uncertainty as well.

Compared with many success stories in industry, theoretic analysis on the disturbance observer itself has attracted relative little attention. One of reasons might be that the original idea of [Ohn87], explained for a simple mechanical model using transfer functions, has already clear intuitive justification. Thus, regarding the design and analysis of the closed-loop system with the disturbance observer, most researches employ the frequency domain tools. As a result, the class of systems under consideration is limited to linear systems (in fact, usually second order systems are considered) and the existing robust stability conditions are mainly based on the small-gain theorem, which are therefore conservative [UH93, Tom96a, GG01, CYC<sup>+</sup>03, KT13]. Several trials have been performed to design and to analyze the disturbance observer in view of well-known frameworks such as  $H_\infty$  control [CCY96, MHMZ98, WT04], sliding mode control [KCO02], unknown input observer [SD02], passivity-based approach [BT99], and so on. However, the behavior and design methodology of individual blocks in the disturbance observer structure and the possibility of extension to more general class of systems (*e.g.*, time-varying linear plants, nonlinear plants, and nonminimum phase plants) have not been clarified yet.

In this dissertation, under an assumption that the bandwidth of Q-filter is enough large (we shall maintain this assumption throughout this dissertation since it make the observation about the behavior of each pole and dynamics of the closed-loop system more easy.), we will rigorously analyze the stability and performance of disturbance observer based control system both in the frequency and time domain. In the frequency domain, we will review the robustness of the disturbance observer and an almost necessary and sufficient condition for robust stability. Afterward, by embedding the internal model, a disturbance observer with modified Q-filter structure will be proposed to enhance the disturbance re-

jection performance. And then, we will study the robustness of the disturbance observer for the case that the relative degree of the plant is unknown. As a counterpart, in the time domain, we will represent the closed-loop system with disturbance observer as the singular perturbation form to enlighten the behavior of each block of the disturbance observer structure and extend its applications to more general class of systems. Then, with respect to the bandwidth of Q-filter, the robust stability and nominal performance recovery of disturbance observer based control scheme with and without unmodeled dynamics will be discussed. Finally, the robust transient as well as steady-state performance recovery of non-linear disturbance observers will be further discussed.

## 1.2 Contributions and Outline of the Dissertation

This dissertation is composed of two parts with respect to their representations. Throughout Chapter 2–5, the analysis is based on the frequency domain approach, whereas the remainder part is analyzed in the state-space. The contributions of each chapter and the organization of this dissertation are as follows:

### **Chapter 2. Robust Stability for Closed-loop System with Disturbance Observer**

As a first step, we introduce the structure of the disturbance observer and review its disturbance rejection performance and robust stability under plant uncertainties. In addition, a condition for robust stability (in some sense, it is almost necessary and sufficient) is presented. The analysis on robust stability for the disturbance observer based control system in this chapter is owed to [SJ09].

### **Chapter 3. Embedding Internal Model in Disturbance Observer with Robust Stability**

In this chapter, we consider a design problem of disturbance observer to achieve the asymptotic disturbance rejection in view of the internal model principle although the conventional disturbance observer merely compensates the disturbance approximately. This chapter is based on the results in [PJSB12, JPBS14] and the contributions of this chapter are as follows:



- We propose a design method for the disturbance observer to embed the internal model of disturbance for rejecting the disturbance asymptotically.
- We present an almost necessary and sufficient condition for robust stability of the proposed disturbance observer based control system.
- For plant uncertainties belong to an arbitrarily large compact set, a constructive design procedure to satisfy the proposed stability condition is provided.
- As a practical example, a simulation for a mechanical positioning system for X-Y table is performed to verify the performance of the proposed disturbance observer.

#### **Chapter 4 Disturbance Observer with Unknown Relative Degree of the Plant**

This chapter deals with the robust stability of the disturbance observer based control system when the relative degree of plant is not exactly known. Most of this chapter is based on [JJSS12, JJS14] and the contributions of this chapter are summarized as

- We analyze the robust stability for the closed-loop system with the disturbance observer when the relative degree of the plant is not equal to that of its nominal model.
- We provide a robust stability condition for the case that the difference between the relative degree of the plant and that of its nominal model is equal to 1.
- A universal design method for the disturbance observer is proposed when the relative degree of the plant is less than or equal to 4.

#### **Chapter 5 Reduced Order Type-k Disturbance Observer under Generalized Q-filter Design**

The main objective of this chapter is to extend the disturbance observer structure proposed in Chapter 2 and 3 for obtaining an understanding of the role of each

block and reducing the order of disturbance observer structure. The contributions of this chapter are listed as follows.

- Based on the observation about the role of each filter, we generalize a Q-filter design scheme and derive a robust stability condition.
- We propose a reduced order type-k disturbance observer in the viewpoint of the generalized Q-filter design scheme.
- We present a Q-filter design procedure guaranteeing the proposed stability condition.
- To clarify the validity of the proposed disturbance observer, a simulation is performed.

## **Chapter 6 State Space Analysis of Disturbance Observer**

In this chapter, based on the singular perturbation theory, we analyze the disturbance observer in the state space to get a deeper understanding of the behavior of each block in its structure and possibilities to enlarge the horizon of its applications. In addition, we show that the disturbance observer can recover the nominal performance in the presence of disturbances and plant uncertainties. Some parts of this chapter are based on [SJ07]. The contributions of this chapter are summarized as follows:

- We represent the disturbance observer based control system as a singular perturbation form by the state space realization.
- We enlighten several aspects of the disturbance observer not well discussed in the frequency domain approach.
- Based on the Lyapunov stability analysis, the robust stability and nominal performance recovery with respect to the time constant of Q-filter is discussed.

## **Chapter 7 Nominal Performance Recovery and Stability Analysis for Disturbance Observer under Unmodeled Dynamics**

This chapter focus on the robust stability and nominal performance recovery of the closed-loop system with the disturbance observer under fast unmodeled dynamics, which is a counterpart of the results in Chapter 4. The contributions of this chapter are as follows:

- We present the robust stability of the disturbance observer based control scheme under the fast unmodeled dynamics using the multi-parameter and multi-time-scale singular perturbation theory.
- We provide that the robust stability and nominal performance of disturbance observer under unmodeled dynamics with respect the bandwidth of Q-filter.

### **Chapter 8 Extensions of Disturbance Observer for Guaranteeing Robust Transient Performance**

In this chapter, we review extensions of disturbance observer to multi-input multi-output (MIMO) nonlinear systems. Furthermore, the robust transient performance recovery of nonlinear disturbance observer with saturating functions is also discussed. Most of this chapter is based on [BS08, BS09].

### **Chapter 9. Conclusions**

This dissertation concludes with some remarks.

# Chapter 2

## Robust Stability for Closed-loop System with Disturbance Observer

Since its simple structure and powerful ability for disturbance rejection, the disturbance observer has been widely applied to industrial applications. In this chapter, we introduce the basic concept and structure of the classical disturbance observer and review a condition for guaranteeing robust stability of the disturbance observer based control system. Finally, in order to verify the validity of the robust stability condition and the disturbance rejection performance, simulations for a mechanical system are presented. The results of this chapter are mainly based on [SJ09].

### 2.1 Structure of Disturbance Observer

The disturbance observer structure (shaded block) with the outer-loop controller  $C(s)$  is shown in Fig. 2.1. The actual plant, denoted by  $P(s)$ , is a single-input single-output linear time-invariant system with the relative degree<sup>1</sup>  $\nu \geq 1$  and the nominal model for  $P(s)$  is denoted by  $P_n(s)$ . The component  $Q(s)$ , known as the 'Q-filter', is a stable low-pass filter. The outer-loop controller  $C(s)$  is designed for  $P_n(s)$  without taking plant uncertainties and/or disturbances into account.

We make the following assumption for the plant.

---

<sup>1</sup>In the transfer function, the relative degree means that the difference between the degree of the numerator and denominator. For more detailed definition, see [Kha02]

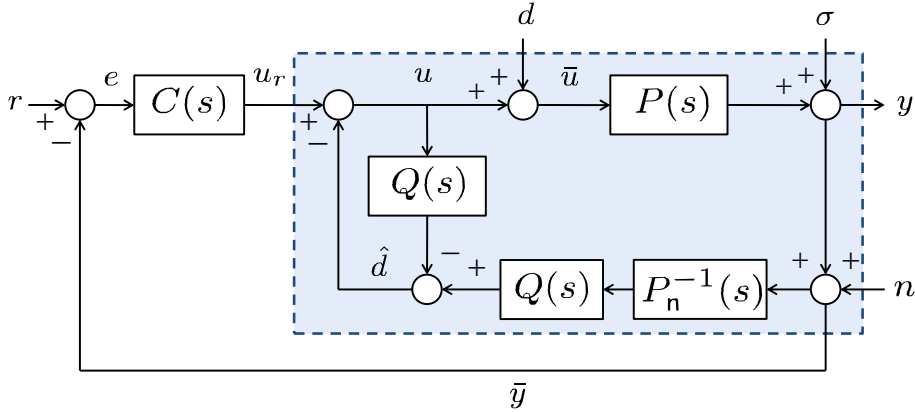


Figure 2.1: The closed-loop system with the disturbance observer structure (shaded block).

**Assumption 2.1.1.** The plant  $P(s)$  belongs to a set  $\mathcal{P}$  defined by

$$\mathcal{P} = \left\{ \frac{\beta_{n-\nu}s^{n-\nu} + \beta_{n-\nu-1}s^{n-\nu-1} + \dots + \beta_0}{\alpha_n s^n + \alpha_{n-1}s^{n-1} + \dots + \alpha_0} : \right. \\ \left. \alpha_i \in [\underline{\alpha}_i, \bar{\alpha}_i], \beta_j \in [\underline{\beta}_j, \bar{\beta}_j], i = 0, \dots, n, j = 0, \dots, n - \nu \right\} \quad (2.1.1)$$

where  $\underline{\alpha}_i$ ,  $\bar{\alpha}_i$ ,  $\underline{\beta}_j$ , and  $\bar{\beta}_j$  are known constants, the intervals  $[\underline{\alpha}_n, \bar{\alpha}_n]$  and  $[\underline{\beta}_{n-\nu}, \bar{\beta}_{n-\nu}]$  do not contain zero<sup>2</sup>, and  $\beta_i$ 's are such that  $\beta_{n-\nu}s^{n-\nu} + \dots + \beta_0$  is Hurwitz (i.e.,  $\mathcal{P}$  consists of minimum phase plants).  $\square$

In fact, the order of nominal model  $P_n(s)$ ,  $\bar{n}$ , may not equal to  $n$ . However, one must choose  $P_n(s)$  such that the relative degree of  $P_n(s)$  is equal to that of  $P(s)$ <sup>3</sup>, minimum phase plant, and  $\beta_{\bar{n}-\nu}^n/\alpha_{\bar{n}}^n$  has the same sign as  $\beta_{n-\nu}/\alpha_n$  where both  $\beta_{\bar{n}-\nu}^n$  and  $\alpha_{\bar{n}}^n$  are nominal values of  $\beta_{n-\nu}$  and  $\alpha_n$ , respectively. For simplicity, we assume that  $P_n(s)$  also belongs to the set  $\mathcal{P}$  (i.e.,  $n = \bar{n}$ ).

The Q-filter is generally designed as [UH93, LT96, CYC<sup>+</sup>03]

$$Q(s) = \frac{c_k(\tau s)^k + \dots + c_0}{(\tau s)^l + a_{l-1}(\tau s)^{l-1} + \dots + a_1(\tau s) + a_0} \quad (2.1.2)$$

<sup>2</sup>It implies that the relative degree,  $\nu$ , and the sign of the high frequency gain,  $\beta_{n-\nu}/\alpha_n$ , of the plant are known *a priori* and do not changed.

<sup>3</sup>The general case when the relative degree of  $P_n(s)$  is different from that of  $P(s)$  will be discussed in Chapter 4 and 7.

where  $c_0 = a_0$  and  $l - k \geq \nu$  so that the Q-filter has a unity DC gain and the transfer function  $Q(s)P_n(s)^{-1}$  becomes proper. All the  $a_i$ 's should be chosen such that the polynomial  $s^l + a_{l-1}s^{l-1} + \dots + a_0$  is Hurwitz. The design parameter  $\tau > 0$  is a time constant, which determines the cut-off frequency of Q-filter.

In Fig. 2.1, the reference input  $r$ , the input disturbance  $d$ , the output disturbance  $\sigma$ , and the measurement noise  $n$  are the input signals of the closed-loop system. In general, it is assumed that the disturbances  $d$  and  $\sigma$  are dominant in the low frequency range, while the noise  $n$  is dominant in the high frequency range. With these signals, the output  $y$  of the closed-loop system becomes

$$y(s) = T_{yr}(s)r(s) + T_{yd}(s)d(s) + T_{y\sigma}(s)\sigma(s) + T_{yn}(s)n(s) \quad (2.1.3)$$

where

$$\begin{aligned} T_{yr}(s) &:= \frac{P(s)P_n(s)C(s)}{Q(s)(P(s) - P_n(s)) + P_n(s)(1 + P(s)C(s))}, \\ T_{yd}(s) &:= \frac{P(s)P_n(s)(1 - Q(s))}{Q(s)(P(s) - P_n(s)) + P_n(s)(1 + P(s)C(s))}, \\ T_{y\sigma}(s) &:= \frac{P_n(s)(1 - Q(s))}{Q(s)(P(s) - P_n(s)) + P_n(s)(1 + P(s)C(s))}, \\ T_{yn}(s) &:= -\frac{P(s)(P_n(s)C(s) + Q(s))}{Q(s)(P(s) - P_n(s)) + P_n(s)(1 + P(s)C(s))}. \end{aligned}$$

By construction, we have that  $Q(j\omega) \approx 1$  in the low frequency range. Therefore, it follows that  $T_{yr}(j\omega) = \frac{P_n(j\omega)C(j\omega)}{1 + P_n(j\omega)C(j\omega)}$ ,  $T_{yd}(j\omega) \approx 0$ , and  $T_{y\sigma}(j\omega) \approx 0$ . In addition, we can ignore the noise  $n(j\omega)$  since it is dominant in the high frequency range. Therefore, the equation (2.1.3) is approximated as

$$y(j\omega) \approx \frac{P_n(j\omega)C(j\omega)}{1 + P_n(j\omega)C(j\omega)} r(j\omega).$$

This implies that, in the low frequency range, the closed-loop system with the disturbance observer structure behaves as the nominal closed-loop system in the absence of uncertainties and disturbances. In other words, in spite of the existence of disturbances and uncertainties, the disturbance observer recovers the nominal performance. Here, the nominal performance means the performance of

the nominal closed-loop system  $P_n(s)C(s)/(1 + P_n(s)C(s))$  without the input and output disturbances. It is important to notice that the above property is only valid when the closed-loop system is internally stable. A condition for robust internal stability of the closed-loop system will be presented in the following section. (See [SJ07, BS08, SJ09] for more details.)

## 2.2 Robust Stability Condition for Closed-loop System with Disturbance Observer

Now, we present a condition for robust stability of the closed-loop system in Fig. 2.1. From Fig. 2.1, the transfer function matrix from  $[r, d, \sigma, n]^T$  to  $[e, \bar{u}, \bar{y}, y]^T$  is computed as

$$\frac{1}{\Delta(s)} \begin{bmatrix} Q(P - P_n) + P_n & -PP_n(1 - Q) & -P_n(1 - Q) & -P_n(1 - Q) \\ P_n C & P_n(1 - Q) & -(P_n C + Q) & -(P_n C + Q) \\ PP_n C & PP_n(1 - Q) & P_n(1 - Q) & P_n(1 - Q) \\ PP_n C & PP_n(1 - Q) & P_n(1 - Q) & -P(P_n C + Q) \end{bmatrix}$$

where  $\Delta(s) := Q(s)(P(s) - P_n(s)) + P_n(s)(1 + P(s)C(s))$ . If this transfer function matrix is stable, then the closed-loop system is said to be internally stable. For convenience, one can represent  $P$ ,  $P_n$ ,  $C$ , and  $Q$  as the ratios of coprime polynomials:  $P(s) = N(s)/D(s)$ ,  $P_n(s) = N_n(s)/D_n(s)$ ,  $C(s) = N_c(s)/D_c(s)$ , and  $Q(s) = N_q(s; \tau)/D_q(s; \tau)$ . Note that, in order to express the explicit dependency of  $\tau$ ,  $N_q(s; \tau)$  and  $D_q(s; \tau)$  will be used instead of  $N_q(s)$  and  $D_q(s)$ , respectively. With this notation, for given  $\tau > 0$ , the characteristic polynomial

$$\delta(s; \tau) := D_c N_q (D_n N - D N_n) + N_n D_q (D D_c + N N_c) \quad (2.2.1)$$

is Hurwitz if and only if the closed-loop system is internally stable [SJ09]<sup>4</sup>. The closed-loop system is said to be robustly internally stable if  $\delta(s; \tau)$  is Hurwitz for all  $P(s) \in \mathcal{P}$ .

<sup>4</sup>In fact, unfortunately, this claim ( $\delta(s; \tau)$  is Hurwitz if and only if the closed-loop system is internally stable) in [SJ09] may not be true by the pole/zero cancellation. However, if  $P_n(s)$  is of minimum phase and  $C(s)$  internally stabilizes  $P_n(s)$ , then the above claim is true.

Although effects of the measurement noise on the overall performance are related to the bandwidth of Q-filter, it is not relevant to robust stability of the closed-loop system. Therefore, regardless of the effect of noise, we focus on the robust stability and performance for rejecting disturbances and compensating model uncertainties under an assumption that the bandwidth of Q-filter is enough large. To deal with the performance of disturbance observer with respect to the noise, noise reduction disturbance observers were proposed in [JS13, HKJ<sup>+</sup>13].

Let us introduce the polynomial  $p_f(s)$  given by

$$p_f(s) := D_{\mathbf{q}}(s; 1) + \left( \lim_{s \rightarrow \infty} \frac{P(s)}{P_n(s)} - 1 \right) N_{\mathbf{q}}(s; 1). \quad (2.2.2)$$

By denoting  $P(s) = (\sum_{j=0}^{n-\nu} \beta_j s^j) / (\sum_{i=0}^n \alpha_i s^i)$  and  $P_n(s) = (\sum_{j=0}^{n-\nu} \beta_j^n s^j) / (\sum_{i=0}^n \alpha_i^n s^i)$  whose coefficients  $\alpha_i^n$  and  $\beta_j^n$  are the nominal values of  $\alpha_i$  and  $\beta_j$ , respectively, the polynomial  $p_f(s)$  is rewritten as

$$p_f(s) = s^l + a_{l-1} s^{l-1} + \dots + a_{k+1} s^{k+1} + \left( a_k + \frac{g - g_n}{g_n} c_k \right) s^k + \dots + \left( a_0 + \frac{g - g_n}{g_n} c_0 \right) \quad (2.2.3)$$

where  $g := \beta_{n-\nu} / \alpha_n$  and  $g_n := \beta_{n-\nu}^n / \alpha_n^n$ . In fact,  $g$  and  $g_n$  are the high frequency gains of  $P(s)$  and  $P_n(s)$ , respectively. By Assumption 2.1.1, there exist positive constants  $\underline{g}$  and  $\bar{g}$  such that  $g$  and  $g_n$  belong to the interval  $[\underline{g}, \bar{g}]$ .

It is important to note that, even if the output disturbance is not taken into account, the characteristic polynomial (2.2.1) of the closed-loop system remains unchanged compared with [SJ09]. Hence, the following theorem, which was proposed in [SJ09] also presents a condition for robust internal stability of the closed-loop system even though we consider both the input and output disturbances.

**Theorem 2.2.1.** [SJ09] Under Assumption 2.1.1, there exists a constant  $\bar{\tau} > 0$  such that, for all  $0 < \tau \leq \bar{\tau}$ , the closed-loop system is robustly internally stable if the following two conditions hold:

1.  $C(s)$  internally stabilizes  $P_n(s)$ ,
2.  $p_f(s)$  is Hurwitz for all  $P(s) \in \mathcal{P}$ .



On the contrary, there is  $\bar{\tau} > 0$  such that, for all  $0 < \tau \leq \bar{\tau}$ , the closed-loop system is not robustly internally stable if at least one of the conditions 1–2 is violated in the sense that  $P_n C / (1 + P_n C)$  has some poles in  $\mathbb{C}^+$ , or some zeros of  $P(s)$  or some roots of  $p_f(s) = 0$  are located in  $\mathbb{C}^+$  for some  $P(s) \in \mathcal{P}$ .  $\square$

**Remark 2.2.1.** Theorem 2.2.1 is not able to determine robust internal stability when some poles of  $P_n C / (1 + P_n C)$ , or some zeros of  $P(s)$ , or some roots of  $p_f(s) = 0$  are located on the imaginary axis in the complex plane, but the remaining poles, zeros, and roots are located in  $\mathbb{C}^-$ . See [JJS11, JJSS12, JJS14] for more about such cases. If we exclude such situations, the conditions 1–2 are not only sufficient but also necessary for robust internal stability. In this sense, we call Theorem 2.2.1 as an almost necessary and sufficient condition for robust stability.  $\square$

Theorem 2.2.1 explains interesting points of the disturbance observer based control scheme under the assumption that the time constant  $\tau$  is sufficiently small. Firstly, it reveals that the minimum phaseness of the plant is one of the necessary conditions for internal stability in the classical disturbance observer<sup>5</sup>. Secondly, if  $P(s)$  is of minimum phase and  $C(s)$  is already designed to internally stabilize  $P_n(s)$ , then condition 2 in Theorem 1 indicates whether the closed-loop system is stable or not. Hence,  $p_f(s)$  plays an important role for guaranteeing robust stability of the closed-loop system under plant uncertainties. In other words, the robust stability is mainly determined by the coefficients  $a_i$ ,  $c_i$ , and the variation of  $g$ . If the variation of  $g$  around its nominal value  $g_n$  is small enough, then, due to the continuity of roots with respect to the coefficients of the equation, the polynomial  $p_f(s)$  remains Hurwitz for small perturbation of  $g$  provided that  $s^l + a_{l-1}s^{l-1} + \dots + a_1s + a_0$  is Hurwitz (i.e., the Q-filter of the form (2.1.2) is stable). This explains why the disturbance observer based control system is known to be robust under small parametric uncertainties.

However, for large uncertainties, the coefficients  $a_i$ 's need to carefully be selected. Although it seems difficult to achieve, under Assumption 2.1.1, one can always select  $a_i$  and  $c_i$  of Q-filter such that  $p_f(s)$  is Hurwitz. Here, we provide

---

<sup>5</sup>However, the non-minimum phase systems are often met in applications. Therefore, a trial had been made to apply the disturbance observer approach to non-minimum phase linear systems [JSS10].

one way to design the coefficients of Q-filter. If one select  $k = 0$ , then  $p_f(s)$  is reduced as

$$p_f(s) = s^l + a_{l-1}s^{l-1} + \cdots + a_1s + \frac{g}{g_n}a_0. \quad (2.2.4)$$

Now, we propose a design procedure so that  $p_f(s)$  in (2.2.4) to be Hurwitz.

### Procedure 1. Q-filter Design Procedure for Robust Stability

*Step 0:* Choose the coefficients  $a_{l-1}, \dots, a_1$  such that the polynomial

$$s^{l-1} + a_{l-1}s^{l-2} + \cdots + a_1$$

is Hurwitz.

*Step 1:* From Lemma A. 3 in Appendix, there exists  $\bar{\gamma}_0$  such that the polynomial

$$s^l + a_{l-1}s^{l-1} + \cdots + a_1s + \gamma_0$$

is Hurwitz for all  $\gamma_0 \in (0, \bar{\gamma}_0)$ . Then, select  $a_0 < (g_n/\bar{g})\bar{\gamma}$ .  $\square$

By the proposed procedure, we can choose the coefficients  $a_i$ 's such that  $p_f(s)$  in (2.2.4) is Hurwitz for all  $g \in [g, \bar{g}]$ . More general design procedure for  $p_f(s)$  in (2.2.3) to satisfy the condition 2 in Theorem 2.2.1 will be discussed in Chapter 3.

Now, we investigate the physical meaning of  $p_f(s)$  by the following remark.

**Remark 2.2.2.** Consider a second-order mechanical system as follows:

$$P(s) = \frac{1}{Js^2 + Bs} \quad (2.2.5)$$

where  $J$  is a moment of inertia and  $B$  is a viscous friction coefficient. From (2.2.5), the uncertain parameter in  $p_f(s)$  is  $1/J$ . Therefore, the inertia variation determines whether  $p_f(s)$  is Hurwitz or not. It is important to notice that, from the viewpoint of physical interpretation,  $p_f(s)$  explains the well-known fact that the robust stability mainly depends on the inertia variation for the mechanical systems, which is pointed out in [KC03b, KKO07].  $\square$

### 2.3 Illustrative Example

In order to verify the robust stability condition proposed in Theorem 2.2.1 and the disturbance rejection performance of the disturbance observer, simulations are performed for a mechanical system of the form

$$P(s) = \frac{1}{Js^2 + Bs}$$

where the moment of inertia  $J$  and the viscous friction  $B$  belong to the intervals  $[0.1, 1]$  and  $[8, 12]$ , respectively. We consider its nominal model as follows:

$$P_n(s) = \frac{1}{J_n s^2 + B_n s}$$

where  $J_n = 1$  and  $B_n = 8$ . Note that  $g_n = 1$  and  $g \in [\underline{g}, \bar{g}]$  where  $\underline{g} = 1$  and  $\bar{g} = 10$ . The outer-loop controller  $C(s)$  is designed as a simple proportional controller  $C(s) = 25$  so that the nominal closed-loop system becomes

$$\frac{P_n(s)C(s)}{1 + P_n(s)C(s)} = \frac{5^2}{s^2 + 2 \times 0.8 \times 5s + 5^2}.$$

The Q-filter with binomial coefficients for disturbance observer is selected as

$$Q_b(s) = \frac{1}{(\tau s)^3 + 3(\tau s)^2 + 3(\tau s) + 1}.$$

Fig. 2.2 shows the step responses of three cases: nominal closed-loop system in the absence of disturbance ('Nominal response'), nominal closed-loop system in the presence of  $d(t) = 5 \sin(2\pi t)$  ('W/O DOB'), and nominal closed-loop system with the disturbance observer with  $Q_b(s)$  in the presence of disturbance ('W/ DOB'). From the figure, it is seen that the disturbance observer compensates the effect of disturbance and recovers the nominal performance.

Now, we focus on the nominal performance recovery by the disturbance observer with respect to the time constant  $\tau$  of Q-filter. Fig. 2.3 shows the error between the step response of the nominal closed-loop system in the absence of disturbance, which is shown in Fig. 2.2 and that of the actual closed-loop system with the disturbance observer for  $\tau = 0.01$  and  $\tau = 0.001$ . It is clearly observed

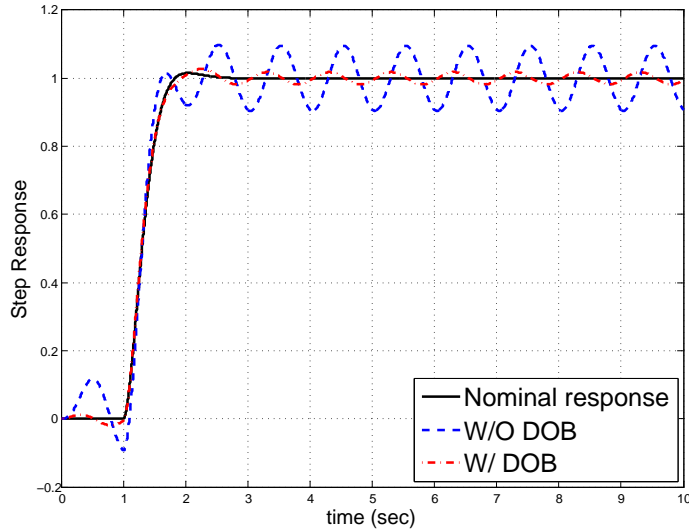


Figure 2.2: Step responses of the nominal closed-loop system in the absence of disturbance ('Nominal response'), the nominal closed-loop system in the presence of the disturbance  $d(t) = 5 \sin(2\pi t)$  ('W/O DOB'), and the nominal closed-loop system with the disturbance observer with  $Q_b(s)$  in the presence of the disturbance ('W/ DOB') when  $\tau = 0.01$ .

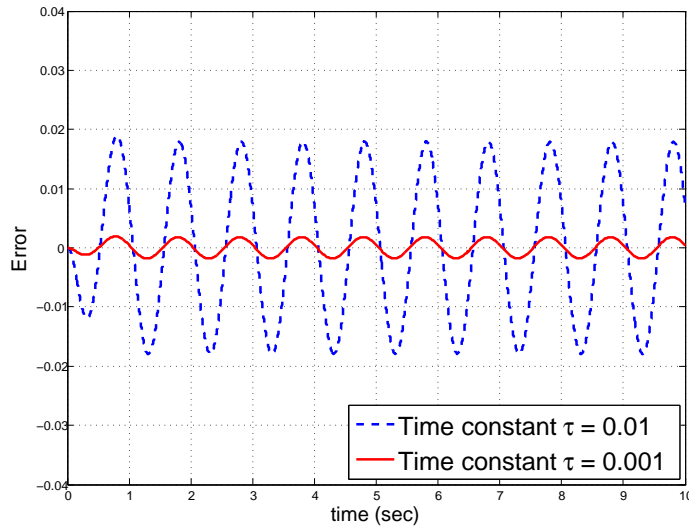


Figure 2.3: The error between the step response of the nominal closed-loop system and that of the actual closed-loop system with the disturbance observer with  $Q_b(s)$  for the time constant  $\tau = 0.01$  ('Time constant  $\tau = 0.01$ ') and  $\tau = 0.001$  ('Time constant  $\tau = 0.001$ ') when  $J = 1$  and  $B = 8$ .

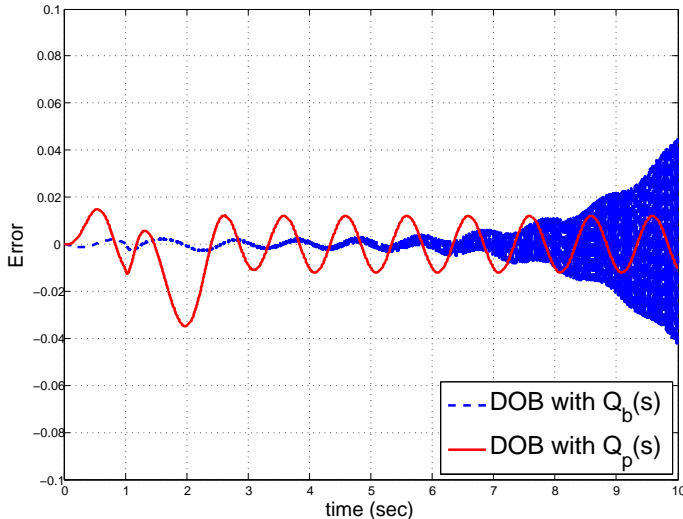


Figure 2.4: The error between the step response of the nominal closed-loop system and that of the actual closed-loop system with the disturbance observer with  $Q_b(s)$  ('DOB with  $Q_b(s)$ ') and  $Q_p(s)$  ('DOB with  $Q_p(s)$ ') when  $J = 0.1$  and  $B = 11.3$ .

that the difference between the output of the nominal closed-loop system and that of the actual closed-loop system becomes smaller (*i.e.*, the nominal performance is recovered) as  $\tau$  gets smaller [CYC<sup>+</sup>03, BS08]. More explicit relation between the nominal performance recovery and  $\tau$  will be discussed in Section 6.4.

Finally, the robust stability condition of Theorem 2.2.1 for the closed-loop system with the disturbance observer under parametric uncertainties is explored. To guarantee robust stability, we select the coefficients of Q-filter such that  $p_f(s)$  is Hurwitz for all  $g \in [1, 10]$ . Following Procedure 1, we select  $l = 3$ ,  $a_2 = 3$ , and  $a_1 = 3$  so that  $s^2 + a_2s + a_1$  is Hurwitz. Using the root-locus plot, we take  $\bar{\gamma}_0 = 9$  such that  $s(s^2 + a_2s + a_1) + \gamma_0$  is Hurwitz for all  $\gamma_0 \in (0, \bar{\gamma}_0)$ . Choose  $a_0 = 0.89 \in (0, (g_n/\bar{g})\bar{\gamma}_0)$ . Then, the proposed Q-filter is designed as

$$Q_p(s) = \frac{0.89}{(\tau s)^3 + 3(\tau s)^2 + 3(\tau s) + 0.89}.$$

From Fig. 2.4, when  $J = 0.1$  and  $B = 11.3$ , it can be seen that the closed-loop system with the disturbance observer with  $Q_b(s)$  becomes unstable since  $p_f(s)$  is not Hurwitz. It is remarked that the proposed disturbance observer with  $Q_p(s)$  works well because it is designed considering plant uncertainties.

# Chapter 3

## Embedding Internal Model in Disturbance Observer with Robust Stability

Design problems for disturbance rejection controllers are mainly classified into two types. Inspired by the internal model principle [Dav76, FW76], one approach is to design a controller so as to embed an internal model of disturbances into its structure and generate a corresponding input signal for compensating the disturbance when the disturbance is modeled as an output of a differential equation whose initial condition is unknown. Following this idea, asymptotic disturbance rejection has been achieved by output regulator [Isi95, Hua04], disturbance accommodation controller [Joh71], proportional integral observer [JWS00, SK10], and so on. Although the disturbance model is required, it has the benefit of exact cancellation of the disturbances in the steady state.

The other approach is to suppress the effect of disturbances, rather than asymptotically cancel them, so that the disturbance rejection is just approximate. One popular control method is based on the disturbance observer. Since the disturbance observer based control has a simple structure for implementation, while it has strong disturbance rejection ability, it has been widely applied in many applications. As discussed in Chapter 2, however, due to lack of disturbance model in the control loop, it rejects the disturbance approximately rather than asymptotically.

In many applications, the disturbance can be modeled such as step, ramp,

sinusoidal, and so on [Dav76]. When the disturbance model is known, based on the internal model principle, a disturbance observer, called 'high order disturbance observer', which can reject a polynomial-in-time type disturbance ( $d_0 + d_1t + \dots$ ) has been already developed [YKIH96, YKMH96, YKIH97, YKMH99, KMH00]. They impose certain restriction on the structure of Q-filter to embed the internal model. Although successful to embed the internal model and to derive a robust stability condition [YKMH99], the stability condition is restrictive in the sense that the plant uncertainty allowed is limited by the reciprocal of  $H_\infty$  norm of complementary sensitivity function, and the results are mainly for the second order systems. Moreover, as the order of disturbance observer (equivalently, the degree of the numerator of Q-filter) grows, this condition tends to be violated [YKIH96].

In this chapter, our concern is to enhance the disturbance rejection performance of the conventional disturbance observer by embedding the internal model assuming that the disturbance model is available. In particular, this chapter shows that the linear disturbance model can be embedded in the so-called Q-filter of the conventional disturbance observer structure, and moreover, the remaining design freedom of Q-filter can be used to robustly stabilize the closed-loop system that has uncertain parameters of arbitrarily large variation. As a result, the proposed disturbance observer based controller can reject not only approximately the unmodeled disturbances but also asymptotically the disturbances of sinusoidal or polynomial-in-time type. Details on the contributions of this chapter are listed below and the results are based on [PJSB12, JPBS14].

- A design method for the disturbance observer to embed the internal model including the sinusoidal as well as the polynomial-in-time type disturbance is proposed. It implies that the disturbance observer can reject not only the bounded low frequency disturbance approximately but also the modeled disturbance asymptotically.
- A modified almost necessary and sufficient robust stability condition is derived for the proposed disturbance observer. It is an extension of the previous result in Theorem 2.2.1 and deals with the case that the coefficients of

Q-filter are not only a constant but also a polynomial depending on a time constant of Q-filter. It is emphasized that the robust stability condition is almost necessary and sufficient, and the uncertain parameters of the plant are allowed to belong to an arbitrarily large (but bounded) compact set.

- A systematic design procedure for Q-filter to satisfy the robust stability condition is proposed. In order to develop the design procedure, we first construct an interval polynomial, which characterizes stability of the closed-loop system, from the coefficients of Q-filter and the bounds of plant uncertainties. Then, this polynomial reduces the robust stability problem as the selection of the coefficients of Q-filter to make the polynomial Hurwitz for all uncertain parameters. To solve this problem, we employ Kharitonov theorem [BCK95] and exploit the structure of the polynomial to show that appropriate coefficients can always be chosen step by step. It is remarked that, compared to previous result in Procedure 1, the proposed design procedure provide more flexibility since it does not restrict the degree of Q-filter.

### 3.1 Design Method for Embedding Internal Model of Disturbance

As discussed in Chapter 2, the disturbance observer can reject disturbances approximately. In fact, the effects of disturbances are reduced as the Q-filter's time constant  $\tau$  goes to zero [CYC<sup>+</sup>03, BS08] (It will be also discussed in Section 6.4). However, it may make the closed-loop system unstable in the presence of unmodeled dynamics [JJSS12, JJS14] and increase the effect of measurement noise [KK99, CYC<sup>+</sup>03]. Thus, in real applications, there are certain limitations on the disturbance rejection performance that can be achieved by reducing  $\tau$ .

While approximate rejection of disturbances might be the best when a model generating the disturbance is not known, let us now explore for exact rejection with knowledge of the disturbance model. The conceptual answer has already been given by the well-known internal model principle, e.g., in [FW76]. The actual question here is where and how to embed the internal model of disturbances in the



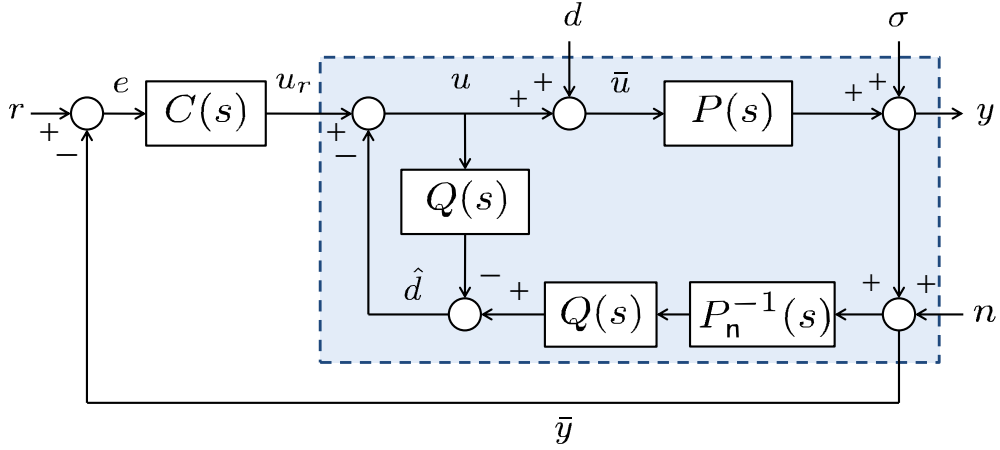


Figure 3.1: The closed-loop system with the disturbance observer structure (dotted-line block).

disturbance observer structure of Fig. 3.1. This embedding should preserve the conventional behavior of the disturbance observer such as approximate rejection of unmodeled low frequency disturbances, and should enable the selection of Q-filter such that the closed-loop system is robustly stable, which was the case discussed in Chapter 2.

In order to endow the disturbance observer with this ability, we consider the transfer functions  $T_{yd}(s)$  and  $T_{y\sigma}(s)$  in (2.1.3) which are transfer functions from the disturbances  $d$  and  $\sigma$  to the output  $y$ , respectively. We represent them as

$$\begin{aligned} T_{yd}(s) &= \frac{D_c(s)N(s)N_n(s)(D_q(s;\tau) - N_q(s;\tau))}{\delta(s;\tau)}, \\ T_{y\sigma}(s) &= \frac{D_c(s)D(s)N_n(s)(D_q(s;\tau) - N_q(s;\tau))}{\delta(s;\tau)} \end{aligned} \quad (3.1.1)$$

where

$$\delta(s;\tau) := N_n(DD_c + NN_c)D_q + N_qD_c(D_nN - DN_n). \quad (3.1.2)$$

Note that the polynomials regarding  $P$ ,  $P_n$ , and  $C$  are already given from the problem, and thus, we may need to embed the internal model utilizing two polynomials  $D_q$  and  $N_q$ . Since the effects of  $D_q$  and  $N_q$  on  $T_{yd}(s)$  and  $T_{y\sigma}(s)$  are the same, we can omit the detailed analysis of the output disturbance  $\sigma$  from now on.

Now, we make the following assumption for the disturbance.

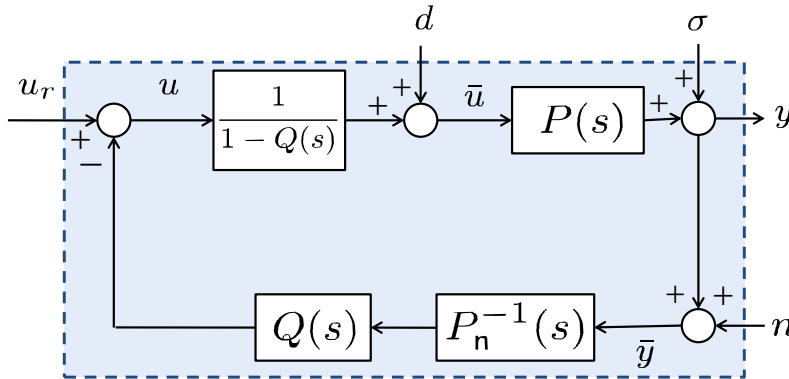


Figure 3.2: Equivalent block diagram of the DOB structure in Fig. 3.1.

**Assumption 3.1.1.** The input disturbance  $d(t)$  has the form<sup>1</sup> of

$$\begin{aligned} d(t) &= \bar{d}(t) + \sum_{i=0}^{k_t} d_i t^i + \sum_{j=1}^{k_s} \sigma_j \sin(\omega_j t + \phi_j) \\ &=: \bar{d}(t) + \tilde{d}(t) \end{aligned} \quad (3.1.3)$$

where  $k_t \geq 0$  and  $k_s \geq 1$  are known integers,  $d_i$ ,  $\sigma_j$ , and  $\phi_j$  are unknown constants while the frequencies  $\omega_j > 0$  are known such that  $\omega_j \neq \omega_{\bar{j}}$  for  $j \neq \bar{j}$ , and  $\bar{d}(t)$  is an unknown but bounded signal whose time derivative is also bounded.  $\square$

Laplace transform of the disturbance component  $\tilde{d}(t)$  has the form of  $\tilde{d}(s) = \sum_{i=0}^{k_t} d_i^*/s^{i+1} + \sum_{j=1}^{k_s} (\tilde{\sigma}_j s + \bar{\sigma}_j)/(s^2 + \omega_j^2)$  where  $d_i^*$ ,  $\tilde{\sigma}_j$ , and  $\bar{\sigma}_j$  are some constants. The observation with (2.1.3), (3.1.1), and (3.1.2) suggests that if we find the coefficients of  $D_q$  and  $N_q$  so that  $D_q - N_q$  contains  $s^{k_t+1} \prod_{j=1}^{k_s} (s^2 + \omega_j^2)$  and if the polynomial  $\delta(s; \tau)$  in (3.1.2) is Hurwitz, then the effect of disturbance  $\tilde{d}(t)$  is completely rejected from the response  $y(t)$  in the steady state. Note that this can also be viewed as the internal model principle [FW76]. In fact, an equivalent

<sup>1</sup>In general, the disturbance is considered as unknown system input including friction, torque ripple, modeling errors, and so on. However, in some applications, one can choose a suitable disturbance model when some information of disturbance is given [Joh71]. Therefore, it is possible to divide the disturbance into two parts: one part is an unknown but bounded low frequency disturbance and the other one is an output of a differential equation whose initial condition is unknown. Therefore, if the model of disturbance is given and the disturbance observer is designed to include the disturbance model, then the effects of modeled disturbance should be asymptotically reduced to zero, regardless of  $\tau$ , by the internal model principle.

block diagram of the disturbance observer is shown in Fig. 3.2. One can see that the rational function  $1/(s^{k_t+1}\prod_{j=1}^{k_s}(s^2 + \omega_j^2))$ , which is the internal model of  $\tilde{d}(t)$ , is embedded in the block  $1/(1 - Q) = D_q/(D_q - N_q)$ .

We now investigate how to design  $D_q$  and  $N_q$  to embed the internal model of disturbance. For this, it is sufficient to find the coefficients satisfying

$$D_q(s; \tau) - N_q(s; \tau) = s^{k_t+1}\prod_{i=1}^{k_s}(s^2 + \omega_i^2)R(s; \tau) \quad (3.1.4)$$

for some polynomial  $R(s; \tau)$ . Our design suggests to set  $\deg(N_q) = k = k_t + 2k_s$  and  $\deg(D_q) = l \geq k + \nu$ , where  $\deg(\cdot)$  implies the degree of the polynomial, and set

$$c_i = a_i, \quad i = 0, \dots, k_t. \quad (3.1.5)$$

By this,  $D_q - N_q$  now contains the factor  $s^{k_t+1}$ , and in order to contain  $\prod_{i=1}^{k_s}(s^2 + \omega_i^2)$ , we ask

$$\begin{aligned} (D_q - N_q)/(\tau s)^{k_t+1}|_{s=\pm j\omega_i} = \\ \left[ (\tau s)^{l-k_t-1} + a_{l-1}(\tau s)^{l-k_t-2} + \dots + a_{k_t+1} - c_k(\tau s)^{k-k_t-1} - \dots - c_{k_t+1} \right]_{s=\pm j\omega_i} = 0 \end{aligned}$$

for all  $i = 1, \dots, k_s$ . For convenience, let us suppose that  $l - k_t$  is even. Then, the above equation leads to the following two equations for real and imaginary parts, respectively:

$$\begin{aligned} a_{k_t+1} - a_{k_t+3}\tau^2\omega_i^2 + \dots + a_{l-1}(-\tau^2\omega_i^2)^{\frac{1}{2}(l-k_t-2)} \\ = c_{k_t+1} - c_{k_t+3}\tau^2\omega_i^2 + \dots + c_{k_t+2k_s-1}(-\tau^2\omega_i^2)^{k_s-1}, \end{aligned} \quad (3.1.6)$$

$$\begin{aligned} a_{k_t+2} - a_{k_t+4}\tau^2\omega_i^2 + \dots + (-\tau^2\omega_i^2)^{\frac{1}{2}(l-k_t-2)} \\ = c_{k_t+2} - c_{k_t+4}\tau^2\omega_i^2 + \dots + c_{k_t+2k_s}(-\tau^2\omega_i^2)^{k_s-1}, \end{aligned} \quad (3.1.7)$$

for all  $i = 1, \dots, k_s$ . If we introduce Vandermonde matrix given by

$$V_i := \begin{bmatrix} 1 & (-\tau^2\omega_1^2)^1 & \dots & (-\tau^2\omega_1^2)^i \\ \vdots & \vdots & & \vdots \\ 1 & (-\tau^2\omega_{k_s}^2)^1 & \dots & (-\tau^2\omega_{k_s}^2)^i \end{bmatrix} \in \mathbb{R}^{k_s \times (i+1)},$$

the equations (3.1.6) and (3.1.7) can be rewritten compactly as

$$\begin{aligned} V_{k_s-1}[c_{k_t+1}, \dots, c_{k_t+2k_s-1}]^T &= V_{\frac{1}{2}(l-k_t-2)} A_{\text{Re}}, \\ V_{k_s-1}[c_{k_t+2}, \dots, c_{k_t+2k_s}]^T &= V_{\frac{1}{2}(l-k_t-2)} A_{\text{Im}} \end{aligned}$$

where  $A_{\text{Re}} = [a_{k_t+1}, \dots, a_{l-1}]^T \in \mathbb{R}^{(l-k_t)/2}$  and  $A_{\text{Im}} = [a_{k_t+2}, \dots, a_{l-2}, 1]^T \in \mathbb{R}^{(l-k_t)/2}$ . Note that  $V_{k_s-1}$  is a square matrix of size  $k_s \times k_s$ , and is nonsingular because  $\det V_{k_s-1} = \prod_{1 \leq i < j \leq k_s} \tau^2(\omega_i^2 - \omega_j^2) \neq 0$  by the assumption that  $\omega_i \neq \omega_j$  for  $i \neq j$  [HJ85]. As a result, the coefficients  $c_i$  for  $i = k_t + 1, \dots, k$  are obtained as a function of  $a_i$ 's (and  $\tau$  as well). The following theorem presents a summary, also with the case when  $l - k_t$  is odd.

**Theorem 3.1.1.** Under Assumption 3.1.1, the closed-loop system of Fig. 3.1 rejects the modeled disturbance  $\tilde{d}(t)$  asymptotically if, for any given  $a_i$ ,  $i = 0, \dots, l - 1$  (where  $l \geq k + \nu$ ), and  $\tau > 0$ , the coefficients  $c_i$ ,  $i = 0, \dots, k$  with  $k = k_t + 2k_s$ , are designed as (3.1.5) and

$$\begin{aligned} [c_{k_t+1}, c_{k_t+3}, \dots, c_{k-1}]^T &= V_{k_s-1}^{-1} V_{\frac{1}{2}(l-k_t-2+k^*)} A_{\text{Re}} \\ [c_{k_t+2}, c_{k_t+4}, \dots, c_k]^T &= V_{k_s-1}^{-1} V_{\frac{1}{2}(l-k_t-2-k^*)} A_{\text{Im}} \end{aligned}$$

where

- when  $l - k_t$  is even ( $k^* = 0$ )

$$\begin{aligned} A_{\text{Re}} &= [a_{k_t+1}, a_{k_t+3}, \dots, a_{l-1}]^T \in \mathbb{R}^{(l-k_t+k^*)/2} \\ A_{\text{Im}} &= [a_{k_t+2}, a_{k_t+4}, \dots, a_{l-2}, 1]^T \in \mathbb{R}^{(l-k_t-k^*)/2} \end{aligned}$$

- when  $l - k_t$  is odd ( $k^* = 1$ )

$$\begin{aligned} A_{\text{Re}} &= [a_{k_t+1}, a_{k_t+3}, \dots, a_{l-2}, 1]^T \in \mathbb{R}^{(l-k_t+k^*)/2} \\ A_{\text{Im}} &= [a_{k_t+2}, a_{k_t+4}, \dots, a_{l-1}]^T \in \mathbb{R}^{(l-k_t-k^*)/2} \end{aligned}$$

and if  $\delta(s; \tau)$  in (3.1.2) is Hurwitz.  $\square$

**Remark 3.1.1.** The closed-loop system with the proposed disturbance observer also rejects the unmodeled disturbance  $\bar{d}(t)$  approximately in the low frequency range, which is determined as the range where  $Q(j\omega) \approx 1$ . This range becomes larger as  $\tau$  gets smaller.  $\square$

**Remark 3.1.2.** When  $\sigma_j = 0$  for  $j = 1, \dots, k_s$  (i.e., the sinusoidal disturbance does not exist in (3.1.3)), by Theorem 3.1.1, the Q-filter is designed as

$$Q(s) = \frac{a_k(\tau s)^k + \dots + a_0}{(\tau s)^l + a_{l-1}(\tau s)^{l-1} + \dots + a_1(\tau s) + a_0}. \quad (3.1.8)$$

Then, with the structure of Q-filter (3.1.8) and the equivalent block diagram of the disturbance observer shown in Fig. 3.2, one can easily see that the block  $1/(1-Q)$  contains  $k+1$  integrators, which implies that the disturbance observer structure has the internal model so that the disturbance of the type  $d_0 + d_1 t + \dots + d_k t^k$  can be exactly rejected. We call a disturbance observer with (3.1.8) as ‘type-k disturbance observer’. For more details, see [PJSB12].  $\square$

After embedding the disturbance model, we still have some freedom of choosing  $a_i$ ’s and  $\tau$ . This freedom will be utilized in the next section in order to robustly stabilize the closed-loop system (i.e., to make  $\delta(s; \tau)$  Hurwitz) in spite of the uncertainty of the plant  $P(s)$ . Here we note that, by the selection of Theorem 3.1.1, the coefficient  $c_i$  is in fact a function of  $a_i$ ’s and  $\tau$ , and the Q-filter of (2.1.2) now becomes

$$Q(s) = \frac{c_k(\tau)(\tau s)^k + \dots + c_{k_t+1}(\tau)(\tau s)^{k_t+1} + c_{k_t}(\tau s)^{k_t} + \dots + c_0}{(\tau s)^l + a_{l-1}(\tau s)^{l-1} + \dots + a_1(\tau s) + a_0} \quad (3.1.9)$$

in which, we explicitly treat  $c_i$  for  $i = k_t+1, \dots, k$  as a function of  $\tau$ . In particular, the following lemma plays a key role in the next section.

**Lemma 3.1.2.** The functions  $c_i(\tau)$ ,  $i = k_t+1, \dots, k$ , obtained from Theorem 3.1.1, are of the form

$$c_i(\tau) = a_i + \tau^2 \tilde{c}_i(\tau) \quad (3.1.10)$$

where  $\tilde{c}_i(\tau)$  is a polynomial of  $\tau$ .  $\square$

*Proof.* The matrix that appears in Theorem 3.1.1 has the form of  $V_{k_s-1}^{-1}V_{\hat{k}} \in \mathbb{R}^{k_s \times (\hat{k}+1)}$  where  $\hat{k} \geq k_s - 1$ . If  $\hat{k} = k_s - 1$ , the assertion follows with  $\tilde{c}_i(\tau) = 0$ . For the case where  $\hat{k} > k_s - 1$ , we decompose  $V_{\hat{k}}$  as  $V_{\hat{k}} = \begin{bmatrix} V_{k_s-1} & \hat{V} \end{bmatrix}$ . Note that the first  $k_s$  columns of  $V_{\hat{k}}$  are the same as those of  $V_{k_s-1}$  by construction and that  $V_{k_s-1}$  can be rewritten as  $V_{k_s-1} = W \text{diag}\{1, \tau^2, \dots, (\tau^2)^{k_s-1}\}$  where  $W = V_{k_s-1}|_{\tau=1}$ . The matrix  $\hat{V}$  can also be represented by  $\hat{V} = \hat{W} \text{diag}\{(\tau^2)^{k_s}, \dots, (\tau^2)^{\hat{k}}\}$  where  $\hat{W} \in \mathbb{R}^{k_s \times (\hat{k}-k_s+1)}$  is a matrix independent of  $\tau$ . Therefore,  $V_{k_s-1}^{-1}V_{\hat{k}} = \begin{bmatrix} I & V_{k_s-1}^{-1}\hat{V} \end{bmatrix}$  where  $V_{k_s-1}^{-1}\hat{V}$  is given by

$$\text{diag}\left\{1, \frac{1}{\tau^2}, \dots, \frac{1}{(\tau^2)^{k_s-1}}\right\} W^{-1}\hat{W} \text{diag}\left\{(\tau^2)^{k_s}, \dots, (\tau^2)^{\hat{k}}\right\},$$

from which one deduces that each component of  $V_{k_s-1}^{-1}\hat{V}$  is a monomial of  $\tau$  whose degree is at least 2.  $\square$

So far, we discuss the performance of the disturbance observer for rejecting the effect of the unmodeled disturbance  $\bar{d}(t)$  approximately with respect to  $\tau$  as well as the modeled disturbance  $\tilde{d}(t)$  asymptotically by the internal model in the Q-filter. However, also note that the above analysis is only valid when the closed-loop system is internally stable under plant uncertainties.

## 3.2 Design of Q-filter for Guranteeing Robust Stability

We now present how to design  $a_i$ 's and  $\tau$  so that the closed-loop system remains stable (i.e.,  $\delta(s; \tau)$  is Hurwitz) for arbitrarily large uncertainty of the plant  $P(s)$  satisfying Assumption 2.1.1. For this, we first derive robust stability condition using the tools developed in [SJ09].

### 3.2.1 Robust Stability Condition of Closed-loop System

A robust stability condition for the disturbance observer already introduced in Theorem 2.2.1. However, differently from the coefficients  $c_i$  of Q-filter in (2.1.2), those in (3.1.9) considered in this chapter are not constants but polynomials depending on  $\tau$  as discussed in Lemma 3.1.2. Therefore, we propose a modified robust stability condition for the proposed disturbance observer.

As discussed in Chapter 2, the closed-loop system is said to be robustly internally stable if and only if  $\delta(s; \tau)$  is Hurwitz for all  $P(s) \in \mathcal{P}$ . To present a robust stability condition, we define a polynomial  $p_f^*(s)$  given by

$$p_f^*(s) = s^l + a_{l-1}s^{l-1} + \cdots + a_{k+1}s^{k+1} + \frac{g}{g_n}a_k s^k + \cdots + \frac{g}{g_n}a_1 s + \frac{g}{g_n}a_0 \quad (3.2.1)$$

The following result presents a condition which ensures robust stability of the closed-loop system.

**Theorem 3.2.1.** Under Assumptions 2.1.1 and 3.1.1, suppose that the following conditions hold.

1.  $C(s)$  internally stabilizes  $P_n(s)$ ,
2.  $a_i$ 's are chosen such that  $p_f^*(s)$  is Hurwitz for all  $P(s) \in \mathcal{P}$ .

Then, there exists a constant  $\bar{\tau} > 0$  such that, for all  $0 < \tau \leq \bar{\tau}$ , the Q-filter 3.1.9 with  $c_i$ 's given by Theorem 3.1.1 guarantees that the closed-loop system is robustly internally stable and that the effect of disturbance component  $\tilde{d}$  is completely removed in the steady state.  $\square$

*Proof.* We follow the techniques developed in [SJ09, Lemma 2 and Theorem 3] keeping in mind that  $c_i = a_i + \tau^2 \tilde{c}_i(\tau)$  where  $\tilde{c}_i(\tau)$  is a polynomial of  $\tau$  (by Lemma 3.1.2).

Let  $p_s^*(s) = N(s)(D_c(s)D_n(s) + N_c(s)N_n(s))$ , whose roots are either the poles of  $P_n C / (1 + P_n C)$  and the zeros of  $P$ , and let  $m = \deg(p_s^*(s)) = \deg(D_c D_n N)$ . By Assumption 2.1.1 and Condition 1, the polynomial  $p_s^*(s)$  is Hurwitz.

Since  $\deg(\delta(s; \tau)) = l + m$ , we need to inspect all  $l + m$  roots of  $\delta(s; \tau)$ . This is a difficult task in general, but it turns out that, as  $\tau \rightarrow 0$ , the  $m$  roots tend to the roots of  $\delta(s; 0)$ , whose degree is  $m$ , and the other  $l$  roots tend to infinity [Lemma A.2 in Appendix]. In fact,  $\delta(s; 0) = a_0 p_s^*(s)$  (by the fact  $N_q(s; 0) = D_q(s; 0) = a_0$ ), and thus, those  $m$  roots are stable for sufficiently small  $\tau > 0$ .

Now, in order to see the behavior of remaining  $l$  roots that tend to infinity as  $\tau \rightarrow 0$ , let us define  $\bar{\delta}(s; \tau) := \tau^m \delta(s/\tau; \tau) = \gamma_1(s; \tau) D_q(s/\tau; \tau) + N_q(s/\tau; \tau) \gamma_2(s; \tau)$  where  $\gamma_1(s; \tau) = \tau^m (D D_c N_n(s/\tau) + N N_c N_n(s/\tau))$  and  $\gamma_2(s; \tau)$

$= \tau^m(D_c D_n N(s/\tau) - D_c D N_n(s/\tau))$ . Because  $m = \deg(D_c D_n N) = \deg(DD_c N_n) > \deg(NN_c N_n)$ , it follows that  $\gamma_1(s; 0)$  and  $\gamma_2(s; 0)$  are well-defined and that  $\lim_{\tau \rightarrow 0} \gamma_1(s; \tau) = \lim_{\tau \rightarrow 0} \tau^m DD_c N_n(s/\tau) = \bar{\gamma}_1 s^m$  and  $\lim_{\tau \rightarrow 0} \gamma_2(s; \tau) = \bar{\gamma}_2 s^m$  for all  $s$  with some constants  $\bar{\gamma}_1 \neq 0$  and  $\bar{\gamma}_2$ . Note that  $\gamma_1(s; \tau)$  and  $\gamma_2(s; \tau)$  are well-defined and continuous for all  $\tau$ . On the other hand, by Lemma 3.1.2, the polynomial  $N_q(s; \tau)$  can be decomposed as  $N_q(s; \tau) = \bar{N}_q(s; \tau) + \tilde{N}_q(s; \tau)$  where  $\bar{N}_q(s; \tau) = a_k(\tau s)^k + \dots + a_1(\tau s) + a_0$  and  $\tilde{N}_q(s; \tau) = \tau^2 \tilde{c}_k(\tau)(\tau s)^k + \dots + \tau^2 \tilde{c}_{k_t+1}(\tau)(\tau s)^{k_t+1}$ . Note that  $\bar{N}_q(s/\tau; \tau) = \bar{N}_q(s; 1)$  (and similarly  $D_q(s/\tau; \tau) = D_q(s; 1)$ ). Also, note that  $\lim_{\tau \rightarrow 0} \tilde{N}_q(s/\tau; \tau) = \tilde{N}_q(s/\tau; \tau)|_{\tau=0} = 0$ .

Putting together, it is seen that, for all  $\tau \geq 0$ , the polynomial  $\bar{\delta}(s; \tau)$  has the degree  $l + m$  and is continuous, and

$$\bar{\delta}(s; 0) = \bar{\gamma}_1 s^m \left( D_q(s; 1) + \frac{\bar{\gamma}_2}{\bar{\gamma}_1} \bar{N}_q(s; 1) \right).$$

Since

$$\frac{\bar{\gamma}_2}{\bar{\gamma}_1} = \frac{\lim_{\tau \rightarrow 0} \tau^m (D_c D_n N(s/\tau) - D_c D N_n(s/\tau))}{\lim_{\tau \rightarrow 0} \tau^m DD_c N_n(s/\tau)} = \lim_{s \rightarrow \infty} \frac{ND_n(s)}{N_n D(s)} - 1 = \frac{g}{g_n} - 1,$$

it is seen that  $\bar{\delta}(s; 0) = \bar{\gamma}_1 s^m p_f^*(s)$ . Let  $s_1^*, \dots, s_l^*$  be the roots of  $p_f^*(s)$ . We note that the  $l + m$  roots of  $\bar{\delta}(s; \tau)$  converge to  $l + m$  roots of  $\bar{\delta}(s; 0)$  as  $\tau$  tends to zero. Since a root  $\bar{s}(\tau)$  of  $\bar{\delta}(s; \tau)$  corresponds to the root  $\bar{s}(\tau)/\tau$  of  $\delta(s; \tau)$ , it is seen that

1. those  $l$  roots of  $\delta(s; \tau)$  going to infinity as  $\tau \rightarrow 0$ , say  $s_i(\tau)$ ,  $i = 1, \dots, l$ , correspond to  $\bar{s}_i(\tau)/\tau$  where  $\bar{s}_i(\tau)$  converges to  $s_i^*$ , respectively,
2. those  $m$  roots of  $\delta(s, \tau)$  that remain finite as  $\tau \rightarrow 0$  correspond to  $\bar{s}_i(\tau)/\tau$  where  $\bar{s}_i(\tau)$  converges to the origin for  $i = 1, \dots, m$ .

Since  $p_f^*(s)$  is Hurwitz from the condition 2, all  $l + m$  roots of  $\delta(s; \tau)$  are found in  $\mathbb{C}^-$  for sufficiently small  $\tau > 0$ . This completes the first part of proof.

The second part the theorem follows from Theorem 3.1.1 and the internal stability of the closed-loop system.  $\square$

**Remark 3.2.1.** The conditions in Theorem 3.2.1 are also necessary for robust



stability in some sense. See Section 2.2 for details.  $\square$

**Remark 3.2.2.** Although the robust stability condition of Theorem 3.2.1 resembles that of Theorem 2.2.1, the latter is on the case where the coefficients  $a_i$ 's and  $c_i$ 's of Q-filter are constant numbers while the former allows  $c_i$ 's to be functions of  $\tau$ . Moreover, Theorem 3.2.1 provides a condition with which the possibility of asymptotic rejection of modeled disturbance as well as robust stability can be checked while that of Theorem 2.2.1 is only for robust stability.  $\square$

**Remark 3.2.3.** The design parameters of disturbance observer are  $a_i$ 's,  $c_i$ 's, and  $\tau$  of Q-filter. Since  $p_f^*(s)$  involves only  $a_i$ 's, one can design these parameters first considering plant uncertainties, and then choose  $c_i$ 's for disturbance rejection by following Theorem 3.1.1. Finally, the parameter  $\tau$  is chosen sufficiently small. This shows that the proposed controller is designed in a systematic way. In fact, the design is fully constructive since the parameters  $a_i$ 's can be also chosen iteratively (see Section 3.2.2).  $\square$

### 3.2.2 Selecting $a_i$ 's for Robust Stability

This section presents a constructive design procedure for the coefficients  $a_i$ 's to satisfy the condition 2 in Theorem 3.2.1 (equivalently, to make the polynomial in (3.2.1) become Hurwitz for all  $g \in [\underline{g}, \bar{g}]$ ). The proposed design procedure is derived by Lemma A. 3 and Remark A. 5.

With unknown  $g \in [\underline{g}, \bar{g}]$  and its nominal value  $g_n$ , we define, for  $j = 0, 1, \dots, k$ ,

$$\begin{aligned} p_j(s; g) := & s^{l-k+j} + a_{l-1}s^{l-k-1+j} + \dots \\ & + a_{k+1}s^{1+j} + \frac{g}{g_n}(a_k s^j + \dots + a_{k-j}). \end{aligned} \quad (3.2.2)$$

Note that  $p_{j+1}(s; g) = s p_j(s; g) + (g/g_n)a_{k-j-1}$  and  $p_k(s; g) = p_f^*(s)$ . Associated with  $p_j(s; g)$ , we define the set of interval polynomials

$$\begin{aligned} \mathcal{I}_j := & \{s^{l-k+j} + \dots + a_{k+1}s^{1+j} + \gamma_k s^j + \dots + \gamma_{k-j} : \\ & \gamma_i \in [(g/g_n)a_i, (\bar{g}/g_n)a_i], i = k-j, \dots, k\}. \end{aligned}$$

The four extreme polynomials for  $\mathcal{I}_j$ , in view of Remark A. 5, are denoted by  $\bar{p}_{j,1}(s), \dots, \bar{p}_{j,4}(s)$ .

We now describe the proposed design procedure of  $a_i$  for  $p_f^*(s)$  to be Hurwitz for all  $g \in [g, \bar{g}]$ . It is a recursive procedure and *Step 0* is the initialization step.

**Procedure 2. Q-filter Design Procedure for Robust Stability**

*Step 0:* Choose the order of Q-filter  $l \geq \nu + k$  and the coefficients  $a_{l-1}, a_{l-2}, \dots, a_{k+1}$  such that the polynomial  $s^{l-k-1} + a_{l-1}s^{l-k-2} + \dots + a_{k+1}$  is Hurwitz.

Then, find a  $\bar{\gamma}_k > 0$  such that  $s^{l-k} + a_{l-1}s^{l-k-1} + \dots + a_{k+1}s + \gamma_k$  is Hurwitz for all  $\gamma_k \in (0, \bar{\gamma}_k)$  and choose  $a_k \in (0, (g_n/\bar{g})\bar{\gamma}_k)$ .

*Step j* ( $j = 1, \dots, k$ ): With the coefficients  $a_{l-1}, a_{l-2}, \dots, a_{k-j+1}$  obtained from the previous steps, construct  $\bar{p}_{j-1,1}(s), \dots, \bar{p}_{j-1,4}(s)$  of  $\mathcal{I}_{j-1}$ . For each  $i = 1, \dots, 4$ , find  $\bar{\gamma}_{k-j,i} > 0$  such that

$$s\bar{p}_{j-1,i}(s) + \gamma_{k-j,i}$$

is Hurwitz for all  $\gamma_{k-j,i} \in (0, \bar{\gamma}_{k-j,i})$ , and let  $\bar{\gamma}_{k-j} := \min_i \bar{\gamma}_{k-j,i}$ . Choose  $a_{k-j} \in (0, (g_n/\bar{g})\bar{\gamma}_{k-j})$ .  $\square$

It is emphasized that each step requires at most four extreme polynomials, and the number of polynomials to be checked does not increase as the step proceeds.

**Remark 3.2.4.** With Procedure 2, one obtains the coefficients  $a_0, \dots, a_{l-1}$ , which determine the denominator of Q-filter. The numerator is left as an additional degree of freedom for other performances. For example, it can be determined for complete rejection of some modeled disturbance as discussed in Section 3.1.  $\square$

**Theorem 3.2.2.** Under Assumption 1, the coefficients  $a_{l-1}, \dots, a_0$  obtained via Procedure 2 ensure that the polynomial  $p_f^*(s)$  of (3.2.1) is Hurwitz for all  $g \in [g, \bar{g}]$ .  $\square$

*Proof.* Since  $p_f^*(s) = p_k(s; g)$ , we prove the assertion by induction for the index  $j$  of  $p_j(s; g)$  given by (3.2.2).

After Step 0 of Procedure 2, we obtain  $a_{l-1}, \dots, a_{k+1}$ , and  $a_k$  such that the polynomial  $s^{l-k} + a_{l-1}s^{l-k-1} + \dots + a_{k+1}s + (g/g_n)a_k$  is Hurwitz for all  $g \in [g, \bar{g}]$

(The existence of  $a_k$  is guaranteed by Lemma A. 3.). This means that  $p_0(s; g)$  is Hurwitz for all  $g \in [g, \bar{g}]$ .

As the induction hypothesis, we assume that  $p_{j-1}(s; g)$  is Hurwitz for all  $g \in [g, \bar{g}]$ . To complete the proof, we consider *Step j* in Procedure 2. With  $a_{l-1}, \dots, a_{k-(j-1)}$  obtained up to *Step j-1*, construct  $\mathcal{I}_{j-1}$  and  $\bar{p}_{j-1,1}(s), \dots, \bar{p}_{j-1,4}(s)$ . Then, Lemma A. 3 ensures that for each  $i = 1, \dots, 4$ , there exists  $\bar{\gamma}_{k-j,i} > 0$  such that  $s\bar{p}_{j-1,i}(s) + \gamma_{k-j,i}$  is Hurwitz for all  $\gamma_{k-j,i} \in (0, \bar{\gamma}_{k-j,i})$ . Let  $\bar{\gamma}_{k-j} = \min_i \bar{\gamma}_{k-j,i}$  and choose  $a_{k-j}$  such that  $0 < a_{k-j} < (g_n/\bar{g})\bar{\gamma}_{k-j}$ . This results in that, for each  $i = 1, \dots, 4$ ,  $s\bar{p}_{j-1,i}(s) + (g/g_n)a_{k-j}$  is Hurwitz for all  $g \in [g, \bar{g}]$ . Since these polynomials are all Hurwitz, it follows from Remark A. 5 that  $p_j(s; g)$  is Hurwitz for all  $g \in [g, \bar{g}]$ . The induction completes when  $j = k$ , and the polynomial  $p_k(s; g)$  is the same as  $p_f^*(s)$ , which completes the proof.  $\square$

### 3.3 Illustrative Example

We apply the proposed disturbance observer to a practical example to evaluate the disturbance rejection performance and robustness against parameter uncertainties.

**Example 3.3.1.** Consider a mechanical positioning system for the X-Y table driven by a linear motor [YKMH99]. An actual plant  $P(s)$  and its nominal model  $P_n(s)$  are given by

$$P(s) = \frac{1}{Js^2 + Bs}, \quad P_n(s) = \frac{1}{J_n s^2 + B_n s}$$

where  $J$  and  $B$  are the mass of the table with load variation and the viscous friction coefficient and  $J_n$  and  $B_n$  are nominal values of  $J$  and  $B$ , respectively. Let  $J \in [1, 6]$ ,  $B = 80$ ,  $J_n = 1$ , and  $B_n = 80$ . For tracking control, a simple proportional control of gain  $K_p$  is employed for the outer-loop controller  $C(s)$ . It is assumed that the disturbance  $\tilde{d}(t) = \sigma_1 \sin(\omega_1 t + \phi_1)$ .

Now, we design a Q-filter to embed the internal model of disturbance. We choose  $k_s = 1$  and  $k_t = 0$  so  $k = 2$ , and, since the relative degree  $\nu$  of the plant is 2, we let  $l = 4 \geq k + \nu$ . Then, by Theorem 3.1.1, the coefficients  $c_i$ 's are

determined as  $c_0 = a_0$ ,  $c_1 = a_1 - a_3(\tau\omega_1)^2$ , and  $c_2 = a_2 - (\tau\omega_1)^2$ . By Procedure 2, we can choose the coefficients  $a_i$ 's such that the polynomial  $p_f^*(s)$  of (3.2.1) is Hurwitz for all  $g \in [g, \bar{g}]$  where  $\underline{g} = 1/6$ ,  $\bar{g} = 1$ , and  $g_n = 1$ .

*Step 0:* Pick  $a_3 = 4$  so that  $s + a_3$  is Hurwitz. Since the polynomial  $s^2 + a_3s + \gamma_2$  is Hurwitz for all  $\gamma_2 > 0$ , we choose  $a_2 = 6$ .

*Step 1:* The four extreme polynomials of  $p_0(s; g)$  yield two different ones  $\bar{p}_{0,1}(s)$  and  $\bar{p}_{0,3}(s)$  as

$$\bar{p}_{0,1} = s^2 + a_3s + \frac{\bar{g}}{g_n}a_2, \quad \bar{p}_{0,3}(s) = s^2 + a_3s + \frac{g}{g_n}a_2.$$

Using the root-locus plot, we take  $\bar{\gamma}_{1,1} = 24$  and  $\bar{\gamma}_{1,3} = 3.83$  such that  $s\bar{p}_{0,j}(s) + \gamma_{1,j}$  is Hurwitz for all  $\gamma_{1,j} \in (0, \bar{\gamma}_{1,j})$ . Let  $\bar{\gamma}_1 = \min\{\bar{\gamma}_{1,1}, \bar{\gamma}_{1,3}\}$  and choose  $a_1 = 3.8 \in (0, (g_n/\bar{g})\bar{\gamma}_1)$ .

*Step 2:* The four extreme polynomials of  $p_1(s; g)$  are given by

$$\begin{aligned} \bar{p}_{1,1}(s) &= s^3 + a_3s^2 + \frac{\bar{g}}{g_n}a_2s + \frac{\bar{g}}{g_n}a_1, \\ \bar{p}_{1,2}(s) &= s^3 + a_3s^2 + \frac{\bar{g}}{g_n}a_2s + \frac{g}{g_n}a_1, \\ \bar{p}_{1,3}(s) &= s^3 + a_3s^2 + \frac{g}{g_n}a_2s + \frac{g}{g_n}a_1, \\ \bar{p}_{1,4}(s) &= s^3 + a_3s^2 + \frac{g}{g_n}a_2s + \frac{\bar{g}}{g_n}a_1. \end{aligned}$$

By the same procedure as *Step 1*, we take  $a_0 = 0.04$ .

With the coefficients obtained above, the Q-filter is designed as

$$Q_p(s) = \frac{\{6 - (\tau\omega_1)^2\}(\tau s)^2 + \{3.8 - 4(\tau\omega_1)^2\}(\tau s) + 0.04}{(\tau s)^4 + 4(\tau s)^3 + 6(\tau s)^2 + 3.8(\tau s) + 0.04}.$$

Now, for comparison, we consider another Q-filter whose coefficients are binomial coefficients (that is often employed in the literature such as [CYC<sup>+</sup>03]):

$$Q_b(s) = \frac{6(\tau s)^2 + 4(\tau s) + 1}{(\tau s)^4 + 4(\tau s)^3 + 6(\tau s)^2 + 4(\tau s) + 1}.$$

It is designed to have the same order and relative degree as  $Q_p(s)$  for fair comparison since the disturbance rejection performance tends to improve as the degree

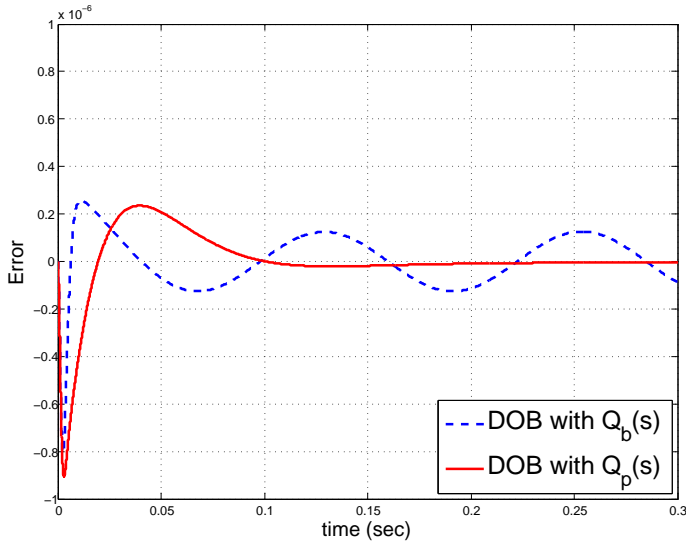


Figure 3.3: The error between the step response of the nominal closed-loop system and that of the actual closed-loop system with the disturbance observer with  $Q_b(s)$  ('DOB with  $Q_b(s)$ ') and  $Q_p(s)$  ('DOB with  $Q_p(s)$ ') when  $J = 1$ .

of the numerator of Q-filter grows (with the same  $\tau$ ) [CYC<sup>+</sup>03]. In addition, simulations are performed with  $J = 1$  and 4.2 to observe the effect of parameter uncertainties. Detailed parameters are as follows:  $\sigma_1 = 1$ ,  $\omega_1 = 2\pi \cdot 8$ ,  $K_p = 2500$ ,  $\phi_1 = 0.5\pi$ , and  $\tau = 0.001$ .

Fig. 3.3 and 3.4 show the error between the step response of the nominal closed-loop system and that of the actual closed-loop system with the disturbance observer with the Q-filter  $Q_b(s)$  having the binomial coefficients and the proposed Q-filter  $Q_p(s)$ . Here, the step response of the nominal closed-loop system means that of  $P_n C / (1 + P_n C)$  without the disturbance. As seen in Fig. 3.3, the disturbance observer with  $Q_p(s)$  completely rejects the effect of disturbance in the steady state, while the one with  $Q_b(s)$  approximately. From Fig. 3.4, it is observed that the closed-loop system with  $Q_b(s)$  is unstable when  $J = 4.2$ . It implies that large plant uncertainties can deteriorate the stability of the closed-loop system with the disturbance observer when it is designed without considering uncertainties. We remark that the proposed disturbance observer works well since it is designed by the proposed systematic procedure considering plant uncertainties.

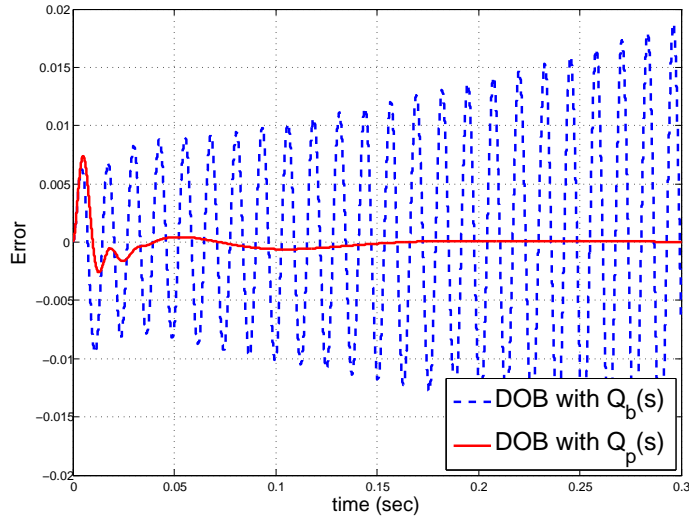


Figure 3.4: The error between the step response of the nominal closed-loop system and that of the actual closed-loop system with the disturbance observer with  $Q_b(s)$  ('DOB with  $Q_b(s)$ ') and  $Q_p(s)$  ('DOB with  $Q_p(s)$ ') when  $J = 4.2$ .

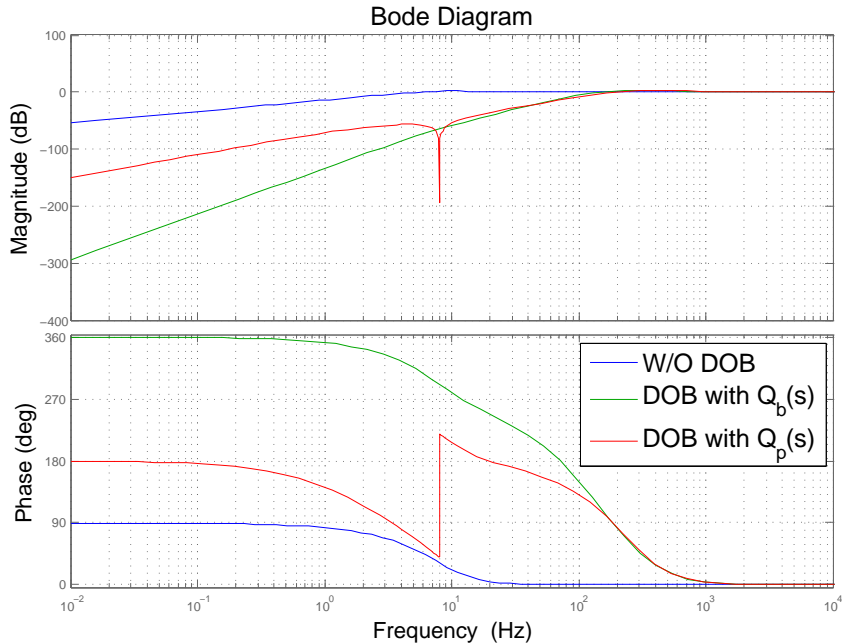


Figure 3.5: Bode diagrams of sensitivity functions without the disturbance observer ('W/O DOB') and with the disturbance observer with  $Q_b(s)$  ('DOB with  $Q_b(s)$ ') and  $Q_p(s)$  ('DOB with  $Q_p(s)$ ') when  $J = 1$ .

The performance of the disturbance observer with  $Q_b(s)$  and  $Q_p(s)$  can be also analyzed in view of the sensitivity function<sup>2</sup> as shown in Fig. 3.5. In the low frequency range, the disturbance rejection performance is improved by both disturbance observers with  $Q_b(s)$  and  $Q_p(s)$ . Especially, in the target frequency (8 Hz), the magnitude of the sensitivity function of the disturbance observer with  $Q_p(s)$  becomes much smaller than that with  $Q_b(s)$  due to the internal model in the disturbance observer structure. On the other hand, the disturbance rejection performance of the disturbance observer with  $Q_b(s)$  is better than that with  $Q_p(s)$  in other frequency ranges since it contains three integrators in  $1/(1 - Q_b(s))$  block as shown in Fig. 3.2. More discussions on the sensitivity function analysis will be provided in the next section.

### 3.4 Discussions on Robustness

In this section, we discuss the robustness of the proposed design procedure 2. In the following subsection, the pros and cons of the proposed Q-filter design procedure is more investigated. And then, the robustness is discussed based on the bode plot approach.

#### 3.4.1 Pros and Cons of Proposed Design Procedure

At each step of the proposed design procedure 2, Kharitonov theorem is employed to guarantee the Hurwitz stability of the interval polynomial  $p_j(s; g)$  for all variation of  $g$ . In fact, Kharitonov theorem provides a necessary and sufficient condition for Hurwitz stability of a family of the interval polynomial when the polynomial coefficients vary independently. However, the coefficients of  $p_j(s; g)$  vary interdependently according to the variation of  $g$ . In other word, if the four extreme polynomials of  $p_j(s; g)$  are Hurwitz, then  $p_j(s; g)$  is Hurwitz. But, the

---

<sup>2</sup>The loop transfer function  $L(s)$  and the sensitivity function  $S(s)$  of the disturbance observer based control system are computed as

$$L(s) = \frac{P(s)(P_n(s)C(s) + Q(s))}{P_n(s)(1 - Q(s))}, \quad S(s) = \frac{P_n(s)(1 - Q(s))}{Q(s)(P(s) - P_n(s)) + P_n(s)(1 + P(s)C(s))}.$$

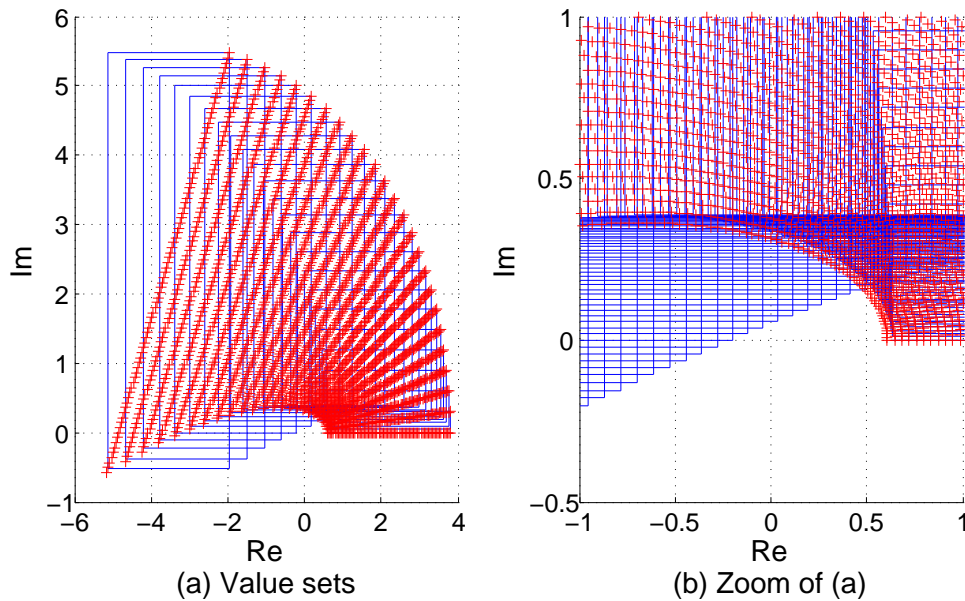


Figure 3.6: The value sets of the four extreme polynomials of  $p_1(s; g)$  ('blue solid line') and  $p_1(s; g)$  ('red plus signs') for each  $\omega \geq 0$ .

converse may not be true. This relationship can be easily understood in view of the value set approach [Definition A. 6 in Appendix].

Recall step 1 of the design procedure in Example 3.3.1. The coefficient  $a_1$  is selected such that the four extreme polynomials of  $p_1(s; g)$  are Hurwitz (*i.e.*,  $p_1(s; g)$  is Hurwitz). Fig. 3.6 shows the value sets of four extreme polynomials  $p_1(s; g)$  and  $p_1(s; g)$  for all  $g \in [g, \bar{g}]$ . By the zero exclusion theorem [Lemma A. 7 in Appendix], both cases are Hurwitz stable since the value sets do not contain the origin. However, the distance between the origin and the value set of four extreme polynomials of  $p_1(s; g)$  is smaller than that of  $p_1(s; g)$ . It implies that the proposed design procedure 2 is conservative in the sense that one might select a small  $a_{k-j}$  such that the four extreme polynomials of  $p_j(s; g)$  be Hurwitz even though the selection of larger  $a_{k-j}$  might be possible. As a result, as the step proceeds, the selected  $a_{k-j}$  becomes smaller although the proposed design procedure provides a systematic method for selecting  $a_{k-j}$ .



### 3.4.2 Bode Diagram Approach

In this section, the robustness of the proposed Q-filter design procedure is investigated in view of the bode diagram approach. For Example 3.3.1, we design the Q-filters with the binomial coefficients ( $Q_{type-1}^b(s)$ ,  $Q_{type-2}^b(s)$ ,  $Q_{type-3}^b(s)$ ,  $Q_{IM}^b(s)$ , and  $Q_{type-4}^b(s)$ ) and the Q-filters by the proposed design procedure ( $Q_{type-1}^p(s)$ ,  $Q_{type-2}^p(s)$ ,  $Q_{type-3}^p(s)$ ,  $Q_{IM}^p(s)$ , and  $Q_{type-4}^p(s)$ ) as follows:

$$\begin{aligned}
Q_{type-1}^b(s) &= \frac{1}{(\tau s)^2 + 2(\tau s) + 1}, & Q_{type-2}^b(s) &= \frac{3(\tau s) + 1}{(\tau s)^3 + 3(\tau s)^2 + 3(\tau s) + 1}, \\
Q_{type-3}^b(s) &= \frac{6(\tau s)^2 + 4(\tau s) + 1}{(\tau s)^4 + 4(\tau s)^3 + 6(\tau s)^2 + 4(\tau s) + 1}, \\
Q_{IM}^b(s) &= \frac{\{6 - (\tau\omega_1)^2\}(\tau s)^2 + \{4 - 4(\tau\omega_1)^2\}(\tau s) + 1}{(\tau s)^4 + 4(\tau s)^3 + 6(\tau s)^2 + 4(\tau s) + 1}, \\
Q_{type-4}^b(s) &= \frac{10(\tau s)^3 + 10(\tau s)^2 + 5(\tau s) + 1}{(\tau s)^5 + 5(\tau s)^4 + 10(\tau s)^3 + 10(\tau s)^2 + 5(\tau s) + 1}, \\
Q_{type-1}^p(s) &= \frac{6}{(\tau s)^2 + 4(\tau s) + 6}, & Q_{type-2}^p(s) &= \frac{6(\tau s) + 3.8}{(\tau s)^3 + 4(\tau s)^2 + 6(\tau s) + 3.8}, \\
Q_{type-3}^p(s) &= \frac{6(\tau s)^2 + 3.8(\tau s) + 0.04}{(\tau s)^4 + 4(\tau s)^3 + 6(\tau s)^2 + 3.8(\tau s) + 0.04}, \\
Q_{IM}^p(s) &= \frac{\{6 - (\tau\omega_1)^2\}(\tau s)^2 + \{3.8 - 4(\tau\omega_1)^2\}(\tau s) + 0.04}{(\tau s)^4 + 4(\tau s)^3 + 6(\tau s)^2 + 3.8(\tau s) + 0.04}, \\
Q_{type-4}^p(s) &= \frac{6(\tau s)^3 + 3.8(\tau s)^2 + 0.04(\tau s) + 0.0006}{(\tau s)^5 + 4(\tau s)^4 + 6(\tau s)^3 + 3.8(\tau s)^2 + 0.04(\tau s) + 0.0006}.
\end{aligned}$$

Fig. 3.7 and 3.8 show the bode diagrams of sensitivity functions and loop transfer functions with Q-filters having the binomial coefficients, respectively. The phase margins by  $Q_{type-1}^b(s)$ ,  $Q_{type-2}^b(s)$ ,  $Q_{type-3}^b(s)$ ,  $Q_{IM}^b(s)$ , and  $Q_{type-4}^b(s)$  are 75.8 deg, 53 deg, 43.5 deg, 43.5 deg, and 38.3 deg, respectively. It implies that, as the order of Q-filter with the binomial coefficients increases, the robustness decreases. On the other hand, Fig. 3.9 and 3.10 show the bode diagrams of sensitivity functions and loop transfer functions with Q-filters by the proposed design procedure, respectively. The phase margins by  $Q_{type-1}^p(s)$ ,  $Q_{type-2}^p(s)$ ,  $Q_{type-3}^p(s)$ ,  $Q_{IM}^p(s)$ , and  $Q_{type-4}^p(s)$  are 70.5 deg, 46.5 deg, 46.5 deg, 46.5 deg, and 46.5 deg, respectively. Thus, the robustness is preserved even though the order of Q-filter by the proposed design procedure increases.

One might think that the above results are not implementable since the control bandwidth of the nominal closed-loop system is much smaller than those of the disturbance observer based control systems. Fig. 3.11 and 3.12 show the bode diagrams of sensitivity functions and loop transfer functions with Q-filters by the proposed design procedure, respectively. In this case, the control bandwidth of the disturbance observer based control systems are designed to be similar to that of the nominal closed-loop system. The phase margins of the nominal closed-loop system and the closed-loop system with  $Q_{type-1}^p(s)$ ,  $Q_{type-2}^p(s)$ ,  $Q_{type-3}^p(s)$ ,  $Q_{IM}^p(s)$ , and  $Q_{type-4}^p(s)$  are 69.9 deg, 49.1 deg, 46.6 deg, 46.6 deg, 48.1 deg, and 46.6 deg, respectively. It means that the robustness is also preserved although the order of the Q-filter is increased. This phenomenon is explained by the bode diagram of each Q-filter as shown in 3.13 and 3.14. As the order of the Q-filter increases, the cut-off frequency and magnitude of each Q-filter designed by the proposed design procedure do not increase even though those of each Q-filter with the binomial coefficients increase. (For more details, see [KK99].)

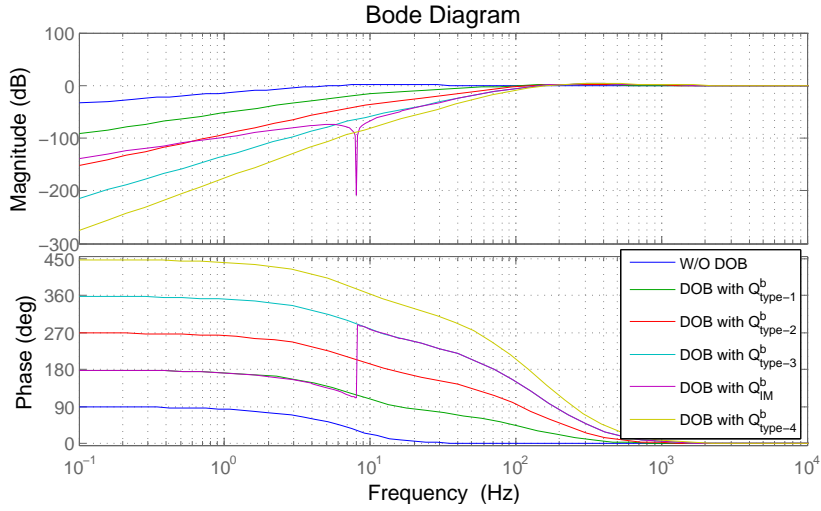


Figure 3.7: Bode diagrams of sensitivity functions without the disturbance observer ('W/O DOB') and with the disturbance observer with  $Q_{type-1}^b(s)$  ('DOB with  $Q_{type-1}^b(s)$ '),  $Q_{type-2}^b(s)$  ('DOB with  $Q_{type-2}^b(s)$ '),  $Q_{type-3}^b(s)$  ('DOB with  $Q_{type-3}^b(s)$ '),  $Q_{IM}^b(s)$  ('DOB with  $Q_{IM}^b(s)$ '), and  $Q_{type-4}^b(s)$  ('DOB with  $Q_{type-4}^b(s)$ ') when  $\tau = 0.001$  and  $\omega_1 = 8 \times 2\pi$ .

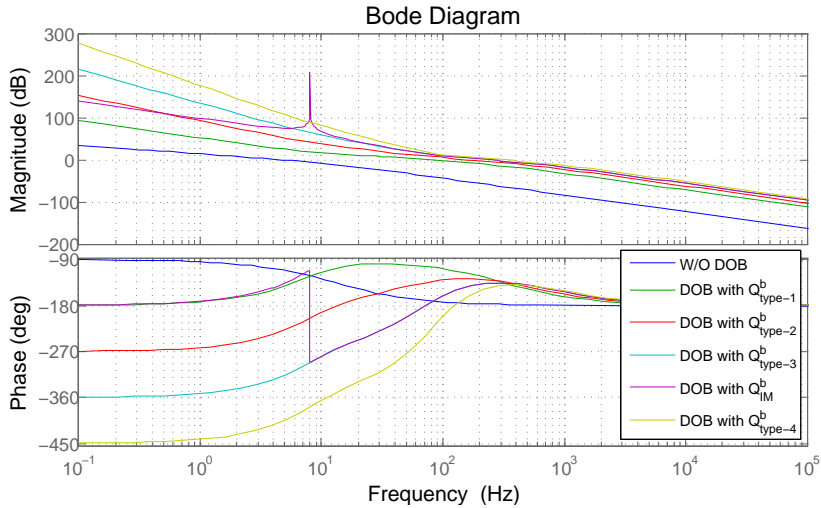


Figure 3.8: Bode diagrams of loop transfer functions without the disturbance observer ('W/O DOB') and with the disturbance observer with  $Q_{type-1}^b(s)$  ('DOB with  $Q_{type-1}^b(s)$ '),  $Q_{type-2}^b(s)$  ('DOB with  $Q_{type-2}^b(s)$ '),  $Q_{type-3}^b(s)$  ('DOB with  $Q_{type-3}^b(s)$ '),  $Q_{IM}^b(s)$  ('DOB with  $Q_{IM}^b(s)$ '), and  $Q_{type-4}^b(s)$  ('DOB with  $Q_{type-4}^b(s)$ ') when  $\tau = 0.001$  and  $\omega_1 = 8 \times 2\pi$ .

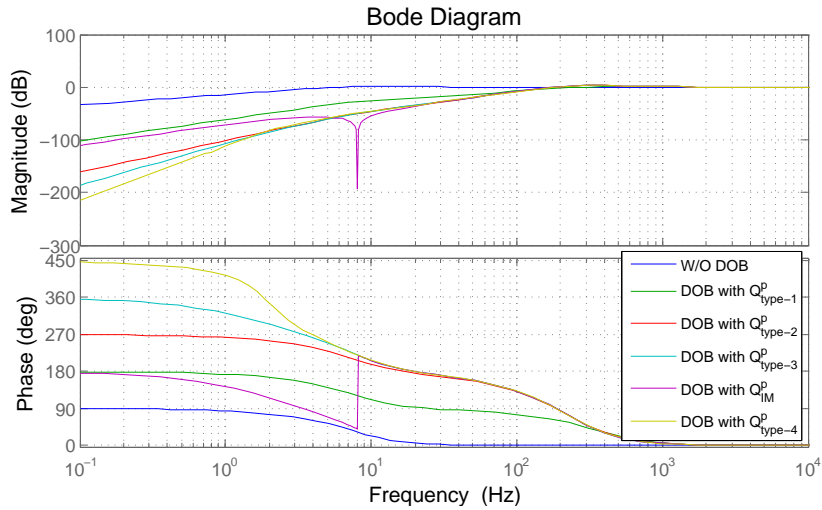


Figure 3.9: Bode diagrams of sensitivity functions without the disturbance observer ('W/O DOB') and with the disturbance observer with  $Q_{type-1}^p(s)$  ('DOB with  $Q_{type-1}^p(s)$ '),  $Q_{type-2}^p(s)$  ('DOB with  $Q_{type-2}^p(s)$ '),  $Q_{type-3}^p(s)$  ('DOB with  $Q_{type-3}^p(s)$ '),  $Q_{IM}^p(s)$  ('DOB with  $Q_{IM}^p(s)$ '), and  $Q_{type-4}^p(s)$  ('DOB with  $Q_{type-4}^p(s)$ ') when  $\tau = 0.001$  and  $\omega_1 = 8 \times 2\pi$ .

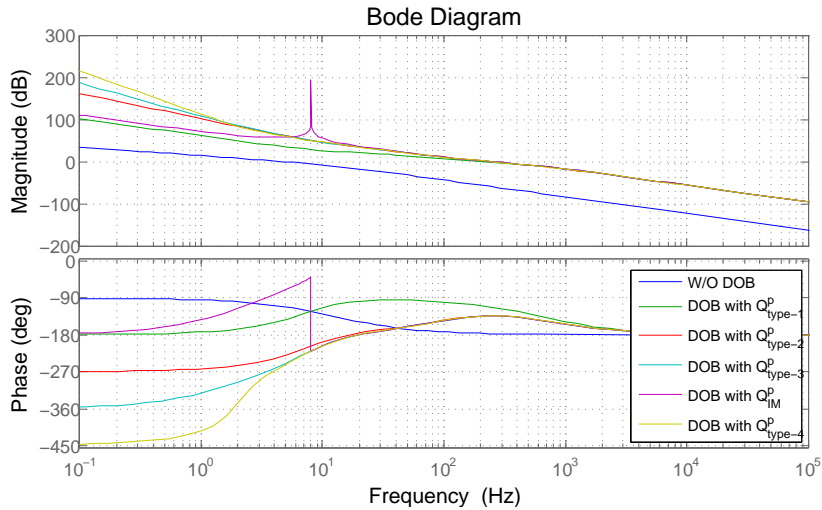


Figure 3.10: Bode diagrams of loop transfer functions without the disturbance observer ('W/O DOB') and with the disturbance observer with  $Q_{type-1}^p(s)$  ('DOB with  $Q_{type-1}^p(s)$ '),  $Q_{type-2}^p(s)$  ('DOB with  $Q_{type-2}^p(s)$ '),  $Q_{type-3}^p(s)$  ('DOB with  $Q_{type-3}^p(s)$ '),  $Q_{IM}^p(s)$  ('DOB with  $Q_{IM}^p(s)$ '), and  $Q_{type-4}^p(s)$  ('DOB with  $Q_{type-4}^p(s)$ ') when  $\tau = 0.001$  and  $\omega_1 = 8 \times 2\pi$ .

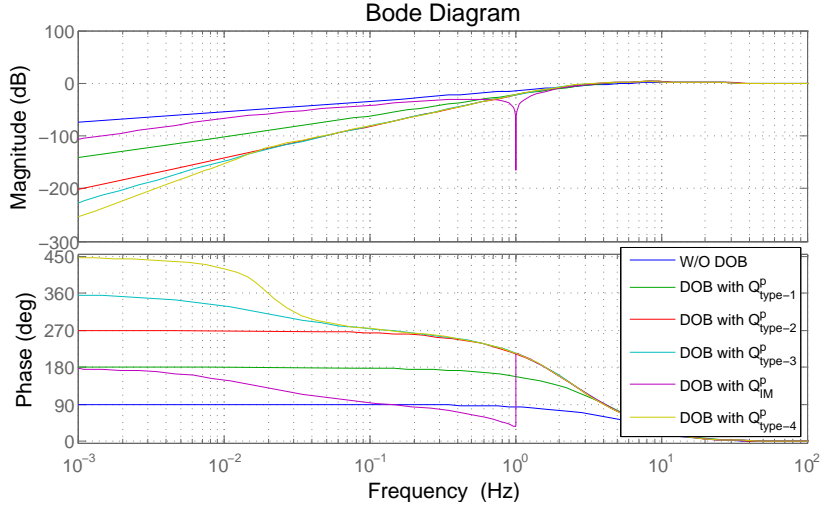


Figure 3.11: Bode diagrams of sensitivity functions without the disturbance observer ('W/O DOB') and with the disturbance observer with  $Q_{type-1}^p(s)$  ('DOB with  $Q_{type-1}^p(s)$ '),  $Q_{type-2}^p(s)$  ('DOB with  $Q_{type-2}^p(s)$ '),  $Q_{type-3}^p(s)$  ('DOB with  $Q_{type-3}^p(s)$ '),  $Q_{IM}^p(s)$  ('DOB with  $Q_{IM}^p(s)$ '), and  $Q_{type-4}^p(s)$  ('DOB with  $Q_{type-4}^p(s)$ ') when  $\tau = 0.1$  and  $\omega_1 = 2\pi$ .

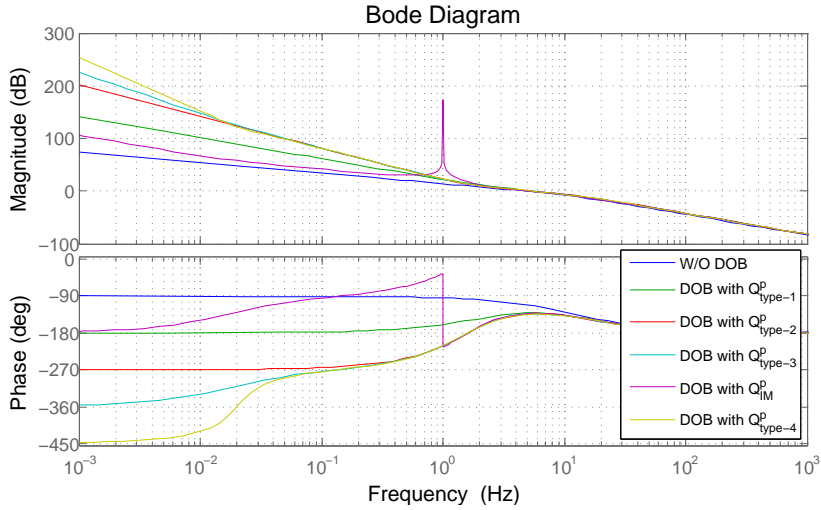


Figure 3.12: Bode diagrams of loop transfer functions without the disturbance observer ('W/O DOB') and with the disturbance observer with  $Q_{type-1}^p(s)$  ('DOB with  $Q_{type-1}^p(s)$ '),  $Q_{type-2}^p(s)$  ('DOB with  $Q_{type-2}^p(s)$ '),  $Q_{type-3}^p(s)$  ('DOB with  $Q_{type-3}^p(s)$ '),  $Q_{IM}^p(s)$  ('DOB with  $Q_{IM}^p(s)$ '), and  $Q_{type-4}^p(s)$  ('DOB with  $Q_{type-4}^p(s)$ ') when  $\tau = 0.1$  and  $\omega_1 = 2\pi$ .

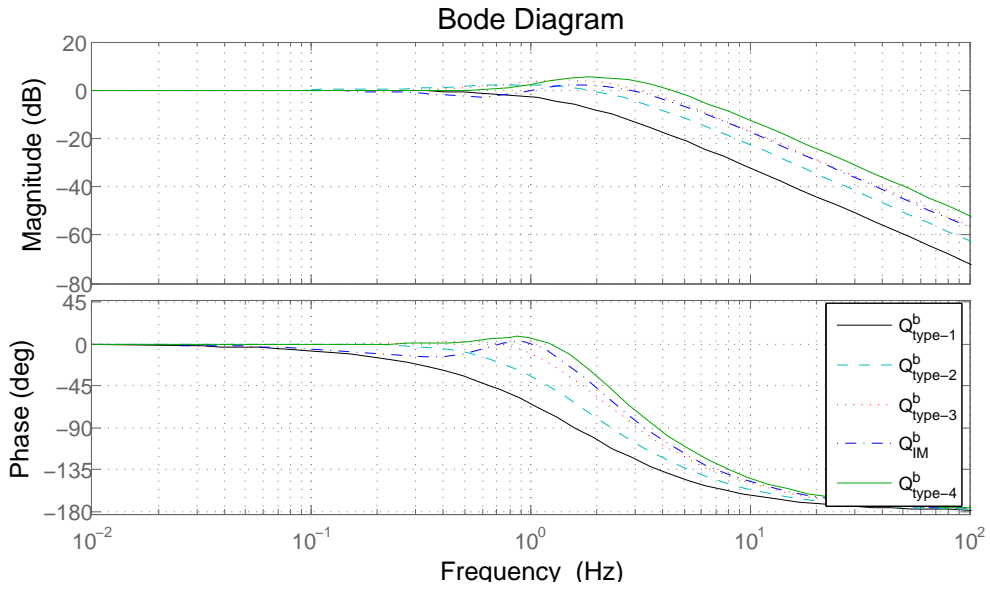


Figure 3.13: Bode diagrams of  $Q_{type-1}^b(s)$ ,  $Q_{type-2}^b(s)$ ,  $Q_{type-3}^b(s)$ ,  $Q_{IM}^b(s)$ , and  $Q_{type-4}^b(s)$  when  $\tau = 0.1$  and  $\omega_1 = 2\pi$ .

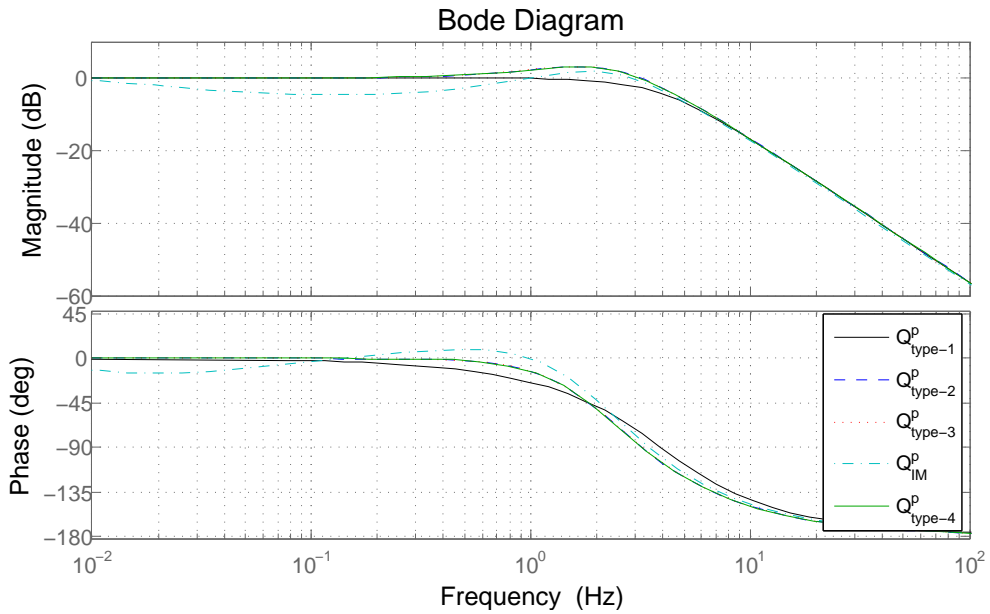


Figure 3.14: Bode diagrams of  $Q_{type-1}^p(s)$ ,  $Q_{type-2}^p(s)$ ,  $Q_{type-3}^p(s)$ ,  $Q_{IM}^p(s)$ , and  $Q_{type-4}^p(s)$  when  $\tau = 0.1$  and  $\omega_1 = 2\pi$ .



# Chapter 4

## Disturbance Observer with Unknown Relative Degree of the Plant

The disturbance observer based controller has been widely used among control engineers since it has a powerful ability of uncertainty compensation and disturbance attenuation. However, this property holds only when the disturbance observer based control system is stable. Therefore, the important question of interest is the robust stability of the closed-loop system under the uncertainty of the plant.

As shown in Chapter 2 and 3, an almost necessary and sufficient stability condition was presented when the time constant of Q-filter is sufficiently small in accordance with the performance enhancement. Under the assumption that actual uncertain plant  $P$  be of minimum phase, it has been shown that, for any given nominal model  $P_n$ , the disturbance observer based control system can be robustly stabilized with an appropriate choice of the Q-filter. However, it is not applicable to the case where the relative degree of real plant is not the same as that of the nominal model.

In this chapter, we study the robust stability of the disturbance observer based control system when the relative degree of plant is not exactly known and so it happens to be different from that of nominal model. This case often occurs in real world control applications. For instance,  $r.deg(P) > r.deg(P_n)$ <sup>1</sup> when the actuator dynamics is ignored, or when there is unmodeled dynamics for the plant.

---

<sup>1</sup> $r.deg(P)$  stands for the relative degree of the transfer function  $P$ .



Although some related work has been presented in [JJS11], it is limited to the case where the relative degree of  $P_n$  is equal to one and the Q-filter is given by the first order system. Inspired by the fact that the characteristic equation for stability is of the form that appears in the ‘higher-order root locus technique’ [Hah81], conditions for robust stability are derived by utilizing the Newton diagram for general cases. Under the standing assumption that the time constant of Q-filter is sufficiently small, the derived conditions reveal a few facts such as:

- if  $r.deg(P) = r.deg(P_n) + 1$ , the robust stability can be achieved by an appropriate design of  $P_n$  as well as  $Q$ , which is contrast to the case where  $r.deg(P) = r.deg(P_n)$  in Chapter 2 (where the selection of  $P_n$  does not matter).
- if  $1 \leq r.deg(P) \leq 2$ , then the robust stability is always achievable.
- if  $r.deg(P) \geq r.deg(P_n) + 2$  or  $r.deg(P_n) > r.deg(P) > 2$ , then the robust stabilization is not possible with sufficiently small  $\tau$  no matter how  $P_n$ ,  $C$ , and  $Q$  are selected.
- a universal design of the disturbance observer can be achieved for the special case where  $r.deg(P)$  is unknown but  $1 \leq r.deg(P) \leq 4$ .

In summary, the lesson of this chapter is that one needs to estimate the relative degree of the plant as close as possible, because, if not, the robust stability may not be achievable with sufficiently small time constant of Q-filter.

## 4.1 Robust Stability

The standard disturbance observer control system is illustrated in Fig. 4.1. In this figure,  $P(s)$  and  $P_n(s)$  represent the uncertain plant and its nominal model, respectively, and signals  $r$ ,  $d$ , and  $n$  represent the reference input, input disturbance and measurement noise, respectively. The controller  $C(s)$  is designed *a priori* using the nominal model  $P_n(s)$  only (The design of  $C(s)$  does not require the information of  $P(s)$ ). The transfer function  $Q(s)$  (called as ‘Q-filter’) is a

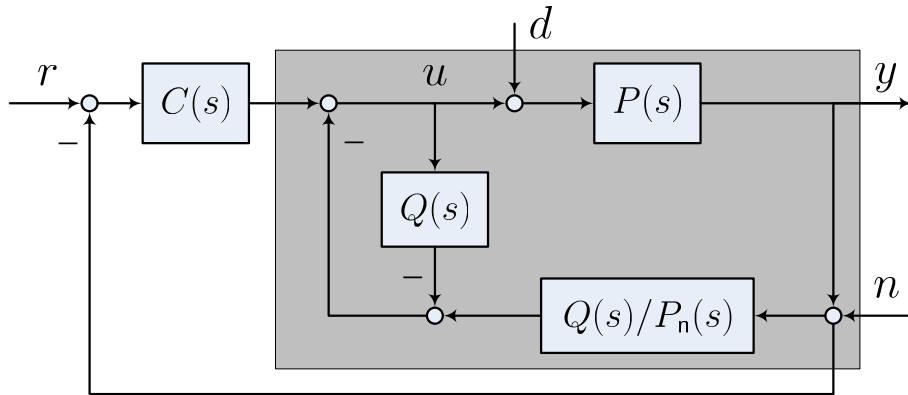


Figure 4.1: Structure of the disturbance observer control system. The shaded region represents the real plant  $P(s)$  augmented with the disturbance observer

stable low pass filter, which usually has the form of

$$Q(s) = \frac{c_k(\tau s)^k + c_{k-1}(\tau s)^{k-1} + \cdots + c_0}{a_l(\tau s)^l + a_{l-1}(\tau s)^{l-1} + \cdots + a_1(\tau s) + a_0} \quad (4.1.1)$$

where  $\tau > 0$  is the filter time constant, and  $k$  and  $l$  are nonnegative integers. Assume that  $c_0 = a_0$  for the unity DC gain and  $l \geq k + r.\text{deg}(P_n)$  to make the transfer function  $Q(s)P_n^{-1}(s)$  proper.

As discussed in Chapter 2, the disturbance observer recovers the nominal performance in the presence of the disturbances and model uncertainties. However, this property is only maintained when the closed-loop system is stable. In this chapter, we will investigate the robust stability of the disturbance observer based control system when  $r.\text{deg}(P) \neq r.\text{deg}(P_n)$ . We assume that  $P(s)$  and  $P_n(s)$  are strictly proper while  $C(s)$  is at least proper. Let us also represent each transfer function  $P$ ,  $P_n$ ,  $C$ , and  $Q$  as the ratios of coprime polynomials:  $P(s) = N(s)/D(s)$ ,  $P_n(s) = N_n(s)/D_n(s)$ ,  $C(s) = N_c(s)/D_c(s)$ , and  $Q(s) = N_Q(s;\tau)/D_Q(s;\tau)$  (in which, the dependence of  $N_Q$  and  $D_Q$  on  $\tau$  is explicitly indicated). Then, it has been shown in Chapter 2 that, for given  $\tau > 0$ , the closed-loop system is internally stable if and only if the characteristic polynomial

$$\delta(s; \tau) := (DD_c + NN_c)N_nD_Q + N_QD_c(ND_n - N_nD) \quad (4.1.2)$$

is Hurwitz. Define

$$p_\alpha(s) := N(N_c N_n + D_c D_n), \quad p_\beta(s) = N_n(N_c N + D_c D) \quad (4.1.3)$$

and let  $m_\alpha := \deg(N D_c D_n)$ ,  $m_\beta := \deg(N_n D_c D)$ , and  $\alpha_i, \beta_i$  be such that

$$\begin{aligned} p_\alpha(s) &= \alpha_{m_\alpha} s^{m_\alpha} + \alpha_{m_\alpha-1} s^{m_\alpha-1} + \cdots + \alpha_0, \\ p_\beta(s) &= \beta_{m_\beta} s^{m_\beta} + \beta_{m_\beta-1} s^{m_\beta-1} + \cdots + \beta_0. \end{aligned} \quad (4.1.4)$$

It should be kept in mind that  $m_\beta - m_\alpha = r.\deg(P) - r.\deg(P_n)$ , and that  $\beta_{m_\beta}/\alpha_{m_\alpha}$  is the ratio of the high frequency gains of  $P(s)$  and  $P_n(s)$ . Let  $\bar{k}$  be such that  $a_0 = c_0, \dots, a_{\bar{k}} = b_{\bar{k}}$  and  $a_{\bar{k}+1} \neq c_{\bar{k}+1}$ , or  $\bar{k} = k$ . Then, it follows that (with  $a_l = 1$  for convenience)

$$\begin{aligned} \delta(s; \tau) &= p_\beta(s) D_Q(s; \tau) + (p_\alpha(s) - p_\beta(s)) N_Q(s; \tau) \\ &= p_\beta(s) \sum_{i=0}^l a_i (\tau s)^i + (p_\alpha(s) - p_\beta(s)) \sum_{i=0}^k b_i (\tau s)^i \\ &= \sum_{i=0}^{\bar{k}} (\tau s)^i a_i p_\alpha(s) \\ &\quad + \sum_{i=\bar{k}+1}^k (\tau s)^i (a_i p_\beta(s) + c_i (p_\alpha(s) - p_\beta(s))) + \sum_{i=k+1}^l (\tau s)^i a_i p_\beta(s). \end{aligned} \quad (4.1.5)$$

Note that  $\deg(\delta(s; \tau)) = l + m_\beta$  if  $\tau > 0$ , and the locations of  $l + m_\beta$  roots, when  $\tau$  is sufficiently small, are of interest because they determine the stability of the closed-loop system. Since  $\delta(s; 0) = a_0 p_\alpha(s)$  and  $\deg(\delta(s; 0)) = m_\alpha$ , it is clear that  $m_\alpha$  roots out of  $l + m_\beta$  roots of  $\delta(s; \tau)$  converge to the roots of  $p_\alpha(s)$  as  $\tau \rightarrow 0$ , while the remaining  $l + m_\beta - m_\alpha$  roots tend to infinity (see [SJ09] for more rigorous arguments).

Here, we recall Theorem 2.2.1 in the viewpoint of the coefficients  $\alpha_i$  and  $\beta_i$ , with the set  $\mathcal{P}$  being a collection of transfer functions whose coefficients belong to certain (known) bounded intervals.

**Theorem 4.1.1.** Suppose that  $r.\deg(P_n) = r.\deg(P)$  and their high frequency gains have the same sign. Then, there exists a constant  $\bar{\tau} > 0$  such that, for

all  $0 < \tau \leq \bar{\tau}$ , the closed-loop system is internally stable if the following three conditions hold:

H1.  $P(s)$  is of minimum phase for all  $P(s) \in \mathcal{P}$ ,

H2.  $P_n C / (1 + P_n C)$  is stable, and

H3. the polynomial

$$p_f(s) := \beta_{m_\beta} \{a_l s^l + a_{l-1} s^{l-1} + \cdots + a_{k+1} s^{k+1} + (a_k - c_k) s^k + \cdots + (a_1 - c_1) s\} \\ + \alpha_{m_\alpha} \{c_k s^k + \cdots + c_1 s + a_0\}$$

is Hurwitz.

On the contrary, there is  $\bar{\tau} > 0$  such that, for all  $0 < \tau \leq \bar{\tau}$ , the closed-loop system is unstable if at least one of the conditions H1–H3 is violated in the sense that,  $P_n C / (1 + P_n C)$  has some poles in  $\mathbb{C}^+$ , or some zeros of  $P(s)$  or some roots of  $p_f = 0$  are located in  $\mathbb{C}^+$ .  $\square$

*Proof.* The conditions H1–H3 are the same as those of Theorem 2.2.1 although the condition H3 is derived using a different method with respect to (4.1.4). Hence, the proof is the same as that of Theorem 2.2.1 and omitted.  $\square$

**Remark 4.1.1.** It is observed that the conditions H1 and H2 are equivalent to  $p_\alpha(s)$  being Hurwitz (see (4.1.3)), so that  $m_\alpha$  roots of  $\delta(s; \tau)$  have negative real parts for sufficiently small  $\tau$ . On the other hand, the condition H3 constrains the other  $l + m_\beta - m_\alpha = l$  (since  $m_\beta = m_\alpha$  if  $r.\deg(P) = r.\deg(P_n)$ ) roots to remain in  $\mathbb{C}^-$ .  $\square$

Theorem 4.1.1 indicates that robust stabilization can be achieved against uncertain parameters, provided that  $C(s)$  stabilizes the nominal model  $P_n(s)$ , and uncertain plant is of minimum phase. Note that the selection of  $P_n(s)$  is not crucial for the robust stabilization provided that  $r.\deg(P_n) = r.\deg(P)$ .

Although Theorem 4.1.1 presents an almost necessary and sufficient condition for stability according to Remark 2.2.1, it is not useful when  $r.\deg(P) \neq r.\deg(P_n)$ . If  $\lim_{s \rightarrow \infty} (P(s)/P_n(s)) = 0$ , which occurs when the relative degree of  $P_n(s)$  is less

than that of  $P(s)$ , then  $p_f(s) = D_Q(s; 1) - N_Q(s; 1)$  has a root at the origin since  $c_0 = a_0$ . For such a case, some stability condition was derived in [JJS11] under the assumption that  $r.deg(P_n) = 1$  and the Q-filter is of the form  $Q(s) = a_0/(a_1\tau s + a_0)$ . However, this is too restrictive to be used in real applications. Furthermore, the polynomial  $p_f(s)$  is not defined when  $r.deg(P) < r.deg(P_n)$ .

When  $r.deg(P) \neq r.deg(P_n)$ , the  $l + m_\beta - m_\alpha$  roots of  $\delta(s; \tau)$ , that go to infinity as  $\tau \rightarrow 0$ , are of particular interest. In order to observe their behavior conveniently, we want to make them go to zero as  $\tau \rightarrow 0$ . This is done by defining  $\bar{\delta}(s; \tau) := s^{l+m_\beta}\delta(1/s; \tau)$ . Then,<sup>2</sup>

$$\bar{\delta}(s; \tau) = \bar{q}_0(s) + \tau\bar{q}_1(s) + \cdots + \tau^l\bar{q}_l(s),$$

$$\bar{q}_i(s) = \begin{cases} a_i(\alpha_{m_\alpha}s^{l+m_\beta-m_\alpha-i} + \cdots + \alpha_0s^{l+m_\beta-i}), & i = 0, 1, \dots, \bar{k}, \\ (a_i - c_i)(\beta_{m_\beta}s^{l-i} + \cdots + \beta_0s^{l+m_\beta-i}) & \\ + c_i(\alpha_{m_\alpha}s^{l+m_\beta-m_\alpha-i} + \cdots + \alpha_0s^{l+m_\beta-i}), & \\ a_i(\beta_{m_\beta}s^{l-i} + \cdots + \beta_0s^{l+m_\beta-i}), & i = \bar{k} + 1, \bar{k} + 2, \dots, k, \\ a_i(\beta_{m_\beta}s^{l-i} + \cdots + \beta_0s^{l+m_\beta-i}), & i = k + 1, k + 2, \dots, l. \end{cases} \quad (4.1.6)$$

Since  $Re(s) < 0$  if and only if  $Re(1/s) < 0$  for a complex variable  $s$ , stability analysis using  $\bar{\delta}$ , instead of  $\delta$ , is justified (assuming that  $\delta(0, \tau) \neq 0$  which is to be seen shortly). As  $\tau \rightarrow 0$ ,  $l + m_\beta - m_\alpha$  roots of  $\bar{\delta}$  are converging to zero whereas the remaining roots converge to  $m_\alpha$  nontrivial roots of  $\bar{q}_0$ . (From now on, the former are called as vanishing roots while the latter as non-vanishing roots.) Since  $\bar{q}_0(s)/s^{l+m_\beta-m_\alpha} = a_0(\alpha_{m_\alpha} + \cdots + \alpha_0s^{m_\alpha})$ , the non-vanishing  $m_\alpha$  roots have negative real parts if and only if  $p_\alpha(s)$  is Hurwitz. Hence, paying attention to the vanishing roots, we can obtain the following Theorems 4.1.2 and 4.1.3 (for the case  $r.deg(P) > r.deg(P_n)$ ) and Theorems 4.1.4 and 4.1.5 (for  $r.deg(P) < r.deg(P_n)$ ), whose proofs are given in Section 4.3.

**Theorem 4.1.2.** Suppose that  $r.deg(P) = r.deg(P_n) + 1$  for all  $P \in \mathcal{P}$ . Then,

<sup>2</sup>For reader's convenience, we write all polynomials in *ascending* order from now on.

there exists  $\bar{\tau}$  such that, for all  $0 < \tau \leq \bar{\tau}$ , the closed-loop system is robustly stable if both conditions H1 and H2 of Theorem 4.1.1 hold and the following three conditions hold:

1.  $\pi(s) := s^{l-1} + \dots + a_{k+1}s^k + (a_k - c_k)s^{k-1} + \dots + (a_1 - c_1)$  is Hurwitz,
2. the signs of high frequency gains  $P$  and  $P_n$  are the same (*i.e.*,  $\beta_{m_\beta}/\alpha_{m_\alpha} > 0$ ) for all  $P \in \mathcal{P}$ ,
3.  $\sigma_+ := \frac{\alpha_{m_\alpha-1}}{\alpha_{m_\alpha}} - \frac{\beta_{m_\beta-1}}{\beta_{m_\beta}} + \frac{\alpha_{m_\alpha}}{\beta_{m_\beta}} \frac{a_0}{a_1-c_1} \left( \frac{a_2-c_2}{a_1-c_1} - \frac{c_1}{a_0} \right) < 0^3$  for all  $P \in \mathcal{P}$ .

□

The case where  $r.\deg(P) > r.\deg(P_n)$  often happens when the actuator dynamics is ignored, or when there is unmodeled dynamics for the plant. The conditions of Theorem 4.1.2 are almost necessary and sufficient in the following sense.

**Theorem 4.1.3.** For given  $P \in \mathcal{P}$  with  $r.\deg(P) > r.\deg(P_n)$ , the closed-loop system is unstable for sufficiently small  $\tau$  if at least one of the following holds:

1.  $r.\deg(P) \geq r.\deg(P_n) + 2$ ,
2.  $P$  has at least one zero in  $\mathbb{C}^+$  (violation of the condition H1 of Theorem 4.1.1),
3.  $P_n C / (1 + P_n C)$  has at least one pole in  $\mathbb{C}^+$  (violation of the condition H2 of Theorem 4.1.1),
4.  $\pi(s)$  has at least one root in  $\mathbb{C}^+$ ,
5.  $\beta_{m_\beta}/\alpha_{m_\alpha} < 0$ ,
6.  $\sigma_+ > 0$ ,
7.  $\bar{k} > 0$ .

□

---

<sup>3</sup> $c_1 = 0$  if  $c_1$  is not present in (4.1.1), and so on.

A lesson from Theorem 4.1.3 is that, if  $r.deg(P) - r.deg(P_n) \geq 2$ , the closed-loop system cannot be stabilized, with small  $\tau$ , no matter how  $C$ ,  $P_n$ , and  $Q$  are chosen. Thus, the estimation of the relative degree of actual plant is essential for the design of the disturbance observer based controller.

**Theorem 4.1.4.** Suppose that  $r.deg(P) < r.deg(P_n)$  for all  $P \in \mathcal{P}$ . Then, there exists  $\bar{\tau}$  such that, for all  $0 < \tau \leq \bar{\tau}$ , the closed-loop system is robustly stable if, for all  $P \in \mathcal{P}$ , both conditions H1 and H2 of Theorem 4.1.1 hold, and

1.  $r.deg(Q) \leq r.deg(P_n) - r.deg(P) + 2$ ,
2.  $N_Q(s; 1)$  is Hurwitz (or a constant),
3.  $P$  and  $P_n$  have the same sign of high frequency gains (i.e.,  $\beta_{m_\beta}/\alpha_{m_\alpha} > 0$ ) if  $r.deg(Q) \geq r.deg(P_n) - r.deg(P) + 1$ ,
4.  $\sigma_- := c_{k-1} - a_{l-1}c_k < 0$  if  $r.deg(Q) = r.deg(P_n) - r.deg(P) + 2$  and  $k \geq 1$ .

□

**Theorem 4.1.5.** For given  $P \in \mathcal{P}$  with  $r.deg(P) < r.deg(P_n)$ , the closed-loop system is unstable for sufficiently small  $\tau$  if at least one of the following holds:

1.  $r.deg(Q) \geq r.deg(P_n) - r.deg(P) + 3$ ,
2.  $P$  has at least one zero in  $\mathbb{C}^+$ ,
3.  $P_n C / (1 + P_n C)$  has at least one pole in  $\mathbb{C}^+$ ,
4.  $N_Q(s; 1)$  has at least one root in  $\mathbb{C}^+$ ,
5.  $\beta_{m_\beta}/\alpha_{m_\alpha} < 0$  while  $r.deg(Q) \geq r.deg(P_n) - r.deg(P) + 1$ ,
6.  $\sigma_- > 0$  while  $r.deg(Q) \geq r.deg(P_n) - r.deg(P) + 2$  and  $k \geq 1$ .

□

Since the  $Q$ -filter is always designed such that  $r.deg(Q) \geq r.deg(P_n)$ , the condition 4 of Theorem 4.1.4 imposes the restriction that  $r.deg(P) \leq 2$ .

## 4.2 A Guideline for Selecting $Q$ and $P_n$

The theorems in the previous section suggest some design guidelines for  $Q$  and  $P_n$ . For example, if the relative degree of the unknown plant is ensured to be less than or equal to two with known sign of high frequency gain, then simply choose  $P_n$  such that  $r.deg(P_n) \geq 3$  with the same sign of high frequency gain, and design  $Q$  with  $k = 0$  and  $l = r.deg(P_n)$ . Then, it is easily seen that all the conditions of Theorem 4.1.4 are satisfied.

On the other hand, the condition 3 of Theorem 4.1.2 allows the following interpretation. Let  $K_p$  denote the high frequency gain of the plant  $P(s)$ , and its numerator and the denominator be written as  $N(s) = K_p(s^{k_p} + b_p s^{k_p-1} + \dots)$  and  $D(s) = s^{l_p} + a_p s^{l_p-1} + \dots$ , respectively. The controller  $C(s)$  and the nominal model  $P_n(s)$  admit the similar expression so that  $K_c, K_n, k_c, l_c, k_n, l_n, a_c, b_c, a_n$ , and  $b_n$  are all defined from  $N_c, D_c, N_n$ , and  $D_n$ . Suppose that  $r.deg(P_n C) \geq 2$  and  $K_n K_p > 0$  (same sign of high frequency gains). Then, since  $m_\alpha = k_p + l_n + l_c$  and  $m_\beta = k_n + l_p + l_c$ , it follows that  $p_\alpha(s) = K_p[s^{m_\alpha} + (a_n + a_c + b_p)s^{m_\alpha-1} + \dots]$  and  $p_\beta = K_n[s^{m_\beta} + (a_p + a_c + b_n)s^{m_\beta-1} + \dots]$ . Thus, the condition 3 of Theorem 4.1.2 is reduced to

$$\left[ a_n + b_p - a_p - b_n + \frac{K_p}{K_n} \frac{a_0}{a_1 - c_1} \left( \frac{a_2 - c_2}{a_1 - c_1} - \frac{c_1}{a_0} \right) \right] < 0,$$

which leads to

$$\sum_{i=1}^{k_n} z_i^n - \sum_{i=1}^{l_n} p_i^n + \frac{K_p}{K_n} \frac{a_0}{a_1 - c_1} \left( \frac{a_2 - c_2}{a_1 - c_1} - \frac{c_1}{a_0} \right) < \sum_{i=1}^{k_p} z_i^p - \sum_{i=1}^{l_p} p_i^p \quad (4.2.1)$$

where poles and zeros of  $P(s)$ , and those of  $P_n(s)$  are denoted by  $p_i^p, z_i^p$ , and  $p_i^n, z_i^n$ , respectively. Therefore, as poles (zeros, respectively) of  $P_n$  are placed further right (left, respectively), it becomes more beneficial for robust stability. However, this may make the design of  $C(s)$  more difficult since the control of stable plant is easier than that of unstable plant. It should be noted that the controller  $C(s)$  does not affect (4.2.1).



### 4.2.1 A Universal Robust Controller

The design guidelines yield a rather interesting observation that, if the uncertain plant has the relative degree at most four (and is of minimum phase whose sign of high frequency gain is known), then a robust controller can be designed, which is ‘universal’ in the sense that it applies to the plant of any order and of any bounded (but arbitrarily large) uncertainty. Just by reducing the parameter  $\tau$ , robust stabilization is achieved.

Let  $\mu(P) = (\text{sum of all zeros of } P) - (\text{sum of all poles of } P)$ , and let  $\bar{\mu}(\mathcal{P}) := \min_{P \in \mathcal{P}} \mu(P)$  and  $\bar{K}_p := \max_{P \in \mathcal{P}} |K_p|$ . Pick the high frequency gain  $K_n$  of the nominal plant  $P_n$  (to be designed) such that  $K_n K_p > 0$ . Let  $Q(s) = a_0 / ((\tau s)^3 + a_2(\tau s)^2 + a_1(\tau s) + a_0)$ , where  $a_1$  and  $a_2$  is designed such that  $s^2 + a_2 s + a_1 = \pi(s)$  is Hurwitz and  $a_0 > 0$  is chosen sufficiently small such that  $p_f(s) = s^3 + a_2 s^2 + a_1 s + (K_p/K_n)a_0$  is Hurwitz for all  $|K_p| \leq \bar{K}_p$ . In fact, it holds if  $0 < a_0 < a_1 a_2 K_n / \bar{K}_p$ , which is found, *e.g.*, by the Routh-Hurwitz test. Now, determine the locations of poles and zeros of  $P_n$  such that its relative degree is 3 and that

$$\mu(P_n) + \frac{\bar{K}_p}{K_n} \frac{a_0 a_2}{a_1^2} < \bar{\mu}(\mathcal{P})$$

is satisfied. Then,  $C$  is designed such that it stabilizes  $P_n$ . The remaining freedom of choice for  $P_n$  and  $C$  can be used to satisfy given performance specifications.

With the design, robust stability follows from the main theorems. If  $r.deg(P)$  is 1 or 2, all the conditions of Theorem 4.1.4 are satisfied. If  $r.deg(P)$  is 3, all the conditions of Theorem 4.1.1 hold. If  $r.deg(P)$  is 4, all the conditions of Theorem 4.1.2 hold. Hence, with sufficiently small  $\tau$ , robust stability is guaranteed.

## 4.3 Technical Proofs

The conditions regarding H1 and H2 in all theorems follow from the same arguments as in Remark 4.1.1, which are related to the polynomial  $p_\alpha(s)$ . Therefore, the proof is mainly to investigate the behavior of  $l + m_\beta - m_\alpha$  vanishing roots of  $\bar{\delta}(s; \tau)$  in (4.1.6) and to see if they remain in  $\mathbb{C}^-$  while converging to the origin. The study could have been facilitated if there is no higher-order terms of  $\tau$  in

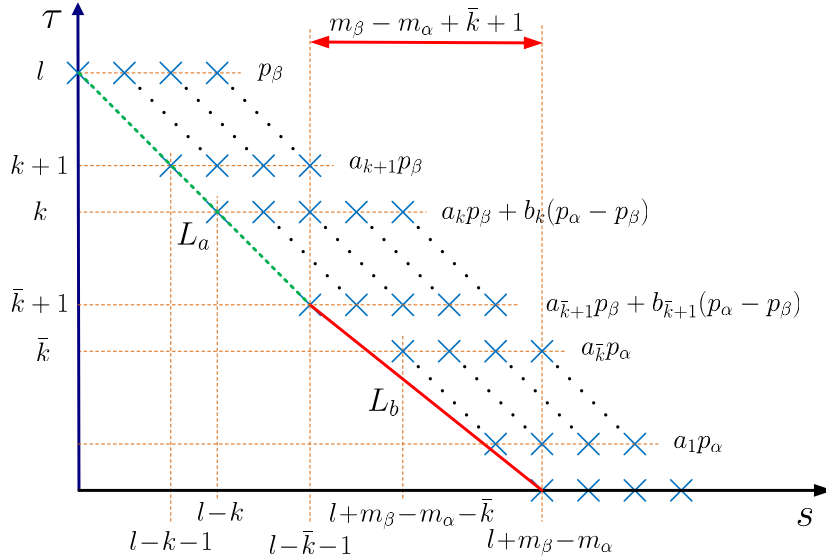


Figure 4.2: Newton diagram for  $\bar{\delta}(s; \tau)$  in (4.1.6) when  $r.\text{deg}(P) > r.\text{deg}(P_n)$  (i.e.,  $m_\beta > m_\alpha$ ).

$\bar{\delta}(s; \tau)$  except the first order one because the classical root-locus method could be employed. However, since this is not the case, we invoke the method of Newton diagram, inspired by the higher-order root-locus method in [Hah81].

**Proof of Theorem 4.1.3:** The vanishing roots of  $\bar{\delta}(s; \tau)$  have the form of  $s^*(\tau) = \gamma\tau^c + o(\tau^c)$  where  $o(\tau^c)$  represents the terms having higher order of  $\tau$  than  $c > 0$ , and  $\gamma$  is a non-zero constant. To find  $c$  and  $\gamma$ , the Newton diagram<sup>4</sup> of  $\bar{\delta}(s; \tau)$  is drawn as in Fig. 4.2, where it is seen that there are two groups of roots. The first

<sup>4</sup>The non-zero coefficient of the term  $\tau^j s^i$  is marked as  $\times$  in the coordinate  $(i, j)$ . Then, a convex hull of all marked  $\times$  is considered, and the line segments with different slopes, located on the boundary in the lower-left side, are found. ( $L_a$  and  $L_b$  in Fig. 4.2.) Let  $N$  be the number of such line segments. From the figure, the following facts are read out: (i) the total number of roots converging to zero as  $\tau \rightarrow 0$  is the index of the leftmost  $\times$  in the row of  $\tau^0$  (which is  $l + m_\beta - m_\alpha$  in Fig. 4.2). (ii) These roots are divided by  $N$  groups. (iii) For each group, there is  $m$  roots of the form  $s_i^*(\tau) = \gamma_i \tau^c + o(\tau^c)$ ,  $1 \leq i \leq m$ , where  $c = -(\text{slope of the line segment})$  and  $m$  is the difference between the horizontal indices of the rightmost mark and the leftmost mark in the line segment. (iv) The value of  $\gamma_i$  is determined by finding roots of the  $m$ -th order polynomial  $\phi(\gamma)$  whose coefficients are the values of those marks that touch the corresponding line segment.

group consists of  $l - \bar{k} - 1$  roots of the form  $\gamma_a \tau^1 + o(\tau^1)$  and the second group has  $m_\beta - m_\alpha + \bar{k} + 1$  roots of the form  $\gamma_b \tau^{(\bar{k}+1/(m_\beta - m_\alpha + \bar{k} + 1))} + o(\dots)$ . It is also seen that  $\gamma_a$  and  $\gamma_b$  satisfy the following two equations, respectively:

$$\phi_a(\gamma) = \beta_{m_\beta} \left[ \sum_{i=k+1}^l a_i \gamma^{l-i} + \sum_{i=\bar{k}+1}^k (a_i - c_i) \gamma^{l-i} \right] = 0,$$

$$\phi_b(\gamma) = (a_{\bar{k}+1} - c_{\bar{k}+1}) \beta_{m_\beta} + \alpha_{m_\alpha} a_0 \gamma^{m_\beta - m_\alpha + \bar{k} + 1} = 0.$$

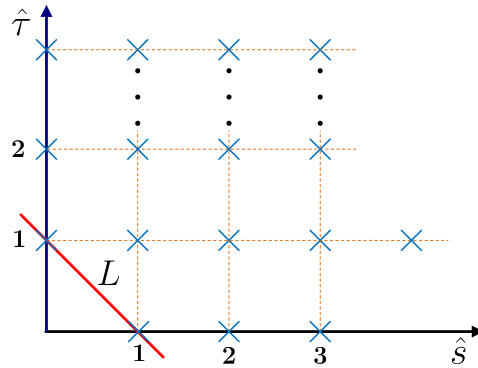
For stability, all the roots of  $\phi_a$  and  $\phi_b$  need to be located in  $\mathbb{C}^-$  because they determine the location of  $s^*(\tau)$  for sufficiently small  $\tau$ . It is clear that a necessary condition for stability is  $m_\beta - m_\alpha + \bar{k}$  is at most one, because, if not, at least one root of  $\phi_b(\gamma)$  is in  $\mathbb{C}^+$ . This explains the conditions 1 and 7. Now assuming  $m_\beta - m_\alpha = 1$  and  $\bar{k} = 0$ , the condition 4 (5, respectively) implies a solution to  $\phi_a(\gamma) = 0$  ( $\phi_b(\gamma) = 0$ , respectively) is in  $\mathbb{C}^+$  (since  $\phi_a(\gamma) = \beta_{m_\beta} \gamma^{l-1} \pi(1/\gamma)$ ). If  $\beta_{m_\beta}/\alpha_{m_\alpha} > 0$ , the second group has two roots  $s^*(\tau) = \pm i\bar{\gamma} \tau^{1/2} + o(\tau^{1/2})$  where  $\bar{\gamma} = \sqrt{(a_1 - c_1)\beta_{m_\beta}/(a_0\alpha_{m_\alpha})}$ . With this, stability is inconclusive and we need to inspect higher order terms.

We let<sup>5</sup>  $s^*(\tau) = (i\bar{\gamma} + \hat{s}(\tau))\tau^{1/2}$  where  $\hat{s}$  is a continuous function to be found such that  $\hat{s}(0) = 0$ . Define  $\hat{\tau} = \tau^{1/2}$  and  $A(\hat{\tau}) = i\bar{\gamma} + \hat{s}(\hat{\tau}^2)$  for convenience, and regard  $\bar{\delta}(s^*(\hat{\tau}^2); \hat{\tau}^2)$  as a polynomial of  $\hat{s}$  with the parameter  $\hat{\tau}$ , that is, from (4.1.6)

$$\begin{aligned} \bar{\delta}(s^*(\hat{\tau}^2); \hat{\tau}^2) &= a_0(\alpha_{m_\alpha} A^{l+1} \hat{\tau}^{l+1} + \alpha_{m_\alpha-1} A^{l+2} \hat{\tau}^{l+2} + \dots) \\ &\quad + (a_1 - c_1)(\beta_{m_\beta} A^{l-1} \hat{\tau}^{l+1} + \beta_{m_\beta-1} A^l \hat{\tau}^{l+2} + \dots) \\ &\quad + c_1(\alpha_{m_\alpha} A^l \hat{\tau}^{l+2} + \alpha_{m_\alpha-1} A^{l+1} \hat{\tau}^{l+3} + \dots) \\ &\quad + (a_2 - c_2)(\beta_{m_\beta} A^{l-2} \hat{\tau}^{l+2} + \beta_{m_\beta-1} A^{l-1} \hat{\tau}^{l+3} + \dots) \\ &\quad + c_2(\alpha_{m_\alpha} A^{l-1} \hat{\tau}^{l+3} + \dots) + \dots =: \hat{\delta}(\hat{s}; \hat{\tau}). \end{aligned}$$

---

<sup>5</sup>As for the case where  $s^*(\tau) = (-i\bar{\gamma} + \hat{s}(\tau))\tau^{1/2}$ , the same conclusion is obtained and the details are omitted.

Figure 4.3: Newton diagram for  $\hat{\delta}(\hat{s}; \hat{\tau})/\hat{\tau}^{l+1}$ .

Collecting the terms in increasing order of  $\hat{\tau}$ , it becomes

$$\begin{aligned} \hat{\delta}(\hat{s}; \hat{\tau}) &= \hat{\tau}^{l+1}[a_0\alpha_{m_\alpha}A^{l+1} + (a_1 - c_1)\beta_{m_\beta}A^{l-1}] \\ &\quad + \hat{\tau}^{l+2}[a_0\alpha_{m_\alpha-1}A^{l+2} + ((a_1 - c_2)\beta_{m_\beta-1} + c_1\alpha_{m_\alpha})A^l + (a_2 - c_2)\beta_{m_\beta}A^{l-2}] \\ &\quad + \hat{\tau}^{l+3}[\dots] + \dots \end{aligned}$$

By expanding with  $A = i\bar{\gamma} + \hat{s}(\hat{\tau}^2)$ , it is seen that the constant term (with respect to  $\hat{s}$ ) in the coefficient of  $\hat{\tau}^{l+1}$  (the lowest power of  $\hat{\tau}$ ) is zero by the definition of  $\bar{\gamma}$ . With this fact, the Newton diagram of  $\hat{\delta}(\hat{s}; \hat{\tau})/\hat{\tau}^{l+1}$  (Fig. 4.3) suggests that it has one root  $\hat{s}^*(\hat{\tau})$  of the form  $\hat{\gamma}\hat{\tau}^1 + o(\hat{\tau}^1)$  and  $\hat{\gamma}$  is the root of

$$\begin{aligned} \hat{\phi}(\hat{\gamma}) &= \left( \frac{\alpha_{m_\alpha-1}\beta_{m_\beta}^2(a_1 - c_1)^2}{\alpha_{m_\alpha}^2 a_0} - \frac{(a_1 - c_1)^2\beta_{m_\beta}\beta_{m_\beta-1}}{\alpha_{m_\alpha} a_0} - \frac{(a_1 - c_1)c_1\beta_{m_\beta}}{a_0} \right. \\ &\quad \left. + (a_2 - c_2)\beta_{m_\beta} \right) - 2(a_1 - c_1)\beta_{m_\beta}\hat{\gamma}. \end{aligned}$$

The condition 6 implies that  $\hat{\gamma}$  is in  $\mathbb{C}^+$ , and so is  $s^*(\tau) = i\bar{\gamma}\tau^{1/2} + \hat{\gamma}\tau^1 + o(\tau^1)$  as  $\tau \rightarrow 0$ .

**Proof of Theorem 4.1.2:** Conclusions of Theorem 4.1.2 are easily derived from the proof of Theorem 4.1.3. Indeed, by the condition 1, it follows that  $a_1 - c_1 > 0$  and  $\bar{k} = 0$ , which yields  $\phi_b(\gamma) = (a_1 - c_1)\beta_{m_\beta} + \alpha_{m_\alpha}a_0\gamma^2$ . Then, the conditions

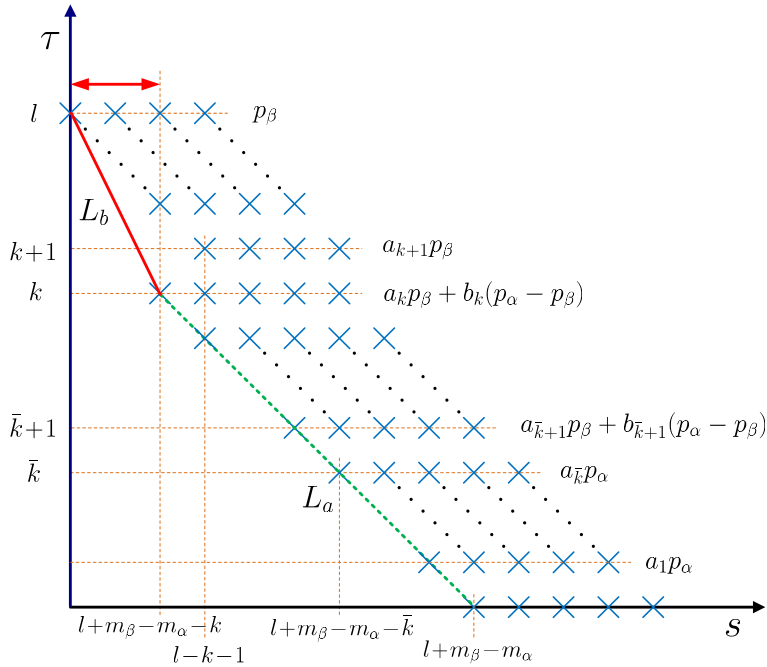


Figure 4.4: Newton diagram for the case  $r.\deg(P) < r.\deg(P_n)$ .

2 and 3 (the condition 1, respectively) imply that all the roots of  $\phi_b$  ( $\phi_a$ , respectively) are located in  $\mathbb{C}^-$ .

**Proof of Theorem 4.1.4:** We now consider the case where  $m_\beta - m_\alpha < 0$ . From the Newton diagram of this case (Fig. 4.4), it is seen that there are two groups of vanishing roots of  $\bar{\delta}(s; \tau)$ . The first group consists of  $k$  roots of the form  $s^*(\tau) = \gamma_a \tau^1 + o(\tau^1)$  where  $\gamma_a$  is the roots of  $\phi_a(\gamma) = c_k + \dots + c_{\bar{k}+1} \gamma^{k-\bar{k}-1} + a_{\bar{k}} \gamma^{k-\bar{k}} + \dots + a_0 \gamma^k = c_k + \dots + c_0 \gamma^k = \gamma^k N_Q(1/\gamma; 1)$ . The condition 2 guarantees that  $\phi_a$  is Hurwitz. On the other hand, it is seen from Fig. 4.4 that the second group has the roots of the form  $s^*(\tau) = \gamma_b \tau^{(l-k)/(l+m_\beta-m_\alpha k)}$ , with  $\gamma_b$  being the roots of  $\phi_b(\gamma) = \beta_{m_\beta} + c_k \alpha_{m_\alpha} \gamma^{l+m_\beta-m_\alpha-k}$ . Note that  $1 \leq l + m_\beta - m_\alpha - k = r.\deg(Q) + r.\deg(P) - r.\deg(P_n) \leq 2$  by the condition 1 and by  $r.\deg(Q) \geq r.\deg(P_n)$ . If its value is 1, then the condition 3 guarantees that  $\phi_b$  is Hurwitz (of first order). If its value is 2 (so that  $l - k > 2$ ), then two roots of the second group are  $s^*(\tau) = (\pm i \bar{\gamma} + \hat{s}(\tau)) \tau^{(l-k)/2}$  where  $\bar{\gamma} = \sqrt{\beta_{m_\beta} / (c_k \alpha_{m_\alpha})}$  and  $\hat{s}$  is a continuous

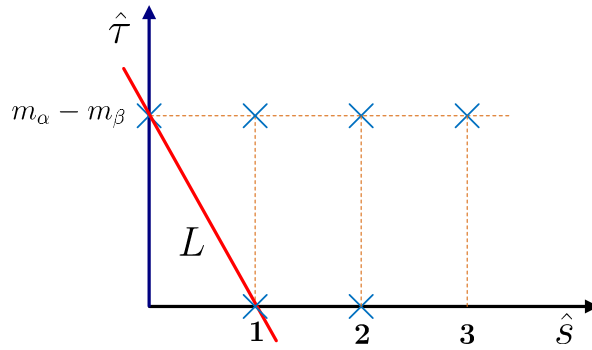


Figure 4.5: Newton diagram for  $\hat{\delta}(\hat{s}; \hat{\tau})/\hat{\tau}^{2l}$  under the condition  $r.\deg(P) < r.\deg(P_n)$ .

function to be found such that  $\hat{s}(0) = 0$ . Let  $\hat{\tau} = \tau^{1/2}$  and  $A(\hat{\tau}) = i\bar{\gamma} + \hat{s}(\hat{\tau}^2)$  so that  $s^*(\hat{\tau}^2) = A\hat{\tau}^{l-k}$ . From (4.1.6), it is seen that the power of  $\hat{\tau}$  in each  $\hat{\tau}^{2j}\bar{q}_j(A\hat{\tau}^{l-k})$  begins with  $(l-k)(l+m_\beta-m_\alpha-j)+2j$  if  $0 \leq j \leq k$ , and with  $(l-k)(l-j)+2j$  if  $k+1 \leq j \leq l$ , and increases by  $(l-k)$  in both cases. Since  $l-k > 2$ , the term of the second lowest power in the polynomial  $\bar{\delta}(A\hat{\tau}^{l-k}, \hat{\tau}^2)$  comes from the lowest power term of  $\hat{\tau}^{2(k-1)}\bar{q}_{k-1}(A\hat{\tau}^{l-k})$  and of  $\hat{\tau}^{l-1}\bar{q}_{l-1}(A\hat{\tau}^{l-k})$  but not from others. Writing  $\bar{\delta}$  in ascending power of  $\hat{\tau}$ , we have

$$\begin{aligned} \bar{\delta}(s^*; \hat{\tau}^2) &= [c_k\alpha_{m_\alpha}A^2 + \beta_{m_\beta}]\hat{\tau}^{2l} + [c_{k-1}\alpha_{m_\alpha}A^3 + a_{l-1}\beta_{m_\beta}A]\hat{\tau}^{2l-m_\beta-m_\alpha} + \dots \\ &= [2ic_k\alpha_{m_\alpha}\bar{\gamma}\hat{s} + (\dots)\hat{s}^2]\hat{\tau}^{2l} + [i\bar{\gamma}(a_{l-1}\beta_{m_\beta} - c_{k-1}\alpha_{m_\alpha}\bar{\gamma}^2) \\ &\quad + (\dots)\hat{s} + (\dots)\hat{s}^2 + (\dots)\hat{s}^3]\hat{\tau}^{2l-m_\beta+m_\alpha} + \dots =: \hat{\delta}(\hat{s}; \hat{\tau}). \end{aligned}$$

The corresponding Newton diagram (Fig. 4.5) suggests that it has one root  $\hat{s}^*(\hat{\tau})$  of the form  $\hat{\gamma}\hat{\tau}^c + o(\hat{\tau}^c)$  where  $c = m_\alpha - m_\beta$  and  $\hat{\gamma}$  is the root of

$$\hat{\phi}(\hat{\gamma}) = 2c_k\alpha_{m_\alpha}\hat{\gamma} + (a_{l-1}\beta_{m_\beta} - c_{k-1}\alpha_{m_\alpha}\bar{\gamma}^2) = 2c_k\alpha_{m_\alpha} \left[ \hat{\gamma} + \frac{\beta_{m_\beta}}{2c_k^2\alpha_{m_\alpha}}(a_{l-1}c_k - c_{k-1}) \right].$$

The condition 4 implies that  $\hat{\phi}$  is Hurwitz. The result is the same with  $A(\hat{\tau}) = -i\bar{\gamma} + \hat{s}(\hat{\tau}^2)$ .

**Proof of Theorem 4.1.5:** Conclusions of Theorem 4.1.5 are easily derived from

the proof of Theorem 4.1.4. Indeed, the condition 4 implies that  $\phi_a(\gamma)$  is not Hurwitz. On the other hand, if the condition 1 holds, then  $\phi_b(\gamma)$  is not Hurwitz because  $l + m_\beta - m_\alpha - k \geq 3$ . Regarding the condition 5, it implies that  $\phi_b(\gamma)$  has at least one root in  $\mathbb{C}^+$ . Finally, suppose that  $\beta_{m_\beta}/\alpha_{m_\alpha} > 0$  while  $r.deg(Q) = r.deg(P_n) - r.deg(P) + 2$ . Then,  $s^*(\tau) = \hat{\gamma}\tau^{m_\alpha - m_\beta} + o(\tau^{m_\alpha - m_\beta})$ . But,  $\hat{\gamma}$  is positive because of the condition 6.

## 4.4 Illustrative Examples

A numerical example is given to illustrate the method presented in Section 4.2.1.

**Example 4.4.1.** Let  $h.gain(P)$  denote the high frequency gain of  $P(s)$  and define sets of transfer functions (having finite coefficients and of minimum phase)

$$\begin{aligned}\mathcal{P}_{12} &= \{P(s) \mid 1 \leq r.deg(P) \leq 2, 0.1 \leq h.gain \leq 8\}, \\ \mathcal{P}_3 &= \{P(s) \mid r.deg(P) = 3, 0.1 \leq h.gain \leq 8\}, \\ \mathcal{P}_4 &= \{P(s) \mid r.deg(P) = 4, 0.1 \leq h.gain \leq 8, \mu(P) \geq 8\}.\end{aligned}$$

It is assumed that the primary control goal is to achieve zero steady-state error (to step response) with overshoot less than 15% and settling time less than 6 seconds. We will show that, for any plant  $P(s) \in \mathcal{P} := \mathcal{P}_{12} \cup \mathcal{P}_3 \cup \mathcal{P}_4$ , a robust controller can be designed in order to achieve the control goal. As discussed in Section 4.2.1, we first choose

$$P_n(s) = \frac{1}{s(s+2)(s+3)}, \quad Q(s) = \frac{1}{(\tau s)^3 + 3(\tau s)^2 + 3(\tau s) + 1}, \quad (4.4.1)$$

which guarantees that, for  $P \in \mathcal{P}_4$ ,

$$\mu(P) - \mu(P_n) \geq 8 - 5 > \frac{8}{3} = \frac{\bar{K}_p a_0 a_2}{K_n a_1^2}. \quad (4.4.2)$$

Next, select

$$C(s) = 5 \quad (4.4.3)$$

so that the unity feedback control system composed of  $P_n(s)$  and  $C(s)$  achieves the

primary control goal. Then, according to Theorem 4.1.2 and 4.1.4, the disturbance observer control system (with small  $\tau$ ) will be stable for any  $P \in \mathcal{P}$ .

To verify the stability as well as the performance, the computer simulations are carried out using the disturbance observer controller with (4.4.1), (4.4.3), and  $\tau = 0.01$ . In addition, the disturbance and the reference inputs are chosen as  $d(t) = \sin(2\pi t)$  and  $r(t) = 1$ . For simulation purpose, we consider the following plants of variation:

$$\begin{aligned} P_{1,a} &= \frac{2}{s+6}, & P_{1,b} &= \frac{0.2}{s+4}, & P_{1,c} &= \frac{5}{s-1}, \\ P_{2,a} &= \frac{2}{(s+2)(s+4)}, & P_{2,b} &= \frac{0.2}{(s+1)(s+3)}, & P_{2,c} &= \frac{5}{(s+2)(s-1)}, \\ P_{3,a} &= \frac{1}{s}P_{2,a}, & P_{3,b} &= \frac{1}{s}P_{2,b}, & P_{3,c} &= \frac{1}{s}P_{2,c}, \\ P_{4,a} &= \frac{1}{s}P_{3,a}, & P_{4,b} &= \frac{1}{s}P_{3,b}, & P_{4,c} &= \frac{s+1}{s(s+8)}P_{3,c}. \end{aligned}$$

It is observed that (a) all the plants except  $P_{4,b}$  belong to  $\mathcal{P}$ , (b) all the plants have different high frequency gains from  $P_n(s)$ , (c) (4.4.2) is satisfied by  $P_{1,a}$ ,  $P_{2,a}$ ,  $P_{3,a}$ ,  $P_{4,a}$ , and  $P_{4,c}$  but not by the others, and (d)  $P_{1,c}$ ,  $P_{2,c}$ , and  $P_{3,c}$  are unstable.

Fig. 4.6 and Fig. 4.7 show the simulation results for  $P_{1,a}$ ,  $P_{1,b}$  and  $P_{2,a}$ ,  $P_{2,b}$ ,  $P_{2,c}$ , respectively. Although there is the disturbance signal  $d(t)$ , it seems that plant outputs are not affected by  $d(t)$ . In addition, it is seen that the performance of each plant can be recovered to that of nominal one so that the primary control goal is achieved for any plant belonging to  $\mathcal{P}_{12}$ . The simulation results for  $P_{3,a}$ ,  $P_{3,b}$ , and  $P_{3,c}$  are depicted in Fig. 4.8. It is also seen that the recovery of the nominal closed-loop system performance is achieved. From Figs. 4.6–4.8, it is verified that, when  $r.deg(P) = r.deg(P_n)$  or  $1 \leq r.deg(P) \leq 2$ , the control system can be stabilized regardless of whether or not the condition (4.4.2) (*i.e.*, 3 of Theorem 4.1.2) is satisfied.

Fig. 4.9 shows the simulation results for  $P_{4,a}$ ,  $P_{4,b}$ , and  $P_{4,c}$ . It is seen that  $P_{4,a}$  and  $P_{4,c}$  can be stabilized by the disturbance observer controller and the nominal performance is recovered. On the other hand, the instability occurs for  $P_{4,b} \notin \mathcal{P}$ , which indicates that the condition (4.4.2) is very critical when  $r.deg(P) = r.deg(P_n) + 1$ .



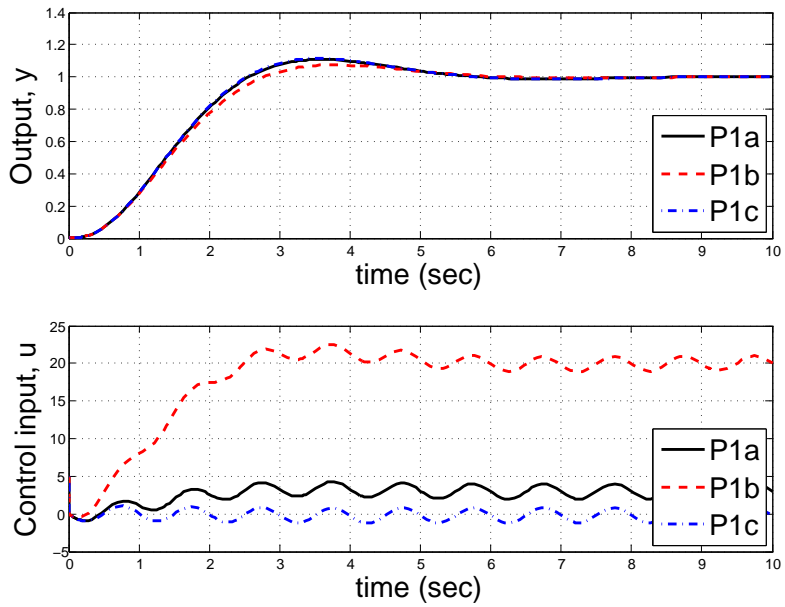


Figure 4.6: Simulation results for  $P_{1,a}$ ,  $P_{1,b}$ , and  $P_{1,c}$  (plants having relative degree 1) in the presence of disturbance  $d(t) = \sin(2\pi t)$

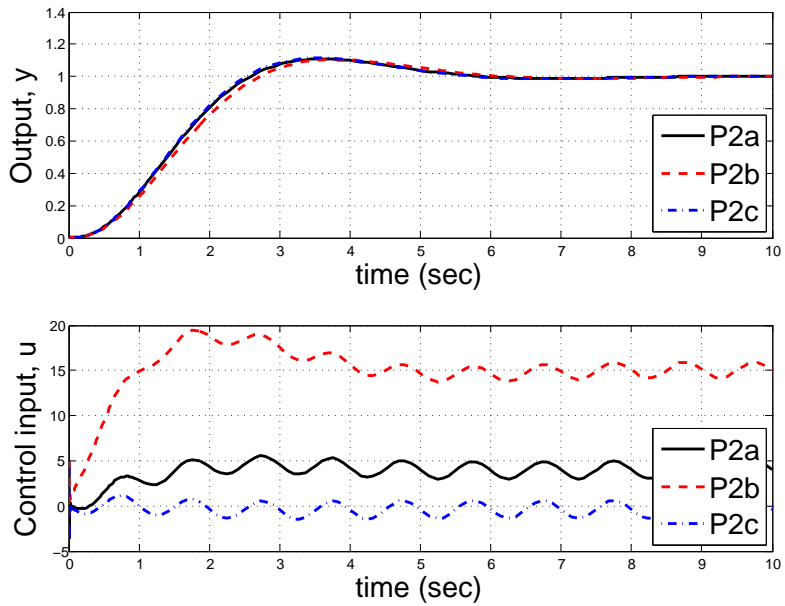


Figure 4.7: Simulation results for  $P_{2,a}$ ,  $P_{2,b}$ , and  $P_{2,c}$  (plants having relative degree 2) in the presence of disturbance  $d(t) = \sin(2\pi t)$

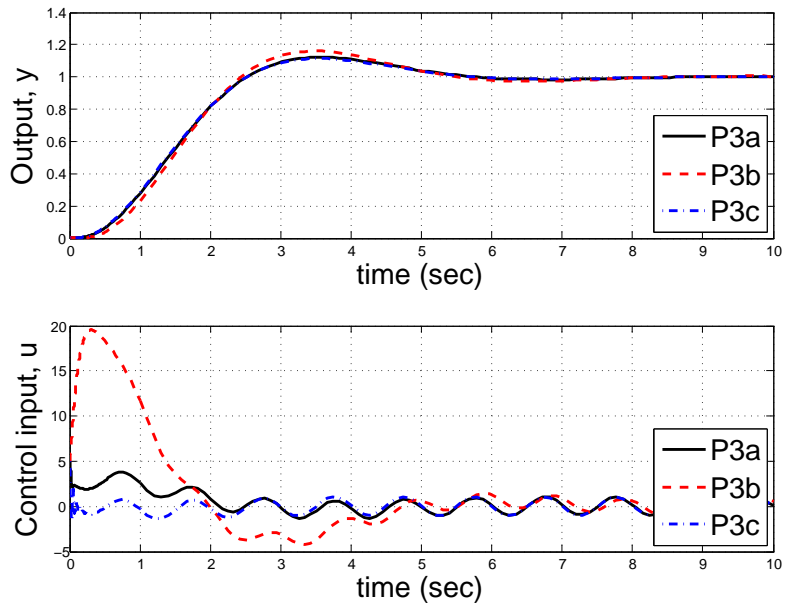


Figure 4.8: Simulation results for  $P_{3,a}$ ,  $P_{3,b}$ , and  $P_{3,c}$  (plants having relative degree 3) in the presence of disturbance  $d(t) = \sin(2\pi t)$

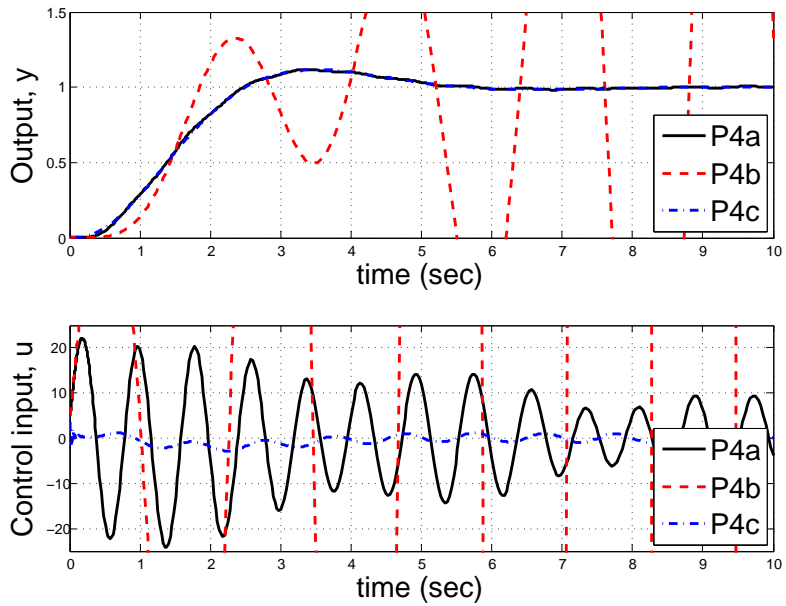


Figure 4.9: Simulation results for  $P_{4,a}$ ,  $P_{4,b}$ , and  $P_{4,c}$  (plants having relative degree 4) in the presence of disturbance  $d(t) = \sin(2\pi t)$

Finally, it should be remarked that, with the help of the disturbance observer controller, the plant output of any  $P(s) \in \mathcal{P}$  is almost indistinguishable from that of nominal model in the absence of the disturbance input.

# Chapter 5

## Reduced Order Type-k Disturbance Observer under Generalized Q-filter

As a robust control scheme, a disturbance observer has been widely employed in industrial applications to reject the effect of disturbances and plant uncertainties. As shown in Chapter 3, the disturbance rejection performance of disturbance observer is mainly determined by the design of two Q-filters, which are the core components of disturbance observer structure. Despite the different roles of each Q-filter, they have been typically designed to have the same structure. In this section, we generalize Q-filters' structures with respect to each Q-filter's objective and derive a robust stability condition for the proposed disturbance observer based control system. To clarify the utility of the generalized Q-filter design framework, a reduced order type-k disturbance observer is proposed to enhance the disturbance rejection performance and to reduce the order of type-k disturbance observer compared with the conventional one, simultaneously. In addition, a constructive Q-filter design procedure for guaranteeing robust stability of the closed-loop system is proposed under parametric uncertainties of plant which belong to an arbitrarily large compact set. Finally, the validity of the proposed disturbance observer is proved by a simulation for the mechanical positioning system.

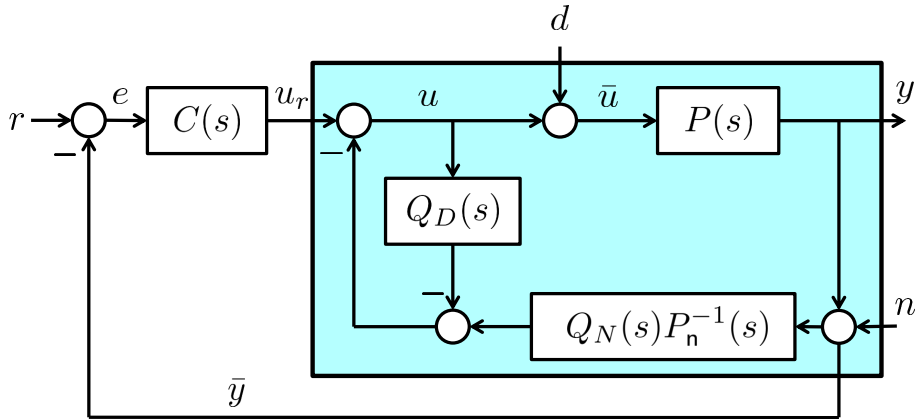


Figure 5.1: Structure of the disturbance observer control system. The shaded region represents the real plant  $P(s)$  augmented with the disturbance observer

## 5.1 Concept of Disturbance Observer with Generalized Q-filter Structure

Fig. 5.1 depicts the configuration of the disturbance observer based control scheme. The input signals  $r$ ,  $d$ , and  $n$  denote the reference input, the disturbance, and the noise, respectively. An uncertain single-input single-output linear time-invariant plant and its nominal model are denoted by  $P(s)$  and  $P_n(s)$ , respectively. The outer-loop controller  $C(s)$  is designed for the nominal model  $P_n(s)$  regardless of the plant uncertainty and disturbance. The blocks  $Q_D(s)$  and  $Q_N(s)$ , which are known as ‘Q-filter’, are stable low-pass filters.

The plant output  $y$  is calculated as

$$\begin{aligned}
 y(s) &= T_{yr}(s) r(s) + T_{yd}(s) d(s) - T_{yn}(s) n(s), \\
 T_{yr}(s) &= \frac{PP_nC}{\Delta(s)}, \quad T_{yd}(s) = \frac{PP_n(1 - Q_D)}{\Delta(s)}, \quad T_{yn}(s) = \frac{PP_nC + PQ_N}{\Delta(s)}, \quad (5.1.1) \\
 \Delta(s) &= PP_nC + PQ_N + P_n(1 - Q_D).
 \end{aligned}$$

Generally, the disturbance  $d$  is dominant in the low frequency range, whereas the noise  $n$  is dominant in the high frequency. As discussed in Chapter 2, in the low

frequency range, (5.1.1) becomes approximately

$$y(jw) \approx \frac{P_n C}{1 + P_n C} r(jw) \quad (5.1.2)$$

since  $Q_D(jw) \approx 1$ ,  $Q_N(jw) \approx 1$ , and  $n(jw) \approx 0$ . It implies that, assuming that all transfer functions are stable, the disturbance observer recovers the nominal closed-loop system  $P_n C / (1 + P_n C)$  in the absence of the disturbance and plant uncertainties.

Let us again consider (5.1.1). One can observe an interesting fact that, when  $Q_D(jw) \approx 1$ , the transfer function from  $d$  to  $y$  is approximate zero (*i.e.*,  $T_{yd}(jw) \approx 0$ ) regardless of  $Q_N(jw)$ . It implies that the disturbance rejection performance mainly depends on  $Q_D(s)$ . On the other hand, the primary objective of  $Q_N(s)$  is to implement an inverse dynamics of the nominal model  $P_n^{-1}(s)$ . In spite of their different objectives, in general, two Q-filters are designed to have the same structure. However, in this section, we design two Q-filters  $Q_D(s)$  and  $Q_N(s)$  independently with respect to the role of each Q-filter.

From these observations, we will specify a generalized Q-filter design framework and discuss robust stability of the disturbance observer based control system with the proposed Q-filter structure. Assume that the plant  $P(s)$  and its nominal model  $P_n(s)$  under consideration satisfy Assumption 2.1.1.

Here, we propose two Q-filters  $Q_D(s)$  and  $Q_N(s)$  with generalized structures as follows:

$$\begin{aligned} Q_D(s) &:= \frac{c_k(\tau s)^k + c_{k-1}(\tau s)^{k-1} + \cdots + c_0}{(\tau s)^l + a_{l-1}(\tau s)^{l-1} + \cdots + a_0}, \\ Q_N(s) &:= \frac{\mathbf{c}_q(\tau s)^q + \mathbf{c}_{q-1}(\tau s)^{q-1} + \cdots + \mathbf{c}_0}{(\tau s)^p + \mathbf{a}_{p-1}(\tau s)^{p-1} + \cdots + \mathbf{a}_0} \end{aligned} \quad (5.1.3)$$

where  $c_0 = a_0$  and  $\mathbf{c}_0 = \mathbf{a}_0$  so that each Q-filter has the unity DC gain. For nonnegative integers  $l$ ,  $k$ ,  $p$ , and  $q$ ,  $l$  and  $k$  are selected as  $l - k \geq 1$ , whereas  $p$  and  $q$  are chosen so that  $p - q \geq \nu$  to make the transfer function  $Q_N(s)P_n^{-1}(s)$  proper. The design parameter  $\tau > 0$  is a time constant, which determines the cut-off frequency of each Q-filter. The design procedure for the coefficients  $a_i$ ,  $c_i$ ,  $\mathbf{a}_i$ , and  $\mathbf{c}_i$  will be presented in Subsection 5.3.

## 5.2 Robust Stability

With the configuration of Fig. 5.1, the transfer function matrix from  $[r, d, n]^T$  to  $[e, \bar{u}, \bar{y}]^T$  is computed as

$$\frac{1}{\Delta(s)} \begin{bmatrix} P_n(1 - Q_D) + PQ_N & -PP_n(1 - Q_D) & -P_n(1 - Q_D) \\ P_n C & P_n(1 - Q_D) & -P_n C - Q_N \\ PP_n C & PP_n(1 - Q_D) & P_n(1 - Q_D) \end{bmatrix} \quad (5.2.1)$$

where  $\Delta(s)$  is in (5.1.1). As discussed in Chapter 2, when the above nine transfer functions are stable, the closed-loop system is said to be internally stable. In addition, the closed-loop system is said to be robustly internally stable if it is internally stable for all  $P(s) \in \mathcal{P}$ . Let us also represent each transfer function  $P$ ,  $P_n$ ,  $C$ ,  $Q_D$ , and  $Q_N$  as the ratio of two coprime polynomials:

$$\begin{aligned} P &= \frac{N(s)}{D(s)}, \quad P_n(s) = \frac{N_n(s)}{D_n(s)}, \quad C(s) = \frac{N_c(s)}{D_c(s)}, \\ Q_D &= \frac{N_{QD}(s; \tau)}{D_{QD}(s; \tau)}, \quad Q_N = \frac{N_{QN}(s; \tau)}{D_{QN}(s; \tau)}. \end{aligned} \quad (5.2.2)$$

In order to express the explicit dependency of  $\tau$ ,  $N_{QD}(s; \tau)$ ,  $D_{QD}(s; \tau)$ ,  $N_{QN}(s; \tau)$ , and  $D_{QN}(s; \tau)$  will be used instead of  $N_{QD}(s)$ ,  $D_{QD}(s)$ ,  $N_{QN}(s)$ , and  $D_{QN}(s)$ , respectively. Then, by a similar way used in [DFT92], for given  $\tau > 0$ , the closed-loop system is internally stable if and only if the characteristic polynomial

$$\begin{aligned} \delta(s; \tau) &= N(N_n N_c D_{QN} + D_n D_c N_{QN}) D_{QD} \\ &\quad + N_n D D_c D_{QN} (D_{QD} - N_{QD}) \end{aligned} \quad (5.2.3)$$

is Hurwitz.

For convenience, define  $m := \deg(DN_n D_c)$ . Then, since transfer functions  $P$ ,  $P_n$ ,  $Q_D$ , and  $Q_N$  are strictly proper, and  $C$  is at least proper, the degree of  $s$  in  $\delta(s; \tau)$  with  $\tau > 0$  is  $m + l + p$ . Therefore, there exist  $m + l + p$  roots of the characteristic equation  $\delta(s; \tau) = 0$ . The following lemma shows the behavior of roots of  $\delta(s; \tau) = 0$  as  $\tau$  goes to zero.

**Lemma 5.2.1.** Let

$$\begin{aligned} p_s(s) &:= N(s)(D_n(s)D_c(s) + N_n(s)N_c(s)), \\ p_f(s) &:= \{D_{QD}(s; 1) - N_{QD}(s; 1)\}D_{QN}(s; 1) \\ &\quad + \left\{ \lim_{s \rightarrow \infty} \frac{P(s)}{P_n(s)} \right\} D_{QD}(s; 1)N_{QN}(s; 1), \end{aligned}$$

and  $s_1^*, \dots, s_m^*$  and  $s_{m+1}^*, \dots, s_{m+l+p}^*$  be the roots of  $p_s(s) = 0$  and  $p_f(s) = 0$ , respectively. Then,  $m + l + p$  roots of  $\delta(s; \tau) = 0$ , say  $s_i(\tau), i = 1, \dots, m + l + p$ , have the property that

$$\begin{aligned} \lim_{\tau \rightarrow 0} s_i(\tau) &= s_i^*, \quad i = 1, \dots, m, \\ \lim_{\tau \rightarrow 0} \tau s_i(\tau) &= s_i^*, \quad i = m + 1, \dots, m + l + p. \end{aligned}$$

□

*Proof.* Since  $D_{QD}(s; 0) = N_{QD}(s; 0) = a_0$  and  $D_{QN}(s; 0) = N_{QN}(s; 0) = \mathbf{a}_0$ ,

$$\lim_{\tau \rightarrow 0} \delta(s; \tau) = a_0 \mathbf{a}_0 N(s)(D_n(s)D_c(s) + N_n(s)N_c(s)).$$

Thus, the first claim is directly proved by Lemma A. 2 in Appendix.

The other  $l + p$  roots of  $\delta(s; \tau) = 0$  go to the infinity as  $\tau$  goes to zero. To investigate the behavior of the  $l + p$  roots, let  $\bar{\delta}(s; \tau) := \tau^m \delta(s/\tau; \tau)$ . Then, we have

$$\begin{aligned} \bar{\delta}(s; \tau) &= \gamma_1(s; \tau)D_{QD}(s; 1)D_{QN}(s; 1) + \gamma_2(s; \tau)D_{QD}(s; 1)N_{QN}(s; 1) \\ &\quad + \gamma_3(s; \tau)D_{QN}(s; 1)\{D_{QD}(s; 1) - N_{QD}(s; 1)\} \end{aligned}$$

where  $\gamma_1(s; \tau) := \tau^m N N_n N_c(s/\tau)$ ,  $\gamma_2(s; \tau) := \tau^m N D_n D_c(s/\tau)$ , and  $\gamma_3(s; \tau) := \tau^m N_n D D_c(s/\tau)$ . Since  $m = \deg(N D_n D_c) = \deg(N_n D D_c) > \deg(N N_n N_c)$ , it follows that  $\lim_{\tau \rightarrow 0} \gamma_1(s; \tau) = 0$ ,  $\lim_{\tau \rightarrow 0} \gamma_2(s; \tau) = \bar{\gamma}_2 s^m$ , and  $\lim_{\tau \rightarrow 0} \gamma_3(s; \tau) = \bar{\gamma}_3 s^m$  for all  $s$  with some nonzero constant  $\bar{\gamma}_2$  and  $\bar{\gamma}_3$ . Then, we obtain

$$\bar{\delta}(s; 0) = \bar{\gamma}_3 s^m \left[ \{D_{QD}(s; 1) - N_{QD}(s; 1)\}D_{QN}(s; 1) + \left\{ \lim_{s \rightarrow \infty} \frac{P(s)}{P_n(s)} \right\} D_{QD}(s; 1)N_{QN}(s; 1) \right]$$



since  $\bar{\gamma}_2/\bar{\gamma}_3 = \lim_{s \rightarrow \infty} P/P_n$ . It follows that

$$\bar{\delta}(s; 0) = \bar{\gamma}_3 s^m p_f(s).$$

It implies that  $\bar{\delta}(s; 0) = 0$  has  $m$  roots at the origin and  $l+p$  roots at  $s_{m+1}^*, \dots, s_{m+l+p}^*$ . In other words, there exist  $l+p$  roots of  $\bar{\delta}(s; \tau) = 0$ , say  $\bar{s}_i(\tau)$ ,  $i = m+1, \dots, m+l+p$ , such that  $\lim_{\tau \rightarrow 0} \bar{s}_i(\tau) = s_i^*$ . Since  $\bar{s}_i(\tau)/\tau$  are roots of  $\delta(s; \tau) = 0$ , the second claim is proved.  $\square$

Based on Lemma 5.2.1, the following theorem presents a condition for robust internal stability of the closed-loop system for all  $P(s) \in \mathcal{P}$ .

**Theorem 5.2.2.** There exists a constant  $\bar{\tau} > 0$  such that, for all  $0 < \tau \leq \bar{\tau}$ , the closed-loop system with (5.1.3) is robustly internally stable if the following two conditions hold:

1.  $C(s)$  internally stabilizes  $P_n(s)$ ,
2.  $p_f(s)$  is Hurwitz.

On the contrary, there is  $\bar{\tau} > 0$  such that, for all  $0 < \tau \leq \bar{\tau}$ , the closed-loop system is not robustly internally stable if at least one of the conditions 1–2 is violated in the sense that  $P_n C/(1 + P_n C)$  has some poles in  $\mathbb{C}^+$ , or some zeros of  $P(s)$  or some roots of  $p_f(s) = 0$  are located in  $\mathbb{C}^+$  for some  $P(s) \in \mathcal{P}$ .  $\square$

*Proof.* Since the denominator of  $P_n C/(1 + P_n C)$  is  $(D_n D_c + N_n N_c)$  and the numerator of  $P(s)$  is  $N(s)$ , the condition 1 and Assumption 2.1.1 imply that the polynomial  $p_s(s)$  is Hurwitz. Thus, the proof follows from Lemma 5.2.1.  $\square$

It is important to note that Theorem 5.2.2 cannot be applied to the case when one of the conditions is marginal (*e.g.*, if some roots of  $p_f(s)$  are located on the imaginary axis). Therefore, in this sense, we call it as an almost necessary and sufficient condition for robust stability.

In addition, Theorem 5.2.2 reveals the following facts: 1) the designer has to design the outer-loop controller  $C(s)$  to stabilize the nominal model  $P_n(s)$  (condition 1), 2) the proposed disturbance observer only can apply to the minimum

phase system, which is a standard assumption for the conventional disturbance observer approach, and 3) the coefficients of two Q-filters  $Q_D(s)$  and  $Q_N(s)$  determine the stability of the closed-loop system (condition 2). Note that the last one is a key condition for robust stability and enlightens new issues on the design of disturbance observer with generalized Q-filters.

**Remark 5.2.1.** If two Q-filters  $Q_D(s)$  and  $Q_N(s)$  are designed as  $Q_D(s) \equiv Q_N(s)$ , then the polynomial  $p_f(s)$  becomes

$$p_f(s) = D_{QD}(s; 1) \times \left[ D_{QD}(s; 1) + \left\{ \lim_{s \rightarrow \infty} \frac{P(s)}{P_n(s)} - 1 \right\} N_{QD}(s; 1) \right]. \quad (5.2.4)$$

Compared with Theorem 2.2.1, the polynomial  $D_{QD}(s; 1)$  is multiplied into  $p_f(s)$  in (5.2.4). In fact, when  $Q_D(s) = Q_N(s)$ , all conditions of Theorem 5.2.2 are equivalent to those in 2.2.1 since  $D_{QD}(s; 1)$  is already Hurwitz if  $D_{QD}(s; 1) + \{\lim_{s \rightarrow \infty} (P/P_n) - 1\} N_{QD}(s; 1)$  is designed to be Hurwitz for all  $P(s) \in \mathcal{P}$ . The difference between Theorem 2.2.1 and the proposed one is from the stable pole/zero cancelation in (5.2.1) corresponding to  $D_{QD}(s; 1)$ .  $\square$

### 5.3 Reduced Order Type-k Disturbance Observer

As discussed before, the design of  $Q_D(s)$  affects the disturbance rejection performance. In order to investigate this intuition, consider  $T_{yd}(s)$  in (5.1.1), which is the transfer function from  $d$  to  $y$ ,

$$T_{yd}(s) = \frac{NN_n D_c D_{QN}(D_{QD} - N_{QD})}{\delta(s; \tau)} \quad (5.3.1)$$

where  $\delta(s; \tau)$  is the characteristic polynomial defined in (5.2.3). It is noticed that the transfer function has the term  $D_{QD}(s; \tau) - N_{QD}(s; \tau)$  in its numerator. If one selects the coefficients  $c_i$ 's such that  $c_i = a_i$ , for all  $i = 0, \dots, k$ , then

$$\begin{aligned} & D_{QD}(s; \tau) - N_{QD}(s; \tau) \\ &= \{(\tau s)^{l-k-1} + a_{l-1}(\tau s)^{l-k-2} + \dots + a_{k+1}\}(\tau s)^{k+1}. \end{aligned} \quad (5.3.2)$$

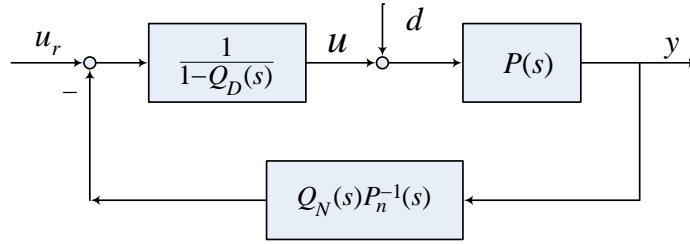


Figure 5.2: The equivalent block diagram of the disturbance observer structure in Fig. 5.1.

Now, assume that the disturbance has the following form:

$$d(s) = \sum_{i=0}^{\bar{k}} \frac{d_i}{s^i}$$

where  $d_i$ 's are unknown constants and  $\bar{k}$  is an unknown nonnegative integer smaller than or equal to  $k + 1$ . By the final value theorem, if  $\delta(s; \tau)$  is Hurwitz, then

$$\lim_{s \rightarrow 0} s T_{yd}(s) d(s) = 0.$$

It implies that the effect of polynomial-in-time disturbance is completely disappeared in the steady state.

This point can also be explained by the internal model principle [FW76]. Fig. 5.2 shows an equivalent block diagram of the disturbance observer structure. Then, one can easily observe that the block  $1/(1 - Q_D(s))$  contains  $k + 1$  integrators, which implies that the disturbance observer structure has the internal model to reject the polynomial-in-time disturbance completely.

On the other hand, the role of  $Q_N(s)$  is for implementing the block  $Q_N(s)P_n^{-1}(s)$ . Therefore, the relative degree of  $Q_N(s)$  has to be larger than or equal to that of  $P_n(s)$ . From these observations, we propose Q-filters' design for reduced order type-k disturbance observer to answer the purpose of each Q-filter as follows:

$$\begin{aligned} Q_D(s) &= \frac{a_k(\tau s)^k + \cdots + a_0}{(\tau s)^{k+1} + a_k(\tau s)^k + \cdots + a_0}, \\ Q_N(s) &= \frac{\mathbf{a}_0}{(\tau s)^\nu + \mathbf{a}_{\nu-1}(\tau s)^{\nu-1} + \cdots + \mathbf{a}_0}. \end{aligned} \quad (5.3.3)$$

Note that  $\nu$  is the relative degree of the plant and  $k$  is selected by the type of disturbance. Now, we call a disturbance observer with two Q-filters in (5.3.3) as ‘reduced order type-k disturbance observer’.

**Remark 5.3.1.** In order to reject the polynomial-in-time disturbance, a type-k disturbance observer has been already proposed in [YKIH96, YKMH99, PJSB12]. However, even if  $\deg(N_n) = 0$ , the order of the type-k disturbance observer with two Q-filters having identical structures is at least  $2(\nu + k)$  although that of the proposed disturbance observer with (5.3.3) is  $\nu + k + 1$ .

In addition, to guarantee the robust stability, a stability condition proposed in [YKMH99]. But, it is conservative since it is derived by the small-gain theorem. Moreover, as the degree of Q-filter’s numerator grows (*i.e.*,  $k$  increases), this condition tends to be violated [YKIH96]. Whereas, by a design procedure which will be proposed later, one can always design the reduced order type-k disturbance observer to guarantee the robust stability of closed-loop system even though uncertain parameters of the plant belong to an arbitrarily large (but bounded) set.  $\square$

The polynomial  $p_f(s)$  for the reduced order type-k disturbance observer is calculated as

$$\begin{aligned} p_{fd}(s) := & s^{\nu+k+1} + \mathbf{a}_{\nu-1}s^{\nu+k} + \dots + \mathbf{a}_1s^{k+2} \\ & + \mathbf{a}_0 \frac{g + g_n}{g_n} s^{k+1} + \mathbf{a}_0 \frac{g}{g_n} a_k s^k + \dots + \mathbf{a}_0 \frac{g}{g_n} a_0. \end{aligned} \quad (5.3.4)$$

where  $g := \beta_{n-\nu}/\alpha_n$  and  $g_n := \beta_{n-\nu}^n/\alpha_n^n$  whose values  $\alpha_n^n$  and  $\beta_{n-\nu}^n$  denote the nominal values of  $\alpha_n$  and  $\beta_{n-\nu}$ , respectively. It is note that, by Assumption 2.1.1,  $g$  and  $g_n$  belong to the interval  $[\underline{g}, \bar{g}]$  where  $\underline{g} = \underline{\beta}_{n-\nu}/\bar{\alpha}_n$  and  $\bar{g} = \bar{\beta}_{n-\nu}/\underline{\alpha}_n$ , and  $g/g_n$  are always positive.

With unknown  $g \in [\underline{g}, \bar{g}]$  and its nominal value  $g_n$ , define, for  $i = 0, \dots, k+1$ ,

$$\begin{aligned} p_i(s; g) := & s^{\nu+i} + \mathbf{a}_{\nu-1}s^{\nu-1+i} + \dots + \mathbf{a}_1s^{1+i} \\ & + \mathbf{a}_0 \frac{g + g_n}{g_n} s^i + \mathbf{a}_0 \frac{g}{g_n} (a_k s^{i-1} + \dots + a_{k+1-i}) \end{aligned} \quad (5.3.5)$$

Note that  $p_{i+1}(s; g) = s p_i(s; g) + \mathbf{a}_0(g/g_n)a_{k-i}$ ,  $p_0(s; g) = s^\nu + \mathbf{a}_{\nu-1}s^{\nu-1} + \dots +$

$\mathbf{a}_1 s + \mathbf{a}_0(g + g_n)/g_n$ , and  $p_{k+1}(s; g) = p_{fd}(s)$ . With respect to  $p_i(s; g)$ , we define the set of interval polynomials

$$\mathcal{I}_i := \left\{ s^{\nu+i} + \mathbf{a}_{\nu-1} s^{\nu-1+i} + \cdots + \mathbf{a}_1 s^{1+i} + \mathbf{a}_0 \frac{g + g_n}{g_n} s^i + \mathbf{a}_0 \frac{g}{g_n} (a_k s^{i-1} + \cdots + a_{k+1-i}) : g \in [\underline{g}, \bar{g}] \right\}$$

The four extreme polynomials for  $\mathcal{I}_i$ , in view of Remark A. 5, are denoted by  $p_{i,0}(s), \dots, p_{i,3}(s)$ .

We are now ready to introduce a Q-filter design procedure so that  $p_{fd}(s)$  is Hurwitz for all  $g \in [\underline{g}, \bar{g}]$  (i.e., the condition 2 in Theorem 5.2.2 is satisfied).

### Procedure 3. Q-filter Design Procedure for Robust Stability

*Step 0:* Select  $k$  in (5.3.3) and the coefficients  $\mathbf{a}_{\nu-1}, \dots, \mathbf{a}_1$  such that the polynomial  $s^{\nu-1} + \mathbf{a}_{\nu-1} s^{\nu-2} + \cdots + \mathbf{a}_2 s + \mathbf{a}_1$  is Hurwitz. Next, pick  $\bar{\kappa}_0 > 0$  such that  $s^\nu + \mathbf{a}_{\nu-1} s^{\nu-1} + \cdots + \mathbf{a}_1 s + \kappa_0$  is Hurwitz for all  $\kappa_0 \in (0, \bar{\kappa}_0)$ . Choose  $\mathbf{a}_0 \in (0, (g_n/(\bar{g} + g_n))\bar{\kappa}_0)$ .

*Step  $m$  ( $m = 1, \dots, k+1$ ):* With the coefficients obtained from the previous steps, consider the four extreme polynomials  $p_{m-1,j}(s)$  of  $\mathcal{I}_{m-1}$ . For each  $j = 0, \dots, 3$ , find  $\bar{\rho}_{k+1-m,j} > 0$  such that

$$s p_{m-1,j}(s) + \rho_{k+1-m,j}$$

is Hurwitz for all  $\rho_{k+1-m,j} \in (0, \bar{\rho}_{k+1-m,j})$ . Then, let  $\bar{\rho}_{k+1-m} := \min_j \bar{\rho}_{k+1-m,j}$ , and choose  $a_{k+1-m} \in (0, (g_n/(\mathbf{a}_0 \bar{g}))\bar{\rho}_{k+1-m})$ .

*Step  $k+2$ :* Construct the Q-filters with the coefficients  $\mathbf{a}_{\nu-1}, \dots, \mathbf{a}_0$  and  $a_k, \dots, a_0$  obtained through the steps 0,  $\dots$ ,  $k+1$ .  $\square$

We also remark that each step requires at most four extreme polynomials and the number of polynomials to be checked does not increase as the step proceeds.

**Theorem 5.3.1.** Under Assumption 2.1.1, the coefficients  $\mathbf{a}_{\nu-1}, \dots, \mathbf{a}_0$  and  $a_k, \dots, a_0$  obtained by the Q-filter design procedure ensure that the polynomial  $p_{fd}(s)$  of (5.3.4) is Hurwitz for all  $g \in [\underline{g}, \bar{g}]$ .  $\square$

*Proof.* In *Step 0*, the coefficients  $\mathbf{a}_{\nu-1}, \dots, \mathbf{a}_0$  are selected such that the polynomial  $s^{\nu-1} + \mathbf{a}_{\nu-1}s^{\nu-2} + \dots + \mathbf{a}_1$  is Hurwitz and  $0 < \mathbf{a}_0((\bar{g} + g_n)/g_n) < \bar{\kappa}_0$ . Thus, by Lemma A. 3, the polynomial  $p_0(s; g)$  is Hurwitz for all  $g \in [g, \bar{g}]$ .

The remaining part of theorem is easily proved by the induction argument. Assume that the polynomial  $p_i(s; g)$  is Hurwitz for all  $g \in [g, \bar{g}]$ . We claim that, with  $a_{k-i}$  from the design procedure, the polynomial  $p_{i+1}(s; g) = sp_i(s; g) + \mathbf{a}_0(g/g_n)a_{k-i}$  is Hurwitz for all  $g \in [g, \bar{g}]$ . For each extreme polynomial  $p_{i,j}(s)$  of  $\mathcal{I}_i$ , Lemma A. 3 guarantees the existence of  $\bar{\rho}_{k-i,j}$  such that  $sp_{i,j}(s) + \rho_{k-i,j}$  is Hurwitz for all  $\rho_{k-i,j} \in (0, \bar{\rho}_{k-i,j})$ , and  $a_{k-i}$  was selected such that  $0 < a_{k-i} < (g_n/\bar{g})\bar{\rho}_{k-i}$  where  $\bar{\rho}_{k-i} = \min_j \bar{\rho}_{k-i,j}$ . Therefore, all extreme polynomials  $p_{i+1,j}(s)$  are Hurwitz since they correspond to the collection of  $sp_{i,j}(s) + (g/g_n)a_{k-i}$ ,  $j = 0, \dots, 3$ . It means that  $p_{i+1}(s; g)$  is Hurwitz for all  $g \in [g, \bar{g}]$ . The proof is completed since  $p_{fd}(s) = p_{k+1}(s; g)$ .  $\square$

## 5.4 Illustrative Examples

In this subsection, an illustrative example is presented to clarify the validity of the reduced order type-k disturbance observer scheme proposed in the previous subsection.

**Example 5.4.1.** Let us consider a mechanical positioning system for the X-Y table operated by a linear motor [YKMH99]. Here, an actual plant and its nominal one are modeled as

$$P(s) = \frac{1}{Js^2 + Bs}, \quad P_n(s) = \frac{1}{J_n s^2 + B_n s} \quad (5.4.1)$$

where  $J \in [0.5, 2]$  is the mass of the table with load variation,  $B = 8$  is the viscous friction coefficient, and  $J_n = 1$  and  $B_n = 8$  are nominal values of  $J$  and  $B$ , respectively. Note that  $g = 1/J$  of  $P(s)$  belongs to a bounded interval  $[0.5, 2] =: [g, \bar{g}]$ , which contains the nominal one  $g_n = 1/J_n = 1$ . To stabilize the nominal model, the outer-loop controller  $C(s)$  is designed as a proportional controller with  $K_p = 25$ .

Assuming that a polynomial-in-time disturbance of at most type-2 enters into

the closed-loop system, we construct a reduced order type-2 disturbance observer by following the proposed Q-filter design procedure.

*Step 0:* We first design  $\mathbf{a}_1 = 2$  such that  $s + \mathbf{a}_1$  is Hurwitz. Since any positive  $\rho_0$  makes  $s^2 + \mathbf{a}_1 s + \rho_0$  Hurwitz, we simply select  $\mathbf{a}_0 = 1 \in (0, \infty)$ .

*Step 1:* Thanks to the selection of  $\{\mathbf{a}_i\}$ 's, two extreme polynomials

$$p_{0,0}(s) = s^2 + \mathbf{a}_1 s + \mathbf{a}_0 \frac{\bar{g} + g_n}{g_n},$$

$$p_{0,2}(s) = s^2 + \mathbf{a}_1 s + \mathbf{a}_0 \frac{g + g_n}{g_n}$$

are Hurwitz. By using the root-locus technique, we take  $\bar{\rho}_{2,0} = 6.1$  and  $\bar{\rho}_{2,2} = 2.9$  such that, for  $j = 0, 2$ ,  $sp_{0,j}(s) + \rho_{2,j}$  is Hurwitz for  $\rho_{2,j} \in (0, \bar{\rho}_{2,j})$ . Let  $\bar{\rho}_2 = \min_j \bar{\rho}_{2,j} = 2.9$  and select  $a_2 = 1.4 \in (0, (g_n/(\mathbf{a}_0 \bar{g})\bar{\rho}_2)$ .

*Step 2-3:* We now have the following four Hurwitz extreme polynomials

$$p_{1,0}(s) = s^3 + \mathbf{a}_1 s^2 + \mathbf{a}_0 \frac{\bar{g} + g_n}{g_n} s + \mathbf{a}_0 \frac{\bar{g}}{g_n} a_2,$$

$$p_{1,1}(s) = s^3 + \mathbf{a}_1 s^2 + \mathbf{a}_0 \frac{\bar{g} + g_n}{g_n} s + \mathbf{a}_0 \frac{g}{g_n} a_2,$$

$$p_{1,2}(s) = s^3 + \mathbf{a}_1 s^2 + \mathbf{a}_0 \frac{g + g_n}{g_n} s + \mathbf{a}_0 \frac{g}{g_n} a_2,$$

$$p_{1,3}(s) = s^3 + \mathbf{a}_1 s^2 + \mathbf{a}_0 \frac{g + g_n}{g_n} s + \mathbf{a}_0 \frac{\bar{g}}{g_n} a_2.$$

With the same procedure in the previous step, we take  $a_1 = 0.0675$  and  $a_0 = 0.0035$ .

*Step 4:* With the coefficients obtained above, we finally propose Q-filters  $Q_D(s)$  and  $Q_N(s)$  as

$$Q_{D,p,type-2}(s) = \frac{1.4(\tau s)^2 + 0.0675(\tau s) + 0.0035}{(\tau s)^3 + 1.4(\tau s)^2 + 0.0675(\tau s) + 0.0035},$$

$$Q_{N,p,type-2}(s) = \frac{1}{(\tau s)^2 + 2(\tau s) + 1}.$$

To compare with the proposed disturbance observer, we make the other Q-filters with binomial coefficients, which have been usually used in the design of

disturbance observer structure [YKIH96], as follows:

$$Q_{D,b}(s) = \frac{3(\tau s)^2 + 3(\tau s) + 1}{(\tau s)^3 + 3(\tau s)^2 + 3(\tau s) + 1}$$

and  $Q_{N,b}(s) = Q_{N,p,type-2}(s)$ . Notice that in this case,  $p_{fd}(s)$  is calculated as

$$\begin{aligned} p_{fd,b}(s) &= s^5 + 2s^4 + \left(\frac{g + g_n}{g_n}\right) s^3 + \frac{g}{g_n} 3s^2 + \frac{g}{g_n} 3s + \frac{g}{g_n} \\ &= s^3(s+1)^2 + \frac{g}{g_n}(s+1)^3 = (s+1)^2 \left\{ s^3 + \frac{g}{g_n}(s+1) \right\}. \end{aligned}$$

Since  $s^3 + (g/g_n)(s+1)$  always has an unstable root for any positive  $g$ ,  $p_{fd,b}(s)$  also does. Therefore, Theorem 5.2.2 indicates that the reduced-order type-2 disturbance observer with the binomial coefficient may destabilize the overall system for a sufficiently small  $\tau$ .

For the simulation, set  $J = 0.6$  and  $r(t) \equiv 0$ , and choose  $\tau$  as 0.003. As shown in Fig. 5.3, the disturbance observer with the binomial coefficients makes the overall system unstable; on the other hand, the stability of the overall closed-loop system is guaranteed with the proposed Q-filter design procedure.

As  $k$ , which is the type of the Q-filter  $Q_D(s)$  increases, the disturbance rejection performance of the resulting type- $k$  disturbance observer becomes better. To verify this argument, we additionally construct reduced order type-0 and type-1 disturbance observers with the coefficients of the Q-filters obtained above; that is to say, each  $Q_D(s)$  is designed as

$$\begin{aligned} Q_{D,p,type-0}(s) &= \frac{1.4}{\tau s + 1.4}, \\ Q_{D,p,type-1}(s) &= \frac{1.4(\tau s) + 0.0675}{(\tau s)^2 + 1.4(\tau s) + 0.0675} \end{aligned}$$

where  $\tau = 0.003$ , while  $Q_N(s)$  is chosen as the same one used in the type-2 disturbance observer.

As shown in Fig. 5.4, when a polynomial-in-time disturbance of type-2 enters into the overall system, the type-2 disturbance observer can reject the modeled disturbance asymptotically, while others induce divergent or constant error in the



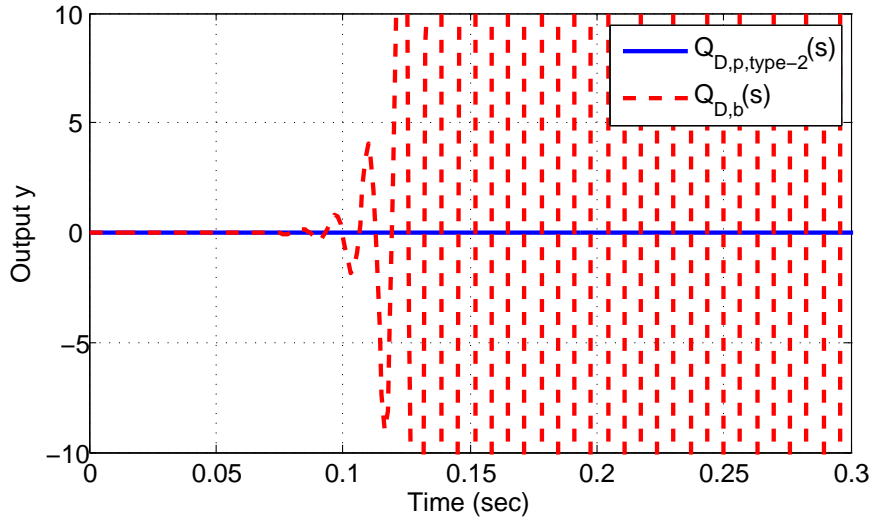


Figure 5.3: The output  $y$  of the overall system with  $Q_{D,p,type-2}(s)$  (solid) and  $Q_{D,b}(s)$  (dashed) when  $d(t) = -2.5t^2 + 10t + 1$

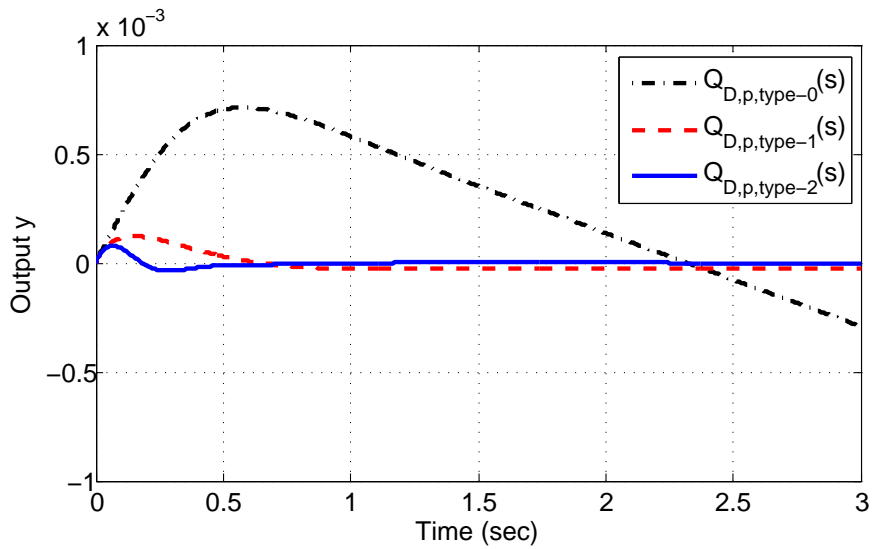


Figure 5.4: The output  $y$  of the overall system with  $Q_{D,p,type-0}(s)$  (dot-dashed),  $Q_{D,p,type-1}(s)$  (dashed), and  $Q_{D,p,type-2}(s)$  (solid) when  $d(t) = -2.5t^2 + 10t + 1$

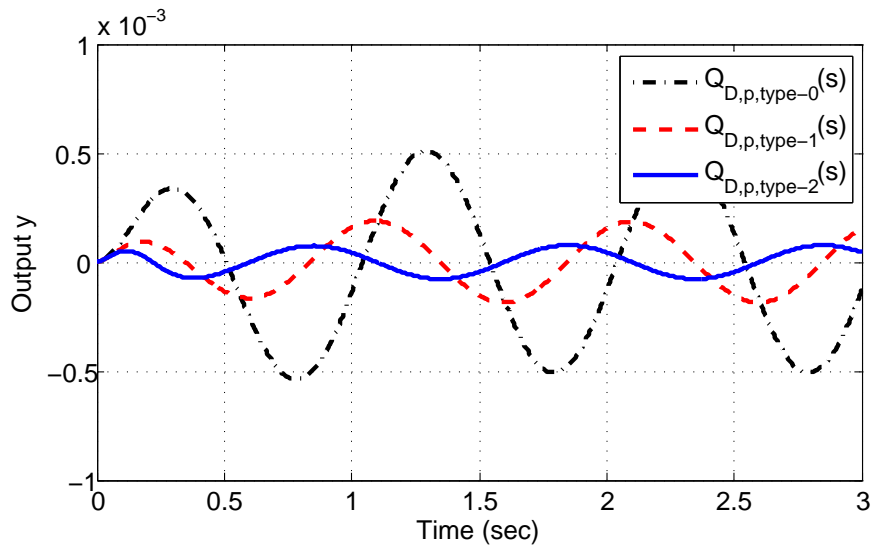


Figure 5.5: The output  $y$  of the overall system with  $Q_{D,p,type-0}(s)$  (dot-dashed),  $Q_{D,p,type-1}(s)$  (dashed), and  $Q_{D,p,type-2}(s)$  (solid) when  $d(t) = 2 \sin(2\pi t)$

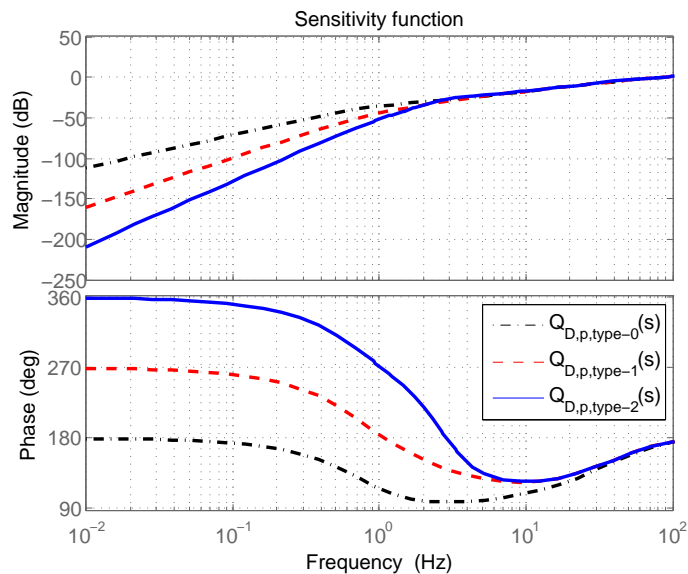


Figure 5.6: Bode plot of sensitivity function of the overall system with  $Q_{D,p,type-0}(s)$  (dot-dashed),  $Q_{D,p,type-1}(s)$  (dashed), and  $Q_{D,p,type-2}(s)$  (solid)

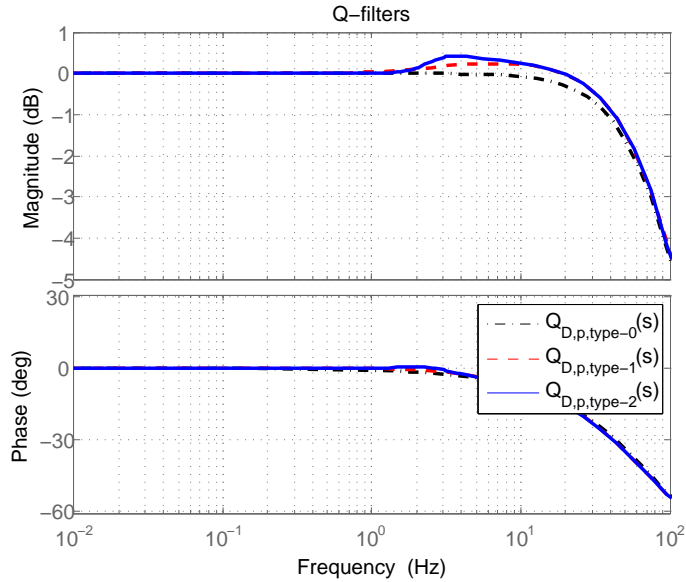


Figure 5.7: Bode plot of Q-filters  $Q_{D,p,type-0}(s)$  (dot-dashed),  $Q_{D,p,type-1}(s)$  (dashed), and  $Q_{D,p,type-2}(s)$  (solid)

steady state due to the lack of the embedded integrators.

In addition to this asymptotic disturbance rejection property, the type-2 disturbance observer also can perform better than type-0 and type-1 even though the disturbance has not the form of polynomial-in-time, as depicted in Fig. 5.5. Indeed, the larger the type of the Q-filter  $Q_D(s)$ , the lower the magnitude of the sensitivity function of the overall system below 2Hz (Fig. 5.6). We remark that this improvement is achieved without increasing the bandwidth of  $Q_D(s)$  (Fig. 5.7).

# Chapter 6

## State Space Analysis of Disturbance Observer

Throughout Chapter 2–3, the conventional linear disturbance observer approach is analyzed in the frequency domain. Although it gives an intuitive explanation for the disturbance observer, we analyze the disturbance observer in the state space for the purpose of extending the horizon of the disturbance observer approach to MIMO (multi-input multi-output) plants, to nonlinear plants, and to non-minimum phase plants and obtaining the deeper understanding of the role of each block.

The contribution of this chapter is

- How the input disturbance  $d$  is estimated and compensated in spite of the uncertainties of the plant. How and why the disturbance observer can be used as a way to robust control. Why the steady-state performance is recovered to the nominal one. These are basic characteristics of the disturbance observer approach, which are already well-known from the frequency domain analysis.
- How the zero dynamics of the plant is replaced by the nominal zero dynamics, and why the zero dynamics of the plant should be stable (*i.e.*, minimum phaseness). This is somewhat new discussion.
- Peaking phenomenon caused by employing Q-filter with large bandwidth is discussed, which possibly degrades the performance during the initial period

for some initial conditions. This implies that the transient performance is not recovered in general, which is a limitation of the conventional linear disturbance observer approach.

- An almost necessary and sufficient condition for robust stability of the plant with model uncertainties, which is the same result in Theorem 2.2.1 are derived when the bandwidth of Q-filter is enough large. It is easy to check and can be applied to not only a plant with unstable poles but also the Q-filter of arbitrary relative degree whose coefficients are not limited to the binomial one.
- Based on Lyapunov stability analysis, a bound of the time constant  $\tau$  for Q-filter is obtained to complete robust stability analysis. Furthermore, the nominal performance recovery of the disturbance observer based control scheme with respect to  $\tau$  is presented.

## 6.1 State Space realization of Disturbance Observer

To begin with the state space analysis, we first realize all the transfer functions in the disturbance observer structure in Fig. 6.1. Then, after a coordinate change, the closed-loop system is put into the standard singular perturbation form. Note that the measurement noise  $n$  is not considered because it is not related to the internal stability.

Consider the following class of uncertain plants<sup>1</sup>, which is a state space realization of  $P(s)$ :

$$\dot{z} = Sz + Gy, \quad y = Cx, \quad (6.1.1a)$$

$$\dot{x} = Ax + B\{F_1z + F_2x + g(u + d)\}, \quad (6.1.1b)$$

where  $\nu$  is the relative degree of  $P(s)$ ,  $x \in \mathbb{R}^\nu$  and  $z \in \mathbb{R}^{n-\nu}$  are the plant state, and  $u \in \mathbb{R}^1$ ,  $y \in \mathbb{R}^1$ , and  $d \in \mathbb{R}^1$  are the plant input, the plant output, and the

---

<sup>1</sup>Note that a single-input single-output linear time-invariant system  $P(s)$  whose relative degree  $\nu$  can always be transformed into the form 6.1.1 such that  $z$ -dynamics is independent of  $x_2, \dots, x_\nu$ . For detailed explanations, refer Chapter 13 in [Kha02]

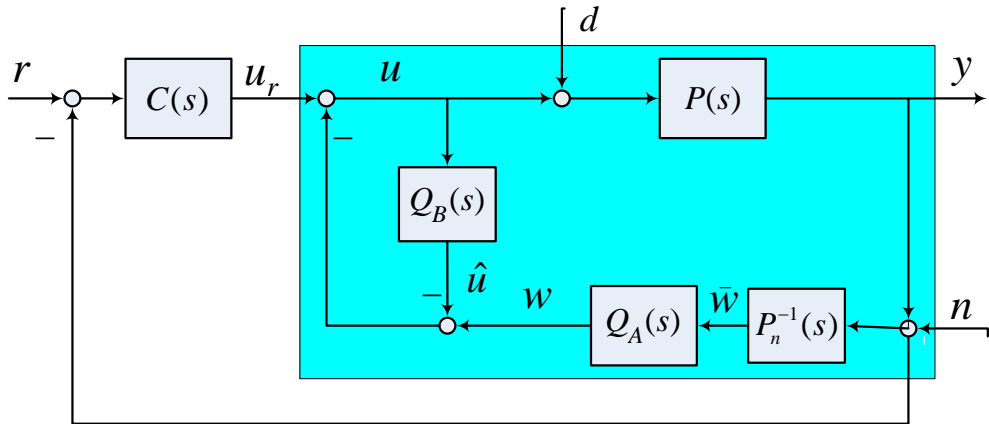


Figure 6.1: Conventional linear disturbance observer structure with the outer-loop controller. Here,  $Q_A(s) = Q_B(s) = Q(s)$ , but unique names are given for convenience.

unknown disturbance, respectively. The matrices  $A$ ,  $B$ , and  $C$  are given by

$$A := \begin{bmatrix} 0_{\nu-1} & I_{\nu-1} \\ 0 & 0_{\nu-1}^T \end{bmatrix}, B := \begin{bmatrix} 0_{\nu-1} \\ 1 \end{bmatrix}, C := \begin{bmatrix} 1 & 0_{\nu-1}^T \end{bmatrix}.$$

The uncertain matrices  $S$ ,  $G$ ,  $F_1$ , and  $F_2$  are of appropriate dimensions and  $g$  is an unknown constant.  $d(t)$  and  $\dot{d}(t)$  are bounded with known constants  $\phi_d$  and  $\phi_{dt}$  such that  $\|d(t)\| \leq \phi_d$  and  $\|\dot{d}(t)\| \leq \phi_{dt}$ , respectively.

**Assumption 6.1.1.** For the uncertain plant (6.1.1), all uncertainties are bounded and their bounds are known *a priori*. In particular, there exist positive constants  $\underline{g}$  and  $\bar{g}$  such that  $\underline{g} \leq g \leq \bar{g}$ .  $\square$

In fact, Assumption 6.1.1 and 2.1.1 are equivalent each other. Therefore, it implies that the relative degree of the plant and the sign of  $g$  are known *a priori*.

**Assumption 6.1.2.** The matrix  $S$  is Hurwitz  $\square$

Assumption 6.1.2 implies that the uncertain plant (6.1.1) is of minimum phase system, which is a conventional assumption on the disturbance observer approach. As a result, the zero dynamics (6.1.1a) in (6.1.1) is input-to-state stable with respect to  $x_1$ .

Now, we represent a nominal model  $P_n(s)$  for the uncertain plant (6.1.1) as follows:

$$\begin{aligned}\dot{z}_n &= \bar{S}z_n + \bar{G}y_n, & y_n &= Cx_n, \\ \dot{x}_n &= Ax_n + B\{\bar{F}_1z_n + \bar{F}_2x_n + g_nu_r\},\end{aligned}\tag{6.1.2}$$

where  $x_n \in \mathbb{R}^\nu$  and  $z_n \in \mathbb{R}^{\bar{n}-\nu}$  are the state,  $u_r \in \mathbb{R}^1$  and  $y_n \in \mathbb{R}^1$  are the control input and the output of the nominal model, respectively. Note that the order of the nominal zero dynamics  $z_n$  may not be equal to that of the zero dynamics (6.1.1a), *i.e.*,  $\bar{n}$  may not be equal to  $n$ .  $\bar{S}$ ,  $\bar{G}$ ,  $\bar{F}_1$ ,  $\bar{F}_2$ , and  $g_n$  are the nominal values of  $S$ ,  $G$ ,  $F_1$ ,  $F_2$ , and  $g$ , respectively.

For the nominal model (6.1.2), consider an output feedback outer-loop controller  $C(s)$  as

$$\dot{\eta} = A_c\eta + B_cr - E_cy_n, \quad u_r = C_c\eta + D_cr - H_cy_n\tag{6.1.3}$$

where  $\eta \in \mathbb{R}^h$  is the state of output feedback controller and  $r$  is the reference input. The matrices  $A_c$ ,  $B_c$ ,  $C_c$ ,  $D_c$ ,  $E_c$ , and  $H_c$  are of appropriate dimensions. It is assumed that  $r(t)$  and  $\dot{r}(t)$  are bounded with known constants  $\phi_r$  and  $\phi_{rt}$  such that  $\|r(t)\| \leq \phi_r$  and  $\|\dot{r}(t)\| \leq \phi_{rt}$ , respectively. Note that, when the outer-loop controller (6.1.3) is considered in the overall closed-loop system,  $y_n$  should be replaced by  $y$ , which is evident and will be applied without mention throughout the paper. Furthermore,  $u_r$ , the function of  $y$ ,  $\eta$ , and  $r$ , will be used for simplification of equations.

We make the following assumption for the nominal closed-loop system.

**Assumption 6.1.3.** The nominal closed-loop system (6.1.2) and (6.1.3) is exponentially stable. It implies that it is input-to-state stable with respect to the reference input  $r$ .  $\square$

As discussed in Chapter 2–3, the outer-loop controller (6.1.3) has to be designed to stabilize the nominal model (6.1.2). Additionally, the specific design of the outer-loop controller is determined by the control objective (*e.g.*, tracking or regulation).

Now, we represent the state space realization of the disturbance observer structure. Since the  $i$ -th derivative of the output  $y$  is  $x_{i+1}$ , the inverse dynamics

of (6.1.1) is obtained from [Isi95] as

$$\begin{aligned}\dot{z} &= Sz + Gy \\ (u + d) &= \frac{1}{g}(-F_1 z - F_2[y, \dot{y}, \dots, y^{(\nu-1)}]^T + y^{(\nu)}).\end{aligned}$$

Motivated by the above exact inverse, we realize the nominal inverse  $\bar{w} = P_n^{-1}(s)y$  (see Fig. 6.1) as the following system

$$\dot{\bar{z}} = \bar{S}\bar{z} + \bar{G}y \quad (6.1.4a)$$

$$\bar{w} = \frac{1}{g_n}(-\bar{F}_1\bar{z} - \bar{F}_2[1, s, s^2, \dots, s^{\nu-1}]^T y + s^\nu y) \quad (6.1.4b)$$

where  $s$  represents the differentiation operator.

Next, a realization of the block  $Q_A(s)$  in Fig. 6.1, where  $Q_A(s)$  is given by (2.1.2), is

$$\begin{aligned}\dot{q} &= \begin{bmatrix} 0 & 1 & 0 & \cdots & 0 \\ 0 & 0 & 1 & \cdots & 0 \\ \vdots & \vdots & \vdots & \ddots & \vdots \\ 0 & 0 & 0 & \cdots & 1 \\ -\frac{a_0}{\tau^l} & -\frac{a_1}{\tau^{l-1}} & -\frac{a_2}{\tau^{l-2}} & \cdots & -\frac{a_{l-1}}{\tau} \end{bmatrix} q + \begin{bmatrix} 0 \\ 0 \\ \vdots \\ 0 \\ 1 \end{bmatrix} \bar{w} \\ &=: A_q(\tau)q + B_q\bar{w} \\ w &= \left[ \frac{c_0}{\tau^l}, \frac{c_1}{\tau^{l-1}}, \dots, \frac{c_k}{\tau^{l-k}}, 0, \dots, 0 \right] q \\ &=: C_q(\tau)q\end{aligned} \quad (6.1.5)$$

where  $q = [q_1, \dots, q_l]^T \in \mathbb{R}^l$ ,  $l - k \geq \nu$ ,  $c_0 = a_0$ , and all  $a_i$ 's are chosen such that the polynomial  $s^l + a_{l-1}s^{l-1} + \dots + a_1s + a_0$  is Hurwitz. The detailed design procedure for coefficients  $a_i$ ,  $c_i$ , and the constant  $\tau$  will be discussed later. Finally, realization of the block  $Q_B(s)$  is identical to (6.1.5) except the corresponding inputs and outputs. That is, referring to Fig. 6.1, we obtain

$$\begin{aligned}\dot{p} &= A_q(\tau)p + B_q(u_r + \hat{u} - w) \\ \hat{u} &= C_q(\tau)p\end{aligned} \quad (6.1.6)$$



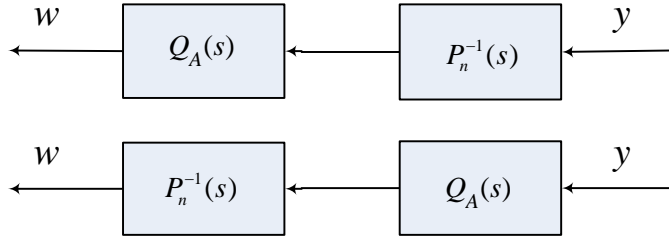


Figure 6.2: Since both systems  $Q_A$  and  $P_n^{-1}$  are linear, two configurations in this figure are equivalent in the steady-state. For implementation the configuration of the bottom is used while the upper one is employed for the stability analysis in this paper.

where  $p = [p_1, \dots, p_l]^T \in \mathbb{R}^l$ .

**Remark 6.1.1.** Obviously, the realization (6.1.4) alone cannot be implemented because it corresponds to an improper transfer function. Instead, the block  $Q_A(s)P_n^{-1}(s)$  is implemented together. Referring to Fig. 6.2 we propose the following implementation in the state space, whose transfer function is proper:

$$\begin{aligned}
 \dot{q} &= A_q q + B_q y \\
 \dot{\bar{z}} &= \bar{S} \bar{z} + \bar{G} C_q q \\
 w &= \frac{1}{g_n} (-\bar{F}_1 \bar{z} - \bar{F}_2 T_\tau q + C_q A_q^\nu q + C_q A_q^{\nu-1} B_q y)
 \end{aligned} \tag{6.1.7}$$

where

$$T_\tau = \begin{bmatrix} C_q \\ C_q A_q \\ \vdots \\ C_q A_q^{\nu-1} \end{bmatrix}.$$

The analysis in this paper uses the combination of (6.1.4) and (6.1.5), instead of (6.1.7), because it greatly simplifies the stability analysis. However, although the input-output responses of two representations are the same, it should be noted that time responses between the two cases are different.  $\square$

Based on the obtained state space realizations, we will represent the closed-loop system as a singular perturbation form. In order to obtain the standard

singular perturbation form, we change coordinates for states  $q$  and  $p$  as follows:

$$\xi_i := \tau_q^{i-(l+1)} q_i, \quad \zeta_i := \tau_q^{i-(l+1)} p_i, \quad i = 1, \dots, l. \quad (6.1.8)$$

On the other hand, since  $s^i y = y^{(i)} = x_{i+1}$ ,  $s^\nu y = \dot{x}_\nu$ , and  $u = u_r + \hat{u} - w$ , the equation for  $\bar{w}$  in (6.1.4b) can again be written in the new coordinates as

$$\begin{aligned} \bar{w} &= \frac{1}{g_n} \left( -\bar{F}_1 \bar{z} - \bar{F}_2 x + F_1 z + F_2 x + g(u_r + \hat{u} - w + d) \right) \\ &= \frac{1}{g_n} \left( -\bar{F}_1 \bar{z} + F_1 z - \bar{F}_2 x + F_2 x + gC_1(\zeta - \xi) + g(u_r + d) \right). \end{aligned} \quad (6.1.9)$$

From (6.1.8) and (6.1.9), the dynamics  $\xi$  and  $\zeta$  become

$$\begin{aligned} \tau \dot{\xi} &= (A_\xi - \frac{g}{g_n} B_\xi C_\xi) \xi + \frac{g}{g_n} B_\xi C_\xi \zeta + \frac{1}{g_n} B_\xi \{ \tilde{F}(z, \bar{z}, x) + g(u_r + d) \}, \quad w = C_\xi \xi, \\ \tau \dot{\zeta} &= -B_\xi C_\xi \xi + (A_\xi + B_\xi C_\xi) \zeta + B_\xi u_r, \quad \hat{u} = C_\xi \zeta \end{aligned} \quad (6.1.10)$$

where  $\tilde{F}(z, \bar{z}, x) = -\bar{F}_1 \bar{z} - \bar{F}_2 x + F_1 z + F_2 x$  and  $A_\xi$ ,  $B_\xi$ , and  $C_\xi$  imply  $A_q$ ,  $B_q$ , and  $C_q$  when  $\tau = 1$ .

Then, from the equation (6.1.1), (6.1.3), (6.1.4), and (6.1.10), the overall closed-loop system can be written as

$$\begin{aligned} \dot{\eta} &= A_c \eta + B_c y_r - E_c y, \quad u_r = C_c \eta + D_c y_r - H_c y, \\ \dot{x} &= A x + B \{ F_1 z + F_2 x + gC_\xi(\zeta - \xi) + g u_r + g d \}, \\ \dot{z} &= S z + G y, \\ \dot{\bar{z}} &= \bar{S} \bar{z} + \bar{G} y, \quad y = C x, \end{aligned} \quad (6.1.11a)$$

and

$$\begin{aligned} \tau \dot{\xi} &= (A_\xi - \frac{g}{g_n} B_\xi C_\xi) \xi + \frac{g}{g_n} B_\xi C_\xi \zeta + \frac{1}{g_n} B_\xi \{ \tilde{F}(z, \bar{z}, x) + g(u_r + d) \}, \\ \tau \dot{\zeta} &= -B_\xi C_\xi \xi + (A_\xi + B_\xi C_\xi) \zeta + B_\xi u_r, \end{aligned} \quad (6.1.11b)$$

From the overall closed-loop system (6.1.11), it is observed that, for relatively small  $\tau$ , the system is in the standard singular perturbation form.

## 6.2 Analysis of Disturbance Observer based on Singular Perturbation Theory

In this section, we will discuss the nominal performance recovery and robust stability for the disturbance observer based control scheme from the singular perturbation theory. It is observed from (6.1.11) that the variables  $x$ ,  $z$ ,  $\bar{z}$ ,  $\eta$ ,  $r$ , and  $d$  are considered as slow variables, while the state  $\xi$  and  $\zeta$  are regarded as fast variables. If the fast dynamics has an isolated equilibrium for each (frozen) slow variables and the equilibrium (depending on  $x$ ,  $z$ ,  $\bar{z}$ ,  $\eta$ ,  $r$ ,  $d$ ) is exponentially stable, then the overall closed-loop system behaves as the reduced system (that is, the overall closed-loop system is restricted to the slow manifold) with sufficiently small  $\tau$ , under the assumption that the slow variables are bounded and not varying fast. In order to show that the disturbance observer recovers the steady-state performance of the nominal closed-loop system (6.1.2) and (6.1.3) and guarantees robust stability of the overall closed-loop system (6.1.11), we first obtain the quasi-steady-state system. And then, we investigate under what condition the overall closed-loop system (6.1.11) is exponential stable and the nominal performance is recovered.

The equilibrium of (6.1.11b) for each frozen slow variables is,

$$\begin{bmatrix} \xi^* \\ \zeta^* \end{bmatrix} = -\mathcal{A}_f^{-1} \begin{bmatrix} \frac{1}{g_n} B_\xi \{ \tilde{F}(z, \bar{z}, x) + g(u_r + d) \} \\ B_\xi u_r \end{bmatrix} \quad (6.2.1)$$

where

$$\mathcal{A}_f = \begin{bmatrix} A_\xi - \frac{g}{g_n} B_\xi C_\xi & \frac{g}{g_n} B_\xi C_\xi \\ -B_\xi C_\xi & A_\xi + B_\xi C_\xi \end{bmatrix}. \quad (6.2.2)$$

After simple calculation using the matrix inversion lemma (Lemma A. 8 in Appendix), each equilibrium is calculated as

$$\begin{aligned} \xi^* &= -\frac{g_n + g}{g_n} (A_\xi - \frac{g}{g_n} B_\xi C_\xi)^{-1} B_\xi u_r, \\ \zeta^* &= \frac{1}{g_n + g} (A_\xi + \frac{g_n}{g_n + g} B_\xi C_\xi)^{-1} B_\xi \{ \tilde{F}(z, \bar{z}, x) + gd - g_n u_r \}. \end{aligned}$$

With the equilibrium (6.2.1), we derive the quasi-steady-state system (*i.e.*, slow dynamics on the slow manifold when  $\tau = 0$ ) as follows:

$$\begin{aligned}\dot{\eta} &= A_c\eta + B_cr - E_cy, & u_r &= C_c\eta + D_cr - H_cy, \\ \dot{x} &= Ax + B\{\bar{F}_1\bar{z} + \bar{F}_2x + g_nu_r\}, \\ \dot{\bar{z}} &= \bar{S}\bar{z} + \bar{G}Cx, \\ \dot{z} &= Sz + GCx, & y &= Cx.\end{aligned}\tag{6.2.3}$$

The quasi-steady-state system (6.2.3) is the key role to explain the nominal performance recovery of the disturbance observer and the extreme case when  $\tau = 0$ . From this reduced system, we find out several interesting points. First, the input disturbance  $d$  is completely rejected from the control input. In addition, the quasi-steady-state subsystem is nothing but the nominal closed-loop system augmented by the zero dynamics of the real plant. Therefore, if the boundary-layer subsystem is exponentially stable, then the overall system behaves like the quasi-steady-state system (6.2.3) after the transient of fast dynamics of  $\xi$  and  $\zeta$ . In this way, the steady-state performance is recovered to the nominal one. Second, in the viewpoint of the outer-loop controller (6.1.3), the plant to be controlled is approximated as the nominal model (6.1.2) that is completely known to the controller designer. Finally, the zero dynamics of the plant (*i.e.*,  $z$ -dynamics of (6.1.1a)) is disconnected from the output  $y$ , that is, becomes unobservable from the output. In fact, it is replaced by the zero dynamics of the nominal model (*i.e.*,  $\bar{z}$ -dynamics of (6.1.2)). These points are explored more in Section 6.3.

Now, we analyze the robust stability of the overall closed-loop system (6.1.11) based on the singular perturbation approach.

**Theorem 6.2.1.** Under Assumption 6.1.1, 6.1.2, and 6.1.3 there exists a positive constant  $\bar{\tau}$  such that, for all  $0 < \tau < \bar{\tau}$ , the overall closed-loop system (6.1.11) is robustly exponentially stable if the matrix  $\mathcal{A}_f$  in (6.2.2) is Hurwitz for all uncertain  $g$ .  $\square$

*Proof.* From the singular perturbation theory, if both the quasi-steady-state and the boundary-layer subsystem are exponentially stable, then the overall closed-loop system is exponentially stable. Since the quasi-steady-state subsystem (6.2.3)

is the nominal closed-loop system (6.1.2) and (6.1.3) augmented by the zero dynamics of the real plant (6.1.1a), from Assumption 6.1.1 and 6.1.2, it follows that (6.2.3) is exponentially stable. On the other hands, the system matrix of the boundary-layer subsystem is nothing but  $\mathcal{A}_f$  of (6.2.2). Therefore, the proof is completed since the matrix  $\mathcal{A}_f$  is Hurwitz.  $\square$

It is emphasized that the matrix  $\mathcal{A}_f$  plays a key role to determine the stability of the overall closed-loop system (6.1.11). If it is satisfied, then (6.1.11) is robustly stable for the sufficiently small  $\tau$ . Next lemma shows the condition for  $a_i$  and  $c_i$ , (*i.e.*, the coefficients of Q-filter) to make  $\mathcal{A}_f$  Hurwitz.

**Lemma 6.2.2.** The matrix  $\mathcal{A}_f$  is Hurwitz if and only if the following two polynomials are Hurwitz:

$$\begin{aligned} p_a(s) &= s^l + a_{l-1}s^{l-1} + \cdots + a_1s + a_0 \\ p_f(s) &= s^l + a_{l-1}s^{l-1} + \cdots + a_{k+1}s^{k+1} \\ &\quad + (a_k + \frac{g - g_n}{g_n}c_k)s^k + \cdots + (a_0 + \frac{g - g_n}{g_n}c_0). \end{aligned} \tag{6.2.4a}$$

$\square$

*Proof.* We compute the characteristic polynomial of the matrix  $\mathcal{A}_f$  as follows. In the derivation, we use the property of the determinant that adding or subtracting a row/column block to another row/column block leaves the determinant unchanged:

$$\begin{aligned} \det \begin{bmatrix} sI - A_\xi + \frac{g}{g_n}B_\xi C_\xi & -\frac{g}{g_n}B_\xi C_\xi \\ B_\xi C_\xi & sI - A_\xi - B_\xi C_\xi \end{bmatrix} &= \det \begin{bmatrix} sI - A_\xi + \frac{g}{g_n}B_\xi C_\xi & sI - A_\xi \\ B_\xi C_\xi & sI - A_\xi \end{bmatrix} \\ &= \det \begin{bmatrix} sI - A_\xi + \frac{g-g_n}{g_n}B_\xi C_\xi & 0 \\ B_\xi C_\xi & sI - A_\xi \end{bmatrix}. \end{aligned}$$

Therefore, the characteristic polynomial of the matrix  $\mathcal{A}_f$  is  $p_a(s)p_f(s)$  where

$$p_a(s) = \det \left[ sI - A_\xi \right], \quad p_f(s) = \det \left[ sI - A_\xi + \frac{g-g_n}{g_n}B_\xi C_\xi \right]$$

which completes the proof.  $\square$

From the analysis in the above, it is clear that the stability of the disturbance observer control scheme under a sufficiently small  $\tau$  is determined by two polynomials  $p_a(a)$  and  $p_f(s)$  of Lemma 6.2.2. As discussed in Section 3.2.2, one can always design the coefficients  $a_i$  and  $c_i$  such that the polynomial  $p_f(s)$  is Hurwitz. In addition, if  $p_f(s)$  is Hurwitz, then  $p_a(s)$  is also Hurwitz since  $g_n \in [\bar{g}, g]$ .

## 6.3 Discussion on Disturbance Observer Approach

This section is for discussing several new findings and reinterpretations obtained from the proposed analysis of disturbance observer in the state space.

### 6.3.1 Relation of Robust Stability Condition between State Space and Frequency Domain Analysis

It is observed that Assumption 2.1.1 and the conditions 1–2 of Theorem 2.2.1 are equivalent to Assumption 6.1.1, 6.1.2, 6.1.3, and the Hurwitzness of  $\mathcal{A}_f$  of Theorem 6.2.1. Therefore, Theorem 2.2.1 is equivalent to Theorem 6.2.1. As a result, Remark 2.2.1 still hold for Theorem 6.2.1.

### 6.3.2 Effect of Zero Dynamics

Looking at the quasi-steady-state model (6.2.3), we observe that the zero dynamics of the plant is disconnected from the output  $y$ , which can be viewed as that the effective disturbance observer makes the zero dynamics almost unobservable. Instead, the nominal zero dynamics (having the state  $\bar{z}$ ) substitutes for the role of the true one. Therefore, in order to have the internal state  $z$  bounded under the effective disturbance observer, minimum phaseness of the plant is necessary so that the  $z$ -dynamics of (6.2.3) becomes input-to-state stable (ISS) with  $x_1$  as the input.

This analysis suggests that, if the outer-loop controller design takes into account the initial conditions of the plant for (slow) transient performance<sup>2</sup> of  $y(t)$ , then it should consider  $x(0)$  and  $\bar{z}(0)$ , but not  $z(0)$ . Note also that, if  $S$  and

---

<sup>2</sup>In this Chapter, 'fast/slow transient' implies the transient response of the fast/slow variables, respectively.

$\bar{S}$ , and  $G$  and  $\bar{G}$ , are similar to each other, respectively, then the  $\bar{z}$ -dynamics of (6.2.3) plays the role of the state observer for  $z$ . Therefore, it is sometimes desirable that the zero dynamics of the plant is fast enough for the nominal state  $\bar{z}(t)$  to converge quickly to its true counterpart  $z(t)$ . It is also noted that, if a state observer is used as a part of the outer-loop controller, then the estimated state for the zero dynamics is more likely to be  $\bar{z}(t)$  rather than  $z(t)$ , because the observer is looking at the quasi-steady-state subsystem when  $\tau$  is sufficiently small.

### 6.3.3 Stability of Nominal Closed-loop System

Assuming the plant  $P(s)$  is of minimum phase, Assumption 6.1.3 is about the stability of  $P_n(s)$  combined with the outer-loop controller  $C(s)$ , and implies the stability of the nominal closed-loop transfer function  $P_n(s)C(s)/(1 + P_nC(s))$  when the unity-feedback configuration is used. Obviously, since the primary goal of the outer-loop controller is to stabilize the nominal closed-loop system, this assumption naturally holds for most cases. Note that a stable  $P_n(s)$  can just be taken without using the outer-loop controller  $C(s)$  because Assumption 6.1.3 is satisfied with  $C(s) \equiv 0$  and a stable  $P_n(s)$ . In this way, a robust stabilization of the plant  $P(s)$  may be achieved by the disturbance observer structure only. (However, our philosophy is that stabilization of  $P_n(s)$  is the responsibility of the outer-loop controller  $C(s)$  if  $P_n(s)$  is not stable. This point is in contrast to [UH93, CYC<sup>+</sup>03], where the stabilization of  $P(s)$  is achieved by designing both  $P_n(s)$  and  $Q(s)$ .)

### 6.3.4 Infinite Gain Property with $p$ -dynamics

It is known that a behind-the-scenes characteristic of the disturbance observer structure is that the Q-filter  $Q_B(s)$  constructs an infinite gain block in the feedback loop. In other words, by noting that Fig. 6.3 is an equivalent to the shaded block of Fig. 6.1, it is observed that the magnitude of  $1/(1 - Q_B(j\omega))$  tends to infinity at low frequencies where  $Q_B(j\omega) \approx 1$ . Indeed, the transfer function  $1/(1 - Q_B(s))$  always has a pole at the origin, and this fact is already reflected in our analysis as that, for (6.1.6) that is  $\dot{p} = (A_q + B_q C_q)p + B(u_r - w)$ , the  $(l, 1)$ -element of the matrix  $A_q + B_q C_q$  is always zero. Therefore, the system (6.1.6)

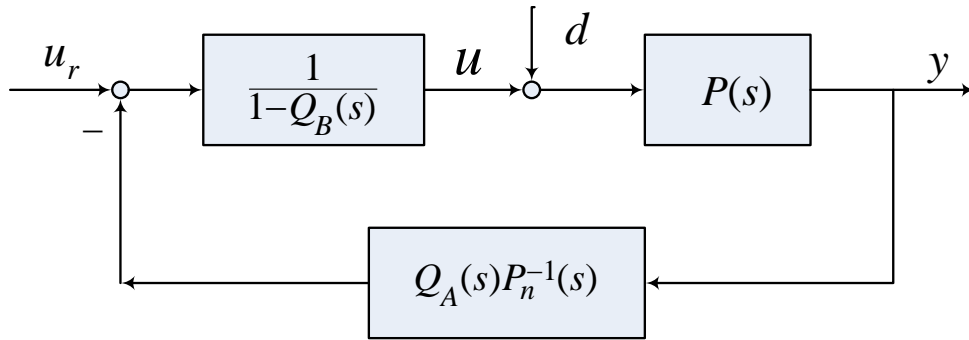


Figure 6.3: Equivalent configuration of the shaded block of Fig. 6.1

is not asymptotically stable by itself. Instead, the combined dynamics of (6.1.6) and (6.1.5) is asymptotically stable for frozen slow variables if the matrix  $\mathcal{A}_f$  is Hurwitz. This point is more easily seen in (6.1.11b). In fact, we note that, the  $(l, 1)$ -element of  $(A_\xi + B_\xi C_\xi)$  for  $\tau \dot{\zeta} = (A_\xi + B_\xi C_\xi)\zeta - B_\xi C_\xi \xi + B_\xi u_r$  of (6.1.11b) is zero, but thanks to the term  $\frac{g}{g_n} B_\xi C_\xi \zeta$  in  $\xi$ -dynamics of (6.1.11b), the Hurwitzness of  $\mathcal{A}_f$  is possible. The source of the term  $\frac{g}{g_n} B_\xi C_\xi \zeta$  is the signal  $\hat{u}$  in  $\bar{w}$  of (6.1.9). Since the appearance of  $\hat{u}$  in  $\bar{w}$  is due to the fact that  $\bar{w}$  depends on  $y^\nu = \dot{x}_\nu$  which has  $\hat{u}$  as one of the inputs to the plant, it can be seen that the helpful term comes through the plant  $P(s)$ . Therefore, if the input to the plant is modified by, for example, the actuator saturation, then the stability of fast dynamics is affected accordingly.

Infinite gain property leads to an interesting fact that, unlike some intuition that the signal  $w$  in Fig. 6.1 is a low-pass filtered signal approximating  $(u + d)$  while  $\hat{u}$  approximates  $u$ , the signal  $w$  is mimicking the external input  $u_r$  and  $\hat{u}$  approximates the important signal  $(1/g)(-\tilde{F}(z, \bar{z}, x) + g_n u_r - g d)$ . (This is easily seen from (6.2.1) keeping in mind that  $w = C_\xi \xi \rightarrow C_\xi \xi^*$  and  $\bar{u} = C_\xi \zeta \rightarrow C_\xi \zeta^*$ .) When the control system with the disturbance observer is working well, the signal  $(u_r - w)$  is nearly zero (but not identically zero) at low frequencies and this small signal is amplified through the almost infinite gain block (see Fig. 6.3) so that the signal  $u$  contains all the necessary signal components for making the overall system be a nominal one with disturbance free.



### 6.3.5 Peaking in Fast Transient

By choosing the design parameter  $\tau$  sufficiently small, the poles of  $Q_A(s)$  (*i.e.*, (6.1.5)) are located far left in the complex plane. More specifically, if  $\lambda_i$ 's are roots of  $s^l + a_{l-1}s^{l-1} + \dots + a_0 = 0$ , then the poles of (6.1.5) are  $\lambda_i/\tau$ . Then, under the structure of (6.1.5), the peaking phenomenon [SK91] happens for the state  $q$ . Peaking phenomenon is briefly summarized as follows. The state  $q(t)$  obeys that  $\|q(t)\| \leq k_1(\tau)e^{-(\lambda/\tau)t}\|q(0)\| + k_2(\tau)\int_0^t e^{-(\lambda/\tau)(t-s)}\bar{w}(s)ds$  with some  $\lambda > 0$  and two positive constants  $k_1$  and  $k_2$  depending on  $\tau$ . While we can speed up the transient by reducing  $\tau$ , the constant  $k_1$  (and  $k_2$ , as well) increases in the order of  $1/\tau^{l-1}$ , which explains the fact that the state  $q(t)$  may have very large value during the initial period for some initial conditions. This initial peaking effect then increases the value of  $w$  (see the real implementation (6.1.7), and also the equation for  $w$  in (6.1.5)). The peaks of  $w$  in the fast transient may perturb the slow state  $x$  during the fast initial period (because  $C_\xi(\zeta - \xi)$  in (6.1.11a) will have unwanted large absolute values then). Peaking phenomenon also happens for the state  $p$  of (6.1.6).

**Remark 6.3.1.** Although the structure of (6.1.11b) (*i.e.*, another representation of (6.1.5) and (6.1.6)) does not seem to show peaking phenomenon for  $\xi$  and  $\zeta$ , the initial condition for  $\xi(0)$  and  $\zeta(0)$  coming from (6.1.8) already reflects the peaking phenomenon of (6.1.5) and (6.1.6), that is, they may be very large with small  $\tau$ .  $\square$

Peaking phenomenon becomes less apparent under the following cases.

1. The parameter  $\tau$  is not very small.
2. The relative degree of the plant is not very high. (For mechanical systems, it is usually two.)
3. The overall system begins its operation on the slow manifold. For example, all the initial conditions of the overall control system including the disturbance  $d(0)$  are zero. (This is the case for some motion control systems.)

In summary, it is not true in general that the conventional linear disturbance observer structure recovers the (slow) transient performance to the nominal one.

A possible remedy to this problem is to modify the disturbance observer structure as suggested in [BS08].

## 6.4 Nominal Performance Recovery with respect to Time Constant of Q-filter

In the stability analysis discussed so far, the bound of  $\tau$  for robust stability of (6.1.11) is not explicitly provided. However, its bound must be determined for the complete stability analysis. Therefore, in this section, we derive the stability analysis based on Lyapunov theory. Furthermore, the nominal performance recovery by the disturbance observer with respect to  $\tau$  is presented.

The closed-loop system (6.1.11) can be compactly written as

$$\begin{aligned}\dot{\mathcal{X}} &= \mathcal{A}_s \mathcal{X} + \mathcal{A}_{xq} \mathcal{Z} + \mathcal{B}_x \mathcal{V}, \\ \tau \dot{\mathcal{Z}} &= \mathcal{A}_f \mathcal{Z} + \mathcal{A}_{qx} \mathcal{X} + \mathcal{B}_q \mathcal{V}\end{aligned}\tag{6.4.1}$$

where  $\mathcal{X} := [\eta; x; z; \bar{z}]$ ,  $\mathcal{Z} := [\xi; \zeta]$ , and  $\mathcal{V} := [r; d]$ . The matrices  $\mathcal{A}_s$ ,  $\mathcal{A}_{xq}$ ,  $\mathcal{B}_x$ ,  $\mathcal{A}_{qx}$ , and  $\mathcal{B}_q$  are as given by

$$\begin{aligned}\mathcal{A}_s &:= \begin{bmatrix} A_c & -E_c C & 0_{h \times n-\nu} & 0_{h \times \bar{n}-\nu} \\ gBC_c & A + B(F_2 - gH_c C) & BF_1 & 0_{\nu \times \bar{n}-\nu} \\ 0_{n-\nu \times h} & GC & S & 0_{n-\nu \times \bar{n}-\nu} \\ 0_{\bar{n}-\nu \times h} & \bar{G}C & 0_{\bar{n}-\nu \times n-\nu} & \bar{S} \end{bmatrix}, \\ \mathcal{A}_{xq} &:= \begin{bmatrix} 0_{h \times l} & 0_{h \times l} \\ -gBC_\xi & gBC_\xi \\ 0_{n \times l} & 0_{n \times l} \\ 0_{\bar{n} \times l} & 0_{\bar{n} \times l} \end{bmatrix}, \quad \mathcal{B}_x := \begin{bmatrix} B_c & 0_{h \times 1} \\ gBD_c & gB \\ 0_{n \times 1} & 0_{n \times 1} \\ 0_{\bar{n} \times 1} & 0_{\bar{n} \times 1} \end{bmatrix}, \\ \mathcal{A}_{qx} &:= \begin{bmatrix} \frac{g}{g_n} B_\xi C_c & \frac{1}{g_n} B_\xi [-\bar{F}_2 + F_2 - gH_c C] & \frac{1}{g_n} B_\xi F_1 & -\frac{1}{g_n} B_\xi \bar{F}_1 \\ B_\xi C_c & -B_\xi H_c C & 0_{l \times n-\nu} & 0_{l \times \bar{n}-\nu} \end{bmatrix}, \\ \mathcal{B}_q &:= \begin{bmatrix} \frac{g}{g_n} B_\xi D_c & \frac{g}{g_n} B_\xi \\ B_\xi D_c & 0_{l \times 1} \end{bmatrix}.\end{aligned}$$

Let  $h(\mathcal{X}, \mathcal{V}) := -\mathcal{A}_f^{-1}(\mathcal{A}_{qx}\mathcal{X} + \mathcal{B}_q\mathcal{V}) = [\xi^*; \zeta^*]$ , which is the isolated equilibrium of (6.1.11b) for each (frozen) slow variables. In fact, it is also equal to  $[\xi^*; \zeta^*]$  in (6.2.1). With  $\mathcal{Y} := \mathcal{Z} - h(\mathcal{X}, \mathcal{V})$ , we have

$$\begin{aligned}\dot{\mathcal{X}} &= \mathcal{F}_s\mathcal{X} + \mathcal{A}_{xq}\mathcal{Y} + (\mathcal{B}_x - \mathcal{A}_{xq}\mathcal{A}_f^{-1}\mathcal{B}_q)\mathcal{V} \\ \dot{\mathcal{Y}} &= \mathcal{F}_q\mathcal{X} + \left(\frac{1}{\tau}\mathcal{A}_f + \mathcal{A}_f^{-1}\mathcal{A}_{qx}\mathcal{A}_{xq}\right)\mathcal{Y} \\ &\quad + \mathcal{A}_f^{-1}\mathcal{A}_{qx}(\mathcal{B}_x - \mathcal{A}_{xq}\mathcal{A}_f^{-1}\mathcal{B}_q)\mathcal{V} + \mathcal{A}_f^{-1}\mathcal{B}_q\dot{\mathcal{V}}.\end{aligned}\tag{6.4.2}$$

where  $\mathcal{F}_s := \mathcal{A}_s - \mathcal{A}_{xq}\mathcal{A}_f^{-1}\mathcal{A}_{qx}$  and  $\mathcal{F}_q := \mathcal{A}_f^{-1}\mathcal{A}_{qx}(\mathcal{A}_s - \mathcal{A}_{xq}\mathcal{A}_f^{-1}\mathcal{A}_{qx})$ . Note that the  $\mathcal{X}$ -dynamics without the term involving  $\mathcal{Y}$  in (6.4.2) is the quasi-steady-state model (6.2.3). In order to show that the closed-loop system (6.1.11) behaves like (6.2.3), let the solution of (6.2.3) be  $\mathcal{X}_N(t)$ , that is,  $\mathcal{X}_N(t)$  satisfies that  $\dot{\mathcal{X}}_N = \mathcal{F}_s\mathcal{X}_N + (\mathcal{B}_x - \mathcal{A}_{xq}\mathcal{A}_f^{-1}\mathcal{B}_q)\mathcal{V}$  where  $\mathcal{F}_s$  is Hurwitz by Assumption 6.1.1 and 6.1.3. The solution  $\mathcal{X}_N(t)$  is hence bounded. Then, with  $\tilde{\mathcal{X}} := \mathcal{X} - \mathcal{X}_N$ , we have  $\dot{\tilde{\mathcal{X}}} = \mathcal{F}_s\tilde{\mathcal{X}} + \mathcal{A}_{xq}\mathcal{Y}$ , while the  $\mathcal{Y}$ -dynamics of (6.4.2) is rewritten as

$$\dot{\mathcal{Y}} = \mathcal{F}_q\tilde{\mathcal{X}} + \left(\frac{1}{\tau}\mathcal{A}_f + \mathcal{A}_f^{-1}\mathcal{A}_{qx}\mathcal{A}_{xq}\right)\mathcal{Y} + \mathcal{B}_r\theta$$

where  $\theta := [\mathcal{X}_N^T, \mathcal{V}^T, \dot{\mathcal{V}}^T]^T$  and  $\mathcal{B}_r$  is

$$\mathcal{B}_r := \begin{bmatrix} \mathcal{A}_f^{-1}\mathcal{A}_{qx}\mathcal{F}_s & \mathcal{A}_f^{-1}\mathcal{A}_{qx}(\mathcal{B}_x - \mathcal{A}_{xq}\mathcal{A}_f^{-1}\mathcal{B}_q) & \mathcal{A}_f^{-1}\mathcal{B}_q \end{bmatrix}.$$

If the matrices  $\mathcal{A}_f$  and  $\mathcal{F}_s$  are Hurwitz, then there exist positive definite matrices  $P_f$  and  $P_s$  such that  $P_f\mathcal{A}_f + \mathcal{A}_f^T P_f = -2I$  and  $P_s\mathcal{F}_s + \mathcal{F}_s^T P_s = -2I$ . Let  $V(\tilde{\mathcal{X}}, \mathcal{Y}) = \frac{1}{2}\tilde{\mathcal{X}}^T P_s \tilde{\mathcal{X}} + \frac{1}{2}\mathcal{Y}^T P_f \mathcal{Y}$ . Then, we obtain

$$\dot{V} \leq -\|\tilde{\mathcal{X}}\|^2 - \frac{1}{\tau}\|\mathcal{Y}\|^2 + \gamma_1\|\tilde{\mathcal{X}}\|\|\mathcal{Y}\| + \gamma_2\|\mathcal{Y}\|^2 + \gamma_3\|\mathcal{Y}\|,$$

where  $\gamma_1 = \|P_s\mathcal{A}_{xq}\| + \|P_f\mathcal{F}_q\|$ ,  $\gamma_2 = \|P_f\mathcal{A}_f^{-1}\mathcal{A}_{qx}\mathcal{A}_{xq}\|$ ,  $\gamma_3 = \|P_f\mathcal{B}_r\| \max_{0 \leq t \leq \infty} \|\theta(t)\|$ . If  $\tau < \bar{\tau} := 1/(\gamma_1^2 + 2\gamma_2)$ , then it can be shown that  $\dot{V} < 0$  when  $\|\mathcal{Y}\| > 2\gamma_3\tau$ .

Now, define  $\bar{V} := \|\tilde{\mathcal{X}}\|^2 + \frac{1}{\tau}\|\mathcal{Y}\|^2$ . Then, it holds that

$$\dot{V} \leq -\frac{1}{2}\bar{V} + \gamma_3\sqrt{\tau}\sqrt{\bar{V}}$$

which means that, if  $\bar{V} > 4\gamma_3^2\tau$ , then  $\dot{V} < 0$ . And, a positive constant  $\mu_1$  is given by

$$\mu_1 := \max_{\bar{V}=4\gamma_3^2\tau} V(\tilde{\mathcal{X}}, \mathcal{Y}).$$

We define the set

$$\Omega_\xi := \{[\tilde{\mathcal{X}}; \mathcal{Y}] : V(\tilde{\mathcal{X}}, \mathcal{Y}) \leq \mu_1\}$$

Then, it is clear that all solutions of  $[\tilde{\mathcal{X}}; \mathcal{Y}]$  converge to the set  $\Omega_\xi$  as  $t \rightarrow \infty$ . If it converges to the set  $\Omega_\xi$ , then it remains the set  $\Omega_\xi$ . By the definition of  $V$  and  $\bar{V}$ ,

$$V = \frac{1}{2}\tilde{\mathcal{X}}^T P_s \tilde{\mathcal{X}} + \frac{1}{2}\mathcal{Y}^T P_f \mathcal{Y} \leq \rho_1 \bar{V}$$

where  $\rho_1 := \max\{\frac{1}{2}\lambda_{\max}(P_s), \frac{1}{2}\lambda_{\max}(P_f)\tau\}$ . For all  $[\tilde{\mathcal{X}}, \mathcal{Y}] \in \Omega_\xi$ ,  $\|\tilde{\mathcal{X}}\|^2 \leq \mu_1 \leq 4\rho_1\gamma_3^2\tau$  and thus,

$$\|\tilde{\mathcal{X}}\| \leq 2\gamma_3\sqrt{\rho_1}\sqrt{\tau}.$$

Since we assume that  $\tau$  is relatively small positive constant and  $\rho_1 = \lambda_{\max}(P_s)/2$  as  $\tau \rightarrow 0$ , the bound of  $\|\mathcal{X} - \mathcal{X}_N\|$  is proportional to the  $\sqrt{\tau}$ . This implies that  $V(\tilde{\mathcal{X}}(t), \mathcal{Y}(t))$  tends to arbitrarily small so that the error  $\mathcal{X}(t) - \mathcal{X}_N(t)$  becomes arbitrarily small, by taking  $\tau$  sufficiently small. Here, we summarize the result as follows.

**Theorem 6.4.1.** Under Assumption 6.1.1, 6.1.2, and 6.1.3, there exists a constant  $\bar{\tau} = 1/(\gamma_1^2 + 2\gamma_2) > 0$  such that, for all  $0 < \tau < \bar{\tau}$ , the closed-loop system (6.1.11) is exponentially stable when  $r = 0$  and  $d = 0$ . Furthermore, the part of the solution (6.1.11) denoted by  $[\eta(t); x(t); \bar{z}(t)]$  satisfies that

$$\limsup_{t \rightarrow \infty} \|[\eta(t); x(t); \bar{z}(t)] - [\eta_N(t); x_N(t); z_N(t)]\| \leq \Gamma_1\sqrt{\tau}$$

where  $\Gamma_1 := 2\gamma_3\sqrt{\rho_1}$  and  $[\eta_N(t); x_N(t); z_N(t)]$  is the solution of the nominal closed-loop system (6.1.2) and (6.1.3).  $\square$

As can be seen in Theorem 6.4.1, the error decreases proportional to  $\sqrt{\tau}$ . It implies that the performance of the disturbance observer is improved as the time constant  $\tau$  goes to zero.



# Chapter 7

## Nominal Performance Recovery and Stability Analysis for Disturbance Observer under Unmodeled Dynamics

Feedback system design including the disturbance observer based control is often achieved by neglecting fast unmodeled dynamics (e.g., actuator or sensor) for reducing design complexity [SD02, LT96]. It is based on an assumption that unmodeled dynamics is fast enough to be negligible. However, the disturbance observer contains two Q-filters as fast dynamics; therefore the assumption may not be satisfied when the time constant of the Q-filter is too small to enhance the disturbance rejection performance. As discussed in Chapter 4, it causes the degradation of performance and may lead to instability. On the other hand, in order to avoid instability caused by unmodeled dynamics, some guidelines for robust stability have been proposed [KK99, CYC<sup>+</sup>03, WT04]. However, they are also based on the small-gain theorem as well as can not deal with the plant with unstable poles.

This chapter presents the nominal performance recovery and stability analysis for the disturbance observer based control scheme under fast unmodeled dynamics. The contribution of this chapter is as follows:

- The stability analysis of disturbance observer based control scheme under the fast unmodeled dynamics is presented using the singular perturbation theory.

- In order to guarantee the robust stability, the explicit bound of a time constant of Q-filter with respect to the unmodeled dynamics is derived based on Lyapunov analysis.
- Finally, this chapter presents that the disturbance observer recovers a nominal performance, which is designed for the nominal model for the plant and the state error between the nominal and actual closed-loop system asymptotically converges to a set whose size is proportional to the square root of the time constant of Q-filter.

## 7.1 Problem Formulation

In this section, we introduce the disturbance observer based control scheme for an uncertain single-input single-output linear plant including unmodeled dynamics to achieve the nominal performance recovery in the presence of the disturbances and uncertainties. After the problem formulation, the overall closed-loop system is transformed to a singular perturbation form.

Consider the following class of uncertain plants:

$$\dot{z} = Sz + Gy, \quad y = Cx, \quad (7.1.1a)$$

$$\dot{x} = Ax + B\{F_1z + F_2x + g(u + d)\}, \quad (7.1.1b)$$

$$\tau_v \dot{v} = A_v v + B_v u_v, \quad u = C_v v, \quad (7.1.1c)$$

where  $x \in \mathbb{R}^\nu$  and  $z \in \mathbb{R}^{n-\nu}$  are the plant state,  $v \in \mathbb{R}^m$  is the state of the unmodeled dynamics, and  $u \in \mathbb{R}^1$ ,  $u_v \in \mathbb{R}^1$ ,  $y \in \mathbb{R}^1$ , and  $d \in \mathbb{R}^1$  are the plant input, the control input, the plant output, and the unknown disturbance, respectively. The matrices  $A$ ,  $B$ , and  $C$  are given by

$$A := \begin{bmatrix} 0_{\nu-1} & I_{\nu-1} \\ 0 & 0_{\nu-1}^T \end{bmatrix}, B := \begin{bmatrix} 0_{\nu-1} \\ 1 \end{bmatrix}, C := \begin{bmatrix} 1 & 0_{\nu-1}^T \end{bmatrix}.$$

The positive constant  $\tau_v$  is a time constant of unmodeled dynamics. The uncertain matrices  $S$ ,  $G$ ,  $F_1$ ,  $F_2$ ,  $A_v$ ,  $B_v$ , and  $C_v$  are of appropriate dimensions and  $g$  is an unknown constant. The disturbance  $d(t)$  and its derivative  $\dot{d}(t)$  are bounded with

known constants  $\phi_d$  and  $\phi_{dt}$  such that  $\|d(t)\| \leq \phi_d$  and  $\|\dot{d}(t)\| \leq \phi_{dt}$ , respectively.

**Assumption 7.1.1.** The uncertain plant (7.1.1) satisfy the following assumptions:

1. All uncertainties are bounded and the bounds are known *a priori*. In particular, there exist positive constants  $\underline{g}$  and  $\bar{g}$  such that  $\underline{g} \leq g \leq \bar{g}$ .
2. The matrix  $S$  is Hurwitz. □

Note that, in the absence of the unmodeled dynamics (7.1.1c), the plant (7.1.1a) and (7.1.1b) under consideration is in the normal form whose relative degree is  $\nu$ . In addition, the condition 2 implies that the plant (7.1.1a) and (7.1.1b) is of minimum phase, which is a conventional assumption on the disturbance observer approach.

**Assumption 7.1.2.** The unmodeled dynamics in the plant (7.1.1c) is exponentially stable (*i.e.*, the matrix  $A_v$  is Hurwitz) and  $-C_v A_v^{-1} B_v = 1$ . Furthermore, the time constant  $\tau_v$  is upper bounded by a positive constant  $\bar{\tau}_v$  which is known *a priori*. □

The above assumption implies that the DC gain of (7.1.1c) equals to one. Even though it is not, a non-unity gain can be integrated into the plant input gain  $g$ .

Now, we consider a nominal model for the uncertain plant (7.1.1) as follows:

$$\begin{aligned} \dot{z}_n &= \bar{S}z_n + \bar{G}y_n, & y_n &= Cx_n, \\ \dot{x}_n &= Ax_n + B\{\bar{F}_1z_n + \bar{F}_2x_n + g_n u_r\}, \end{aligned} \tag{7.1.2}$$

where  $x_n \in \mathbb{R}^\nu$  and  $z_n \in \mathbb{R}^{\bar{n}-\nu}$  are the state,  $u_r \in \mathbb{R}^1$  and  $y_n \in \mathbb{R}^1$  are the control input and the output of the nominal model, respectively. Notice that the order of the nominal zero dynamics  $z_n$  may not be equal to that of the zero dynamics (7.1.1a), *i.e.*,  $\bar{n}$  may not be equal to  $n$ .  $\bar{S}$ ,  $\bar{G}$ ,  $\bar{F}_1$ ,  $\bar{F}_2$ , and  $\bar{g}$  are the nominal values of  $S$ ,  $G$ ,  $F_1$ ,  $F_2$ , and  $g$ , respectively.

For the nominal model (7.1.2), consider an output feedback outer-loop controller as

$$\dot{\eta} = A_c\eta + B_cr - E_c y_n, \quad u_r = C_c\eta + D_cr - H_c y_n \tag{7.1.3}$$



where  $\eta \in \mathbb{R}^h$  is the state of output feedback controller and  $r$  is the reference input. The matrices  $A_c$ ,  $B_c$ ,  $C_c$ ,  $D_c$ ,  $E_c$ , and  $H_c$  are of appropriate dimensions. It is assumed that  $r(t)$  and  $\dot{r}(t)$  are bounded with known bounds  $\phi_r$  and  $\phi_{rt}$  such that  $\|r(t)\| \leq \phi_r$  and  $\|\dot{r}(t)\| \leq \phi_{rt}$ , respectively. As discussed in Chapter 6, when (7.1.3) is employed in the actual closed-loop system,  $\bar{y}$  should be replaced by  $y$ . In addition,  $u_r$ , the function of  $\eta$ ,  $r$ , and  $y$ , will be often used for simplification.

**Assumption 7.1.3.** The nominal closed-loop system (7.1.2) and (7.1.3) is exponentially stable. It implies that it is input-to-state stable with respect to the reference input  $r$ .  $\square$

As discussed in the previous chapters, Assumption 7.1.3 implies that the outer-loop controller (7.1.3) has to be designed to stabilize the nominal model (7.1.2).

Now, we will show that the plant (7.1.1) with the disturbance observer behaves as the disturbance-free nominal model (7.1.2) in the presence of the disturbance and model uncertainties. The disturbance observer as an inner-loop controller is proposed as

$$\dot{\bar{z}} = \bar{S}\bar{z} + \bar{G}\bar{w}, \quad w = \frac{1}{g_n}(-\bar{F}_1\bar{z} - \bar{F}_2\bar{w}^\dagger + \bar{w}^\nu), \quad (7.1.4a)$$

$$\dot{q} = A_q(\tau)q + B_q y, \quad \bar{w} = C_q(\tau)q, \quad (7.1.4b)$$

$$\dot{p} = A_q(\tau)p + B_q u_v, \quad \hat{u} = C_q(\tau)p, \quad (7.1.4c)$$

$$u_v = u_r + \hat{u} - w \quad (7.1.4d)$$

where  $\bar{z} \in \mathbb{R}^{\bar{n}-\nu}$ ,  $q \in \mathbb{R}^l$ , and  $p \in \mathbb{R}^l$  are the state,  $\bar{w}^\dagger = [\bar{w} \ \dot{\bar{w}} \ \dots \ \bar{w}^{\nu-1}]^T$ , and  $\bar{w}^i$  is the  $i$ -th derivative of the output  $\bar{w}$ . The matrices  $A_q(\tau)$ ,  $B_q$ , and  $C_q(\tau)$  are

$$A_q(\tau) := \begin{bmatrix} 0 & 1 & \dots & 0 \\ 0 & 0 & \dots & 0 \\ \vdots & \vdots & \ddots & \vdots \\ 0 & 0 & \dots & 1 \\ -\frac{a_0}{\tau^l} & -\frac{a_1}{\tau^{l-1}} & \dots & -\frac{a_{l-1}}{\tau} \end{bmatrix}, \quad B_q := \begin{bmatrix} 0 \\ 0 \\ \vdots \\ 0 \\ 1 \end{bmatrix},$$

$$C_q(\tau) := \begin{bmatrix} \frac{c_0}{\tau^l} & \frac{c_1}{\tau^{l-1}} & \dots & \frac{c_k}{\tau^{l-k}} & 0 & \dots & 0 \end{bmatrix}.$$

where  $l - k \geq \nu$ ,  $c_0 = a_0$ , and all  $a_i$ 's are chosen such that the polynomial  $s^l + a_{l-1}s^{l-1} + \dots + a_1s + a_0$  is Hurwitz. The detailed design procedure for coefficients  $a_i$ ,  $c_i$ , and  $\tau$  will be discussed later.

It is important to note that the disturbance observer in (7.1.4) is a state-space realization of the conventional disturbance observer, which is already proposed in Chapter 6. The dynamics (7.1.4a) has the same structure as an inverse dynamics of (7.1.2) and the dynamics (7.1.4b) and (7.1.4c) are the controllable canonical form realizations of a stable low-pass filter known as Q-filter. In addition, since  $l - k \geq \nu$ , the signal  $\bar{w}^\nu$  and  $\bar{w}^\dagger$  can be implemented from the state of (7.1.4b) and the output  $y$ .

Let us exchange the dynamics (7.1.4a) with (7.1.4b) as follows:

$$\dot{\bar{z}} = \bar{S}\bar{z} + \bar{G}y, \quad \bar{w} = \frac{1}{g_n}(-\bar{F}_1\bar{z} - \bar{F}_2y^\dagger + y^\nu), \quad (7.1.5a)$$

$$\dot{q} = A_q(\tau)q + B_q\bar{w}, \quad w = C_q(\tau)q, \quad (7.1.5b)$$

$$\dot{p} = A_q(\tau)p + B_qu_v, \quad \hat{u} = C_q(\tau)p, \quad (7.1.5c)$$

$$u_v = u_r + \hat{u} - w \quad (7.1.5d)$$

where  $y^\dagger = [y \ \dot{y} \ \dots \ y^{\nu-1}]$  and  $y^i$  is the  $i$ -th derivative of the output  $y$ . By virtue of the linearity, the input-output behavior between  $y$  and  $w$  of (7.1.4a) and (7.1.4b) is the same as that of (7.1.5a) and (7.1.5b). Throughout this chapter, for simple analysis, the dynamics (7.1.5) is used instead of (7.1.4), although the time response of  $q$  in (7.1.5) is different from that of (7.1.4).

In order to obtain a singular perturbation form, we change coordinates for states  $q$  and  $p$  as follows:

$$\xi_i := \tau^{i-(l+1)}q_i, \quad \zeta_i := \tau^{i-(l+1)}p_i. \quad (7.1.6)$$

With (7.1.6), the dynamics of  $\xi$ ,  $\zeta$ , and  $v$  are represented as

$$\begin{bmatrix} \tau\dot{\xi} \\ \tau\dot{\zeta} \\ \tau_v\dot{v} \end{bmatrix} = \mathcal{A}_u \begin{bmatrix} \xi \\ \zeta \\ v \end{bmatrix} + \begin{bmatrix} \frac{1}{g_n}B_\xi\{\tilde{F}(z, \bar{z}, x) + gd\} \\ B_\xi u_r \\ B_v u_r \end{bmatrix}, \quad (7.1.7)$$

where

$$\mathcal{A}_u := \begin{bmatrix} A_\xi & O_{l \times l} & \frac{g}{g_n} B_\xi C_v \\ -B_\xi C_\xi & A_\xi + B_\xi C_\xi & O_{l \times m} \\ -B_v C_\xi & B_v C_\xi & A_v \end{bmatrix},$$

$\tilde{F}(z, \bar{z}, x) := -\bar{F}_1 \bar{z} - \bar{F}_2 x + F_1 z + F_2 x$ , and  $A_\xi$ ,  $B_\xi$ , and  $C_\xi$  imply  $A_q$ ,  $B_q$ , and  $C_q$  when  $\tau_q = 1$ , respectively.

Then, from the equation (7.1.1), (7.1.3), (7.1.5a), and (7.1.7), the overall closed-loop system can be written as

$$\begin{aligned} \dot{\eta} &= A_c \eta + B_c r - E_c y, & u_r &= C_c \eta + D_c r - H_c y, \\ \dot{x} &= A x + B \{F_1 z + F_2 x + g(C_v v + d)\}, \\ \dot{z} &= S z + G y, \\ \dot{\bar{z}} &= \bar{S} \bar{z} + \bar{G} y, & y &= C x, \end{aligned} \tag{7.1.8a}$$

and

$$\begin{bmatrix} \tau \dot{\xi} \\ \tau \dot{\zeta} \\ \tau_v \dot{v} \end{bmatrix} = \mathcal{A}_u \begin{bmatrix} \xi \\ \zeta \\ v \end{bmatrix} + \begin{bmatrix} \frac{1}{g_n} B_\xi \{ \tilde{F}(z, \bar{z}, x) + g d \} \\ B_\xi u_r \\ B_v u_r \end{bmatrix}. \tag{7.1.8b}$$

From the overall closed-loop system (7.1.8), it is observed that, for relatively small  $\tau_v$  and  $\tau$ , the system is in the multi-parameter or the multi-time-scale singular perturbation form<sup>1</sup>.

## 7.2 Stability and Performance Analysis based on Singular Perturbation Theory

In this section, we will discuss the nominal performance recovery and robust stability for the disturbance observer based control scheme under the unmodeled dynamics using the singular perturbation theory. In order to present the nominal

---

<sup>1</sup>If time constants  $\tau$  and  $\tau_v$  are in same order, then the system is in the multi-parameter singular perturbation form [LS83], [KK79]. Otherwise, it is in the multi-time-scale singular perturbation form [LR85].

performance recovery of the disturbance observer based control system, we first obtain the quasi-steady-state system from the overall closed-loop system (7.1.8) for the extreme case  $\tau = \tau_v = 0$ . And then, we investigate under what condition the overall closed-loop system (7.1.8) is exponential stable and the nominal performance is recovered.

### 7.2.1 Nominal Performance Recovery

It is observed from (7.1.8) that the variables  $x$ ,  $z$ ,  $\bar{z}$ ,  $\eta$ ,  $r$ , and  $d$  are considered as slow variables, while the state  $\xi$ ,  $\zeta$ , and  $v$  are regarded as fast variables. If the fast dynamics has an isolated equilibrium for each (frozen) slow variables and the equilibrium (depending on  $x$ ,  $z$ ,  $\bar{z}$ ,  $\eta$ ,  $r$ ,  $d$ ) is exponentially stable, then the overall closed-loop system behaves as the quasi-steady-state system (*i.e.*, the overall closed-loop system is restricted to the slow manifold) with sufficiently small  $\tau$  and  $\tau_v$ , under the assumption that the slow variables are bounded and not varying fast.

The equilibrium of (7.1.8) for each frozen slow variables is,

$$\begin{bmatrix} \xi^* \\ \zeta^* \\ v^* \end{bmatrix} = -\mathcal{A}_u^{-1} \begin{bmatrix} \frac{1}{g_n} B_\xi \{ \tilde{F}(z, \bar{z}, x) + gd \} \\ B_\xi u_r \\ B_v u_r \end{bmatrix}. \quad (7.2.1)$$

With the help of the matrix inversion lemma (Lemma A. 8 in Appendix), each equilibrium is computed as

$$\xi^* = -\frac{g_n + g}{g_n} (A_\xi - \frac{g}{g_n} B_\xi C_\xi)^{-1} B_\xi u_r, \quad (7.2.2)$$

$$\zeta^* = \frac{1}{g_n + g} (A_\xi + \frac{g_n}{g_n + g} B_\xi C_\xi)^{-1} B_\xi \{ \tilde{F}(z, \bar{z}, x) + gd - g_n u_r \}, \quad (7.2.3)$$

$$v^* = \frac{1}{g} A_v^{-1} B_v \{ \tilde{F}(z, \bar{z}, x) + gd - g_n u_r \}. \quad (7.2.4)$$

With the equilibrium, we derive the quasi-steady-state system (*i.e.*, slow dy-

namics on the slow manifold when  $\tau = \tau_v = 0$ ) as follows:

$$\begin{aligned}\dot{\eta} &= A_c\eta + B_cr - E_cy, & u_r &= C_c\eta + D_cr - H_cy, \\ \dot{x} &= Ax + B\{\bar{F}_1\bar{z} + \bar{F}_2x + g_nu_r\}, \\ \dot{\bar{z}} &= \bar{S}\bar{z} + \bar{G}Cx, \\ \dot{z} &= Sz + GCx, & y &= Cx.\end{aligned}\tag{7.2.5}$$

The quasi-steady-state system (7.2.5) is also the key role to explain the nominal performance recovery of the disturbance observer based control scheme and the extreme case when  $\tau = \tau_v = 0$ . In fact, the quasi-steady-state system (7.2.5) is equivalent to (6.2.3). Since we already mentioned about the quasi-steady-state system (6.2.3) in Section 6.2, we omit the detailed explanation here.

Now, we analyze robust stability for the overall closed-loop system (7.1.8) based on the singular perturbation approach with respect to the ratio between  $\tau$  and  $\tau_v$ .

## 7.2.2 Multi-time-scale Singular Perturbation Analysis

In this section, we first discuss the case that the time constants  $\tau$  and  $\tau_v$  are in different order. When  $\tau_v \ll \tau$  (*i.e.*, the unmodeled dynamics is much faster than  $p$  and  $q$ -dynamics), (7.1.8) can be considered as the three-time scale singular perturbation form.

**Theorem 7.2.1.** Under Assumption 7.1.1, 7.1.2, and 7.1.3, there exists a positive constant  $\bar{\tau}$  such that, for all  $0 < \tau_v \ll \tau < \bar{\tau}$ , the overall closed-loop system (7.1.8) is robustly exponentially stable if the matrix  $\mathcal{A}_f$

$$\mathcal{A}_f := \begin{bmatrix} A_\xi - \frac{g}{g_n}B_\xi C_\xi & \frac{g}{g_n}B_\xi C_\xi \\ -B_\xi C_\xi & A_\xi + B_\xi C_\xi \end{bmatrix}\tag{7.2.6}$$

is Hurwitz for all uncertain  $g$ . □

*Proof.* Since  $\tau_v \ll \tau$ , we consider  $v$ -dynamics in (7.1.8) as fast dynamics, while the other dynamics are slow dynamics. From the singular perturbation theory, if both the quasi-steady-state and the boundary-layer subsystem are exponentially

stable, then the overall closed-loop system is exponentially stable. By Assumption 7.1.2, it follows that the boundary-layer subsystem ( $v$ -dynamics) is exponentially stable.

In the next step, we will show that the quasi-steady-state subsystem is exponentially stable. Since  $C_v A_v^{-1} B_v = -1$ , the quasi-steady-state system is easily calculated as follows:

$$\begin{aligned}\dot{\eta} &= A_c \eta + B_c r - E_c y, & u_r &= C_c \eta + D_c r - H_c y, \\ \dot{x} &= A x + B \{F_1 z + F_2 x + g C_\xi (\zeta - \xi) + g u_r + g d\}, \\ \dot{z} &= S z + G y, \\ \dot{\bar{z}} &= \bar{S} \bar{z} + \bar{G} y, & y &= C x,\end{aligned}\tag{7.2.7a}$$

and

$$\tau \begin{bmatrix} \dot{\xi} \\ \dot{\zeta} \end{bmatrix} = \mathcal{A}_f \begin{bmatrix} \xi \\ \zeta \end{bmatrix} + \begin{bmatrix} \frac{1}{g_n} B_\xi \{ \tilde{F}(z, \bar{z}, x) + g u_r + g d \} \\ B_\xi u_r \end{bmatrix},\tag{7.2.7b}$$

Now, it can be observed that (7.2.7) is the two-time scale singular perturbation form. In fact, it is exactly same as the system (6.1.11) in Section 6.1. By the same manner in Section 6.2, the dynamics (7.2.7a) and (7.2.7b) are considered as slow and fast dynamics, respectively. After a simple calculation, it is easy to see that (7.2.5) is its quasi-steady-state subsystem. From Assumption 7.1.1 and 7.1.3, it follows that (7.2.5) is exponentially stable. The proof is completed since the matrix  $\mathcal{A}_f$  is Hurwitz.  $\square$

It is emphasized that the matrix  $\mathcal{A}_f$  plays a key role to determine the stability of the overall closed-loop system (7.1.8). If it is satisfied, then (7.1.8) is robustly stable for the sufficiently small  $\tau$ . The detailed procedure so as to make the matrix  $\mathcal{A}_f$  Hurwitz was discussed in Section 3.2.2 and 6.2.

**Remark 7.2.1.** When the dynamics of Q-filter is much faster than the unmodeled dynamics  $v$  (*i.e.*,  $\tau \ll \tau_v$ ), the stability of the overall closed-loop system does not guaranteed. Since  $\tau \ll \tau_v$ , the dynamics of Q-filter are considered as fast

dynamics. Then, from (7.1.8), the system matrix of  $\xi$  and  $\zeta$  is

$$\begin{bmatrix} A_\xi & O_{l \times l} \\ -B_\xi C_\xi & A_\xi + B_\xi C_\xi \end{bmatrix}$$

and always has one eigenvalue at the origin. Therefore, the singular perturbation theory cannot be employed since the boundary-layer system is not exponentially stable. In fact, if the relative degree of  $v$ -dynamics is greater than one, then robust stabilization is impossible when the time constant  $\tau$  is much smaller than  $\tau_v$  as discussed in Chapter 4.  $\square$

### 7.3 Nominal Performance Recovery by Disturbance Observer under Unmodeled Dynamics

In the stability analysis discussed so far, the explicit bound of  $\tau$  for robust stability of (7.1.8) is not provided. However, in order to complete the stability analysis, the bound of  $\tau$  must be provided with respect to  $\tau_v$ , especially when the time constants  $\tau$  and  $\tau_v$  are in same order. In addition, the relation between the time constant  $\tau$  and the nominal performance recovery by the disturbance observer will be presented. In fact, as can be seen in Section 6.4, the error decreases proportional to  $\sqrt{\tau}$ . It implies that the performance of the disturbance observer is improved as the time constant  $\tau$  tends to be small. However, in contrast with Chapter 6, we cannot make the time constant  $\tau$  arbitrarily small when unmodeled dynamics exists. Furthermore, it may make the closed-loop system unstable. Now, we investigate the nominal performance recovery of the disturbance observer under unmodeled dynamics with respect to  $\tau$ .

For the convenience, (7.1.8) can be compactly written as

$$\begin{aligned} \dot{\mathcal{X}} &= \bar{\mathcal{A}}_s \mathcal{X} + \mathcal{A}_{xv} \mathcal{Z}_2 + \bar{\mathcal{B}}_x \mathcal{V}, \\ \tau \dot{\mathcal{Z}}_1 &= \bar{\mathcal{A}}_f \mathcal{Z}_1 + \bar{\mathcal{A}}_{qx} \mathcal{X} + \mathcal{A}_{qv} \mathcal{Z}_2 + \bar{\mathcal{B}}_q \mathcal{V}, \\ \tau_v \dot{\mathcal{Z}}_2 &= \mathcal{A}_v \mathcal{Z}_2 + \mathcal{A}_{vx} \mathcal{X} + \mathcal{A}_{vq} \mathcal{Z}_1 + \mathcal{B}_v \mathcal{V} \end{aligned} \quad (7.3.1)$$

where  $\mathcal{X} = [\eta; x; z; \bar{z}]$ ,  $\mathcal{Z}_1 := [\xi; \zeta]$ ,  $\mathcal{Z}_2 := v$ ,  $\mathcal{V} := [r; d]$ , and the matrices  $\bar{\mathcal{A}}_s$ ,  $\mathcal{A}_{xv}$ ,

$\bar{\mathcal{A}}_f$ ,  $\bar{\mathcal{A}}_{qx}$ ,  $\mathcal{A}_{qv}$ ,  $\mathcal{A}_{vx}$ ,  $\mathcal{A}_{vq}$ ,  $\bar{\mathcal{B}}_x$ ,  $\bar{\mathcal{B}}_q$ , and  $\mathcal{B}_v$  are

$$\begin{aligned} \bar{\mathcal{A}}_s &:= \begin{bmatrix} A_c & -E_c C & 0_{h \times n-\nu} & 0_{h \times \bar{n}-\nu} \\ 0_{\nu \times h} & A + B F_2 & B F_1 & 0_{\nu \times \bar{n}-\nu} \\ 0_{n-\nu \times h} & G C & S & 0_{n-\nu \times \bar{n}-\nu} \\ 0_{\bar{n}-\nu \times h} & \bar{G} C & 0_{\bar{n}-\nu \times n-\nu} & \bar{S} \end{bmatrix}, \quad \mathcal{A}_{xv} := \begin{bmatrix} 0_{h \times m} \\ g B C_v \\ 0_{n-\nu \times m} \\ 0_{\bar{n}-\nu \times m} \end{bmatrix}, \\ \bar{\mathcal{A}}_f &:= \begin{bmatrix} A_\xi & 0_{l \times l} \\ -B_\xi C_\xi & A_\xi + B_\xi C_\xi \end{bmatrix}, \quad \mathcal{A}_{vx} := \begin{bmatrix} B_v C_c & -B_v H_c C & 0_{m \times n-\nu} & 0_{m \times \bar{n}-\nu} \end{bmatrix}, \\ \mathcal{A}_{qv} &:= \begin{bmatrix} \frac{g}{g_n} B_\xi C_v \\ 0_{l \times m} \end{bmatrix}, \quad \bar{\mathcal{A}}_{qx} := \begin{bmatrix} 0_{l \times h} & \frac{1}{g_n} B_\xi [-\bar{F}_2 + F_2] & \frac{1}{g_n} B_\xi F_1 & -\frac{1}{g_n} B_\xi \bar{F}_1 \\ B_\xi C_c & -B_\xi H_c C & 0_{l \times n-\nu} & 0_{l \times \bar{n}-\nu} \end{bmatrix}, \\ \mathcal{A}_{vq} &:= \begin{bmatrix} -B_v C_\xi & B_v C_\xi \end{bmatrix}, \quad \bar{\mathcal{B}}_x := \begin{bmatrix} B_c & 0_h \\ 0_\nu & g B \\ 0_{n-\nu} & 0_{n-\nu} \\ 0_{\bar{n}-\nu} & 0_{\bar{n}-\nu} \end{bmatrix}, \quad \bar{\mathcal{B}}_q := \begin{bmatrix} 0_l & \frac{g}{g_n} B_\xi \\ B_\xi D_c & 0_l \end{bmatrix}, \\ \mathcal{B}_v &:= \begin{bmatrix} B_v D_c & 0_m \end{bmatrix}. \end{aligned}$$

Let  $h_1(\mathcal{X}, \mathcal{V}) := -\mathcal{A}_f^{-1}(\mathcal{A}_{qx}\mathcal{X} + \mathcal{B}_q\mathcal{V})$  and  $h_2(\mathcal{X}, \mathcal{Z}_1, \mathcal{V}) := -\mathcal{A}_v^{-1}(\mathcal{A}_{vx}\mathcal{X} + \mathcal{A}_{vq}\mathcal{Z}_1 + \mathcal{B}_v\mathcal{V})$  where

$$\begin{aligned} \mathcal{A}_{qx} &:= \begin{bmatrix} \frac{g}{g_n} B_\xi C_c & \frac{1}{g_n} B_\xi [-\bar{F}_2 + F_2 - g H_c C] & \frac{1}{g_n} B_\xi F_1 & -\frac{1}{g_n} B_\xi \bar{F}_1 \\ B_\xi C_c & -B_\xi H_c C & 0_{l \times n-\nu} & 0_{l \times \bar{n}-\nu} \end{bmatrix}, \\ \mathcal{B}_q &:= \begin{bmatrix} \frac{g}{g_n} B_\xi D_c & \frac{g}{g_n} B_\xi \\ B_\xi D_c & 0_{l \times 1} \end{bmatrix}. \end{aligned}$$

In fact,  $h_1(\mathcal{X}, \mathcal{V}) = [\xi^*; \zeta^*]$  and  $h_2(\mathcal{X}, \mathcal{Z}_1, \mathcal{V}) = v^*$  when  $\mathcal{Z}_1 = h_1(\mathcal{X}, \mathcal{V})$  which are the equilibrium in (7.2.2). With  $\mathcal{Y}_1 := \mathcal{Z}_1 - h_1(\mathcal{X}, \mathcal{V})$  and  $\mathcal{Y}_2 := \mathcal{Z}_2 - h_2(\mathcal{X}, \mathcal{Z}_1, \mathcal{V})$ ,



we have

$$\begin{aligned}
\dot{\mathcal{X}} &= \mathcal{F}_s \mathcal{X} + \mathcal{A}_{xq} \mathcal{Y}_1 + \mathcal{A}_{xv} \mathcal{Y}_2 + (\mathcal{B}_x - \mathcal{A}_{xq} \mathcal{A}_f^{-1} \mathcal{B}_q) \mathcal{V} \\
\dot{\mathcal{Y}}_1 &= \mathcal{F}_q \mathcal{X} + \left( \frac{1}{\tau} \mathcal{A}_f + \mathcal{A}_f^{-1} \mathcal{A}_{qx} \mathcal{A}_{xq} \right) \mathcal{Y}_1 + \left( \frac{1}{\tau} \mathcal{A}_{qv} + \mathcal{A}_f^{-1} \mathcal{A}_{qx} \mathcal{A}_{xv} \right) \mathcal{Y}_2 \\
&\quad + \mathcal{A}_f^{-1} \mathcal{A}_{qx} (\mathcal{B}_x - \mathcal{A}_{xq} \mathcal{A}_f^{-1} \mathcal{B}_q) \mathcal{V} + \mathcal{A}_f^{-1} \mathcal{B}_q \dot{\mathcal{V}} \\
\dot{\mathcal{Y}}_2 &= \mathcal{F}_v \mathcal{X} + \left( \frac{1}{\tau} \mathcal{A}_v^{-1} \mathcal{A}_{vq} \mathcal{A}_f + \mathcal{A}_v^{-1} \mathcal{A}_{vx} \mathcal{A}_{xq} \right) \mathcal{Y}_1 \\
&\quad + \left( \frac{1}{\tau_v} \mathcal{A}_v + \frac{1}{\tau} \mathcal{A}_v^{-1} \mathcal{A}_{vq} \mathcal{A}_{qv} + \mathcal{A}_v^{-1} \mathcal{A}_{vx} \mathcal{A}_{xv} \right) \mathcal{Y}_2 \\
&\quad + \mathcal{A}_v^{-1} \mathcal{A}_{vx} (\mathcal{B}_x - \mathcal{A}_{xq} \mathcal{A}_f^{-1} \mathcal{B}_q) \mathcal{V} + \mathcal{A}_v^{-1} \mathcal{B}_v \dot{\mathcal{V}}
\end{aligned} \tag{7.3.2}$$

where  $\mathcal{F}_s := \mathcal{A}_s - \mathcal{A}_{xq} \mathcal{A}_f^{-1} \mathcal{A}_{qx}$ ,  $\mathcal{F}_q := \mathcal{A}_f^{-1} \mathcal{A}_{qx} (\mathcal{A}_s - \mathcal{A}_{xq} \mathcal{A}_f^{-1} \mathcal{A}_{qx})$ ,  $\mathcal{F}_v := \mathcal{A}_v^{-1} \mathcal{A}_{vx} (\mathcal{A}_s - \mathcal{A}_{xq} \mathcal{A}_f^{-1} \mathcal{A}_{qx})$ , and

$$\begin{aligned}
\mathcal{A}_s &:= \begin{bmatrix} A_c & -E_c C & 0_{h \times n-\nu} & 0_{h \times \bar{n}-\nu} \\ gBC_c & A + B(F_2 - gH_c C) & BF_1 & 0_{\nu \times \bar{n}-\nu} \\ 0_{n-\nu \times h} & GC & S & 0_{n-\nu \times \bar{n}-\nu} \\ 0_{\bar{n}-\nu \times h} & \bar{G}C & 0_{\bar{n}-\nu \times n-\nu} & \bar{S} \end{bmatrix}, \\
\mathcal{A}_{xq} &:= \begin{bmatrix} 0_{h \times l} & 0_{h \times l} \\ -gBC_\xi & gBC_\xi \\ 0_{n \times l} & 0_{n \times l} \\ 0_{\bar{n} \times l} & 0_{\bar{n} \times l} \end{bmatrix}, \quad \mathcal{B}_x := \begin{bmatrix} B_c & 0_{h \times 1} \\ gBD_c & gB \\ 0_{n \times 1} & 0_{n \times 1} \\ 0_{\bar{n} \times 1} & 0_{\bar{n} \times 1} \end{bmatrix}.
\end{aligned}$$

Note that the  $\mathcal{X}$ -dynamics without the term involving  $\mathcal{Y}_1$  and  $\mathcal{Y}_2$  in (7.3.2) is the quasi-steady-state model (7.2.5). Then, with  $\tilde{\mathcal{X}} = \mathcal{X} - \mathcal{X}_N$ , we have  $\dot{\tilde{\mathcal{X}}} = \mathcal{F}_s \tilde{\mathcal{X}} + \mathcal{A}_{xq} \mathcal{Y}_1 + \mathcal{A}_{xv} \mathcal{Y}_2$ , while the  $\mathcal{Y}_1$  and  $\mathcal{Y}_2$ -dynamics of (7.3.2) are rewritten as

$$\begin{aligned}
\dot{\mathcal{Y}}_1 &= \mathcal{F}_q \tilde{\mathcal{X}} + \left( \frac{1}{\tau} \mathcal{A}_f + \mathcal{A}_f^{-1} \mathcal{A}_{qx} \mathcal{A}_{xq} \right) \mathcal{Y}_1 \\
&\quad + \left( \frac{1}{\tau} \mathcal{A}_{qv} + \mathcal{A}_f^{-1} \mathcal{A}_{qx} \mathcal{A}_{xv} \right) \mathcal{Y}_2 + \mathcal{B}_r \theta \\
\dot{\mathcal{Y}}_2 &= \mathcal{F}_v \tilde{\mathcal{X}} + \left( \frac{1}{\tau} \mathcal{A}_v^{-1} \mathcal{A}_{vq} \mathcal{A}_f + \mathcal{A}_f^{-1} \mathcal{A}_{qx} \mathcal{A}_{xq} \right) \mathcal{Y}_1 \\
&\quad + \left( \frac{1}{\tau_v} \mathcal{A}_v + \frac{1}{\tau} \mathcal{A}_v^{-1} \mathcal{A}_{vq} \mathcal{A}_{qv} + \mathcal{A}_v^{-1} \mathcal{A}_{vx} \mathcal{A}_{xv} \right) \mathcal{Y}_2 + \bar{\mathcal{B}}_r \theta
\end{aligned} \tag{7.3.3}$$

where  $\theta := [\mathcal{X}_N^T, \mathcal{V}^T, \dot{\mathcal{Y}}^T]^T$ ,

$$\begin{aligned}\mathcal{B}_r &:= \begin{bmatrix} \mathcal{F}_q & \mathcal{A}_f^{-1} \mathcal{A}_{qx} (\mathcal{B}_x - \mathcal{A}_{xq} \mathcal{A}_f^{-1} \mathcal{B}_q) & \mathcal{A}_f^{-1} \mathcal{B}_q \end{bmatrix}, \\ \bar{\mathcal{B}}_r &:= \begin{bmatrix} \mathcal{F}_v & \mathcal{A}_v^{-1} \mathcal{A}_{vx} (\mathcal{B}_x - \mathcal{A}_{xq} \mathcal{A}_f^{-1} \mathcal{B}_q) & \mathcal{A}_v^{-1} \mathcal{B}_v \end{bmatrix}.\end{aligned}$$

By Assumption 7.1.2 and 7.1.3, the matrix  $\mathcal{F}_s$  and  $\mathcal{A}_v$  are Hurwitz. If the matrix  $\mathcal{A}_f$  is Hurwitz, then there exist positive definite matrices  $P_f$ ,  $P_s$ , and  $P_v$  such that  $P_s \mathcal{F}_s + \mathcal{F}_s^T P_s = -2I$ ,  $P_f \mathcal{A}_f + \mathcal{A}_f^T P_f = -2I$ , and  $P_v \mathcal{A}_v + \mathcal{A}_v^T P_v = -2I$ . Let  $V_2(\tilde{\mathcal{X}}, \mathcal{Y}_1, \mathcal{Y}_2) = \frac{1}{2} \tilde{\mathcal{X}}^T P_s \tilde{\mathcal{X}} + \frac{1}{2} \mathcal{Y}_1^T P_f \mathcal{Y}_1 + \frac{1}{2} \delta \mathcal{Y}_2^T P_v \mathcal{Y}_2$  where a positive constant  $\delta$  will be chosen later. Then, we obtain

$$\begin{aligned}\dot{V}_2 &\leq -\|\tilde{\mathcal{X}}\|^2 - \frac{1}{\tau} \|\mathcal{Y}_1\|^2 - \frac{\delta}{\tau_v} \|\mathcal{Y}_2\|^2 + \gamma_1 \|\tilde{\mathcal{X}}\| \|\mathcal{Y}_1\| + (\gamma_2 + \delta \gamma_7) \|\tilde{\mathcal{X}}\| \|\mathcal{Y}_2\| \\ &\quad + (\gamma_4 \frac{1}{\tau} + \gamma_5 + \delta \frac{1}{\tau} \gamma_8 + \delta \gamma_9) \|\mathcal{Y}_1\| \|\mathcal{Y}_2\| + \gamma_3 \|\mathcal{Y}_1\|^2 + (\delta \frac{1}{\tau} \gamma_{10} + \delta \gamma_{11}) \|\mathcal{Y}_2\|^2 \\ &\quad + \gamma_6 \|\mathcal{Y}_1\| + \delta \gamma_{12} \|\mathcal{Y}_2\|\end{aligned}$$

where

$$\begin{aligned}\gamma_1 &= \|P_s \mathcal{A}_{xq} + \mathcal{F}_q^T P_f\|, \quad \gamma_2 = \|P_s \mathcal{A}_{xv}\|, \quad \gamma_3 = \|P_f \mathcal{A}_f^{-1} \mathcal{A}_{qx} \mathcal{A}_{xq}\|, \quad \gamma_4 = \|P_f \mathcal{A}_{qv}\|, \\ \gamma_5 &= \|P_f \mathcal{A}_f^{-1} \mathcal{A}_{qx} \mathcal{A}_{xv}\|, \quad \gamma_6 = \|P_f \mathcal{B}_r\| \max_{0 \leq t \leq \infty} \|\theta(t)\|, \quad \gamma_7 = \|\mathcal{F}_v^T P_v\|, \\ \gamma_8 &= \|P_v \mathcal{A}_v^{-1} \mathcal{A}_{vq} \mathcal{A}_f\|, \quad \gamma_9 = \|P_v \mathcal{A}_f^{-1} \mathcal{A}_{qx} \mathcal{A}_{xq}\|, \quad \gamma_{10} = \|P_v \mathcal{A}_v^{-1} \mathcal{A}_{vq} \mathcal{A}_{qv}\|, \\ \gamma_{11} &= \|P_v \mathcal{A}_v^{-1} \mathcal{A}_{vx} \mathcal{A}_{xv}\|, \quad \gamma_{12} = \|P_v \bar{\mathcal{B}}_r\| \max_{0 \leq t \leq \infty} \|\theta(t)\|.\end{aligned}$$

We choose  $\delta$  such that  $32\gamma_2^2 \bar{\tau}_v \leq \delta \leq 1/(32\gamma_7^2 \bar{\tau}_v)$  and assume  $\bar{\tau}_v \leq 1/(16\gamma_{11})$ . It is possible because we already assume that the time constant of unmodeled dynamics,  $\tau_v$ , is sufficiently small. By Assumption 7.1.1, 7.1.2, and 7.1.3, values of  $\gamma_1 - \gamma_{12}$  also can be obtained. If we select  $\tau$  that satisfies  $\tau^\dagger < \tau < \bar{\tau}$  where

$$\begin{aligned}\tau^\dagger &:= \max\{16\gamma_{10} \bar{\tau}_v, 64\gamma_4^2 \frac{1}{\delta} \bar{\tau}_v, 64\gamma_8^2 \delta \bar{\tau}_v\}, \\ \bar{\tau} &:= \min\left\{\frac{1}{8(2\gamma_1^2 + \gamma_3)}, \frac{\delta}{64\gamma_5^2 \bar{\tau}_v}, \frac{1}{64\delta\gamma_9^2 \bar{\tau}_v}\right\},\end{aligned}$$

then it can be shown that  $\dot{V}_2 < 0$  when  $\|\mathcal{Y}_1\| > 2\gamma_6\tau$  and  $\|\mathcal{Y}_2\| > 2\gamma_{12}\tau_v$ . Define

$\bar{V}_2 := \frac{1}{2}\|\tilde{\mathcal{X}}\|^2 + \frac{1}{\tau}\|\mathcal{Y}_1\|^2 + \frac{\delta}{\tau_v}\|\mathcal{Y}_2\|^2$ . Then, it holds that

$$\dot{V}_2 \leq -\frac{1}{2}\bar{V}_2 + \frac{\sqrt{2}}{4}\bar{\gamma}(\tau, \tau_v)\sqrt{\bar{V}_2}$$

where  $\bar{\gamma}(\tau, \tau_v) := 4 \max\{\gamma_6, \gamma_{12}\} \cdot \max\{\sqrt{\tau}, \sqrt{\tau_v/\delta}\}$ . If  $\|\bar{V}_2\| > \frac{1}{2}\bar{\gamma}^2(\tau, \tau_v)$ , then  $\dot{V}_2 < 0$ . And, a positive constant  $\mu_2$  is given by

$$\mu_2 := \max_{\bar{V}_2 = \frac{1}{2}\bar{\gamma}^2(\tau, \tau_v)} V_2(\tilde{\mathcal{X}}, \mathcal{Y}_1, \mathcal{Y}_2)$$

Now, we define the set  $\Omega_v := \{[\tilde{\mathcal{X}}; \mathcal{Y}_1; \mathcal{Y}_2] | V_2(\tilde{\mathcal{X}}, \mathcal{Y}_1, \mathcal{Y}_2) \leq \mu_2\}$ . It is obvious that the state  $[\tilde{\mathcal{X}}; \mathcal{Y}_1; \mathcal{Y}_2]$  converges to the set  $\Omega_v$  as  $t \rightarrow \infty$ . Also,

$$V_2 = \frac{1}{2}\tilde{\mathcal{X}}^T P_s \tilde{\mathcal{X}} + \frac{1}{2}\mathcal{Y}_1^T P_f \mathcal{Y}_1 + \frac{\delta}{2}\mathcal{Y}_2^T P_v \mathcal{Y}_2 \leq \rho_2 \bar{V}_2$$

where  $\rho_2 := \max\{\lambda_{\max}(P_s), \frac{1}{2}\lambda_{\max}(P_f)\tau, \frac{1}{2}\lambda_{\max}(P_v)\tau_v\}$ . For all  $[\tilde{\mathcal{X}}, \mathcal{Y}_1, \mathcal{Y}_2] \in \Omega_\alpha$ ,  $\|\tilde{\mathcal{X}}\|^2 \leq \mu_2 \leq \frac{1}{2}\rho_2\bar{\gamma}^2(\tau, \tau_v)$  and thus,

$$\|\tilde{\mathcal{X}}\| \leq \sqrt{\frac{\rho_2}{2}}\bar{\gamma}(\tau, \tau_v).$$

Since we assume that  $\tau_v$  is relatively small positive constant,  $\rho_2 = \lambda_{\max}(P_s)/2$  as  $\tau$  is reduced and the bound of  $\|\mathcal{X} - \mathcal{X}_N\|$  is proportional to the  $\bar{\gamma}(\tau, \tau_v)$ . It means that  $V_2$  tends to small depending on  $\tau$  so the error  $\mathcal{X}(t) - \mathcal{X}_N(t)$  becomes small, by taking  $\tau$  appropriately.

**Theorem 7.3.1.** Under Assumption 7.1.1, 7.1.2, and 7.1.3, for a sufficiently small  $\bar{\tau}_v$ , there exist positive constants  $\tau^\dagger = \max\{16\gamma_{10}\bar{\tau}_v, 64\gamma_4^2\frac{1}{\delta}\bar{\tau}_v, 64\gamma_8^2\delta\bar{\tau}_v\}$  and  $\bar{\tau} = \min\{\frac{1}{8(2\gamma_1^2+\gamma_3)}, \frac{\delta}{64\gamma_5^2\bar{\tau}_v}, \frac{1}{64\delta\gamma_9^2\bar{\tau}_v}\}$  such that, for all  $\tau^\dagger < \tau < \bar{\tau}$ , the overall closed-loop system (7.1.8) is exponential stable when  $y_r = 0$  and  $d = 0$ . Furthermore, the part of solution of (7.1.8) denoted by  $[c(t); x(t); z(t); \bar{z}(t)]$  satisfies that

$$\limsup_{t \rightarrow \infty} \|[c(t); x(t); \bar{z}(t)] - [c_N(t); x_N(t); \bar{z}_N(t)]\| \leq \Gamma_2 \bar{\gamma}(\tau_q, \tau_v)$$

where  $\Gamma_2 := \sqrt{\rho_2/2}$  and  $[c_N(t); x_N(t); \bar{z}_N(t)]$  is the solution of the nominal closed-loop system (7.1.2) and (7.1.3).  $\square$

Compared to results in Section 6.4, the error  $\mathcal{X}(t) - \mathcal{X}_N(t)$  cannot become arbitrarily small in Theorem 7.3.1 because the time constant  $\tau$ , which is the design parameter of the disturbance observer is bounded by  $\tau_v$ . If  $\tau$  is selected too small to reduce the error, it can lead to the instability of the overall closed-loop system.

**Remark 7.3.1.** In Theorem 7.3.1, we assume that the upper bound of the time constant of unmodeled dynamics  $\bar{\tau}_v$  is smaller than  $1/(16\gamma_{11})$  where  $\gamma_{11}$  is determined by the uncertain system under consideration. It seems to be conservative, and thus difficult to apply in real applications. However, when the relative degree of the plant is equal to or greater than 2,  $\gamma_{11} = 0$  and  $1/(16\gamma_{11}) = \infty$ . Therefore, for an arbitrarily  $\bar{\tau}_v$ , this assumption is always satisfied. Furthermore, in this case,  $\gamma_{10}$  is also equal to 0. On the other hand, when the relative degree of the plant is equal to 1, for an arbitrarily small  $\tau$ , robust stabilization of the disturbance observer based control system can always be achieved regardless of  $\tau_v$ , which was discussed in Chapter 4.  $\square$

**Remark 7.3.2.** When the time constant of unmodeled dynamics  $\tau_v$  is sufficiently small compared with the time constant of Q-filter  $\tau$  (*i.e.*,  $\tau_v \ll 1$  and  $\tau_v \ll \tau$ ), the upper and lower bounds of time constant become  $\tau^\dagger \approx 0$  and  $\bar{\tau} = \frac{1}{8(2\gamma_1^2 + \gamma_3)}$ , respectively. In addition, the magnitude of  $\bar{\gamma}(\tau, \tau_v)$  is determined by not  $\tau_v$  but  $\tau$ . As a result, Theorem 7.3.1 provides the same results as Theorem 6.4.1.  $\square$



# Chapter 8

## Extensions of Disturbance Observer for Guaranteeing Robust Transient Performance

In control system design, the existence of disturbances and model uncertainties is unavoidable. To overcome this problem, a disturbance observer approach has been widely used in industry [UH91, UH93, BT99, SD02, BSPS10, LT96, KK99, CYC<sup>+</sup>03]. The versatility of the disturbance observer for many applications comes from its simple structure as well as powerful ability for rejecting disturbances and compensating model uncertainties. Furthermore, the disturbance observer is convenient for use because it is an inner-loop controller, that is, if it is added in the inner-loop, then the existing (pre-designed outer-loop) controller is enabled without taking into account effects from disturbances and model uncertainties.

Although the characteristic of the disturbance observer is easily understood in the frequency domain, an analysis was performed in the state-space domain based on the singular perturbation theory for the purpose of obtaining the deeper understanding of the effects of each block as shown in Chapter 6 and 7. Under an assumption that the cutoff frequency of the Q-filter is sufficiently fast, they exhibit well-known properties as well as some interesting points:

- it shows not only the input disturbance is almost completely rejected but also the plant with the disturbance observer, inner-loop blocks, behaves as a nominal model of the plant.

- the zero dynamics of the plant is replaced by the zero dynamics of the nominal model. It means that the zero dynamics of the plant is nearly unobservable from the output and implies why the zero dynamics should be stable (i.e., minimum phase system).

However, the classical linear disturbance observer does not ensure the recovery of transient response. In order to guarantee the robust transient response and to extend to nonlinear systems, a modified nonlinear disturbance observer, in which all the benefits of the classical one are still preserved, was suggested [BS08]. MIMO (multi-input multi-output) extensions having the same number of inputs and outputs with a linear nominal model was also proposed [BS09].

In this chapter, we review a modified nonlinear disturbance observer and show that it recovers the nominal trajectory, that is, steady-state as well as transient trajectory, which is designed for nominal model.

## 8.1 Extensions to MIMO Nonlinear Systems

We consider uncertain MIMO nonlinear systems having the same number of inputs and outputs given in the Byrnes-Isidori normal form [Isi95] as follows:

$$\begin{aligned} \dot{z} &= F_0(z, x), \\ \dot{x} &= A^m x + B^m (F(z, x, t) + G(z, x, t)(u + d)), \\ y &= C^m x \end{aligned} \tag{8.1.1}$$

where  $u \in \mathbb{R}^m$ ,  $d \in \mathbb{R}^m$ , and  $y \in \mathbb{R}^m$  are the control input, unknown disturbance, and output, respectively.  $x \in \mathbb{R}^\nu$  and  $z \in \mathbb{R}^{n-\nu}$  are system states such that  $x = [x_1; \dots; x_m]$  and  $x_i = [x_{i1}, \dots, x_{i\nu_i}]^T \in \mathbb{R}^{\nu_i}$  with  $\nu = \nu_1 + \dots + \nu_m$ . The matrices  $A^m \in \mathbb{R}^{\nu \times \nu}$ ,  $B^m \in \mathbb{R}^{\nu \times m}$ , and  $C^m \in \mathbb{R}^{m \times \nu}$  are defined as  $A^m = \text{diag}\{A_1^m, \dots, A_m^m\}$ ,  $B^m = \text{diag}\{B_1^m, \dots, B_m^m\}$ , and  $C^m = \text{diag}\{C_1^m, \dots, C_m^m\}$ , in which

$$A_i^m := \begin{bmatrix} 0_{\nu_i-1} & I_{\nu_i-1} \\ 0 & 0_{\nu_i-1}^T \end{bmatrix}, \quad B_i^m := \begin{bmatrix} 0_{\nu_i-1} \\ 1 \end{bmatrix}, \quad C_i^m := \begin{bmatrix} 1 & 0_{\nu_i-1}^T \end{bmatrix}.$$

Here, we assume that the functions  $F_0$ ,  $F$ , and  $G$  are twice continuously differentiable ( $\mathfrak{C}^2$ ) but uncertain<sup>1</sup>.

We now consider a disturbance-free nominal model of (8.1.1) as

$$\begin{aligned}\dot{\bar{z}} &= \bar{F}_0(\bar{z}, \bar{x}) \\ \dot{\bar{x}} &= A^m \bar{x} + B^m(\bar{F}[\bar{z}; \bar{x}] + \bar{G}u_r) \\ \bar{y} &= C^m \bar{x}\end{aligned}\tag{8.1.2}$$

where  $\bar{F}_0(\bar{z}, \bar{x})$ ,  $\bar{F}[\bar{z}; \bar{x}]$ , and  $\bar{G}$  the nominal counterparts of  $F_0(z, x)$ ,  $F(z, x, t)$ , and  $G(z, x, t)$ , respectively. Note that  $\bar{F}$  and  $\bar{G}$  are constant matrices so that the  $\bar{x}$ -dynamics becomes linear, while  $\bar{F}_0$  is assumed to be  $\mathfrak{C}^2$ .<sup>2</sup> We also assume that an (dynamic) output feedback outer-loop controller  $C$  is designed *a priori* for the nominal plant (8.1.2), which is represented by

$$\begin{aligned}\dot{\eta} &= \Gamma(\eta, \bar{y}, r), \quad \eta \in \mathbb{R}^l \\ u_r &= \gamma(\eta, \bar{y}, r), \quad u_r \in \mathbb{R}^m\end{aligned}\tag{8.1.3}$$

where  $\Gamma$  and  $\gamma$  are  $\mathfrak{C}^2$  functions, and  $r$  is a vector of  $\mathfrak{C}^2$  reference command. It is assumed that  $r(t)$  and  $\dot{r}(t)$  are bounded so that  $r(t) \in S_r$ ,  $t \geq 0$ , where  $S_r$  is a known compact set.

**Assumption 8.1.1.** For the considered class of references  $r(t)$ , the nominal closed-loop system (8.1.2) and (8.1.3) has the following properties:

1. the solution  $[\bar{z}(t); \bar{x}(t); \eta(t)]$  of (8.1.2) and (8.1.3) evolves in a bounded, connected, and open set  $U \in \mathbb{R}^{n+l}$  if the initial condition  $[\bar{z}(0); \bar{x}(0); \eta(0)]$  is located in a compact set  $S \in U$ .
2. each solution  $[\bar{z}(t); \bar{x}(t); \eta(t)]$  initiated in  $S$  is locally asymptotically stable.

□

---

<sup>1</sup>Considering uncertain single-input single-output (SISO) nonlinear systems, we assume that  $F$  and  $G$  are not depend on the time.

<sup>2</sup>When we consider a SISO nonlinear nominal model,  $\bar{F}_0$ ,  $\bar{F}$ , and  $\bar{G}$  are  $\mathfrak{C}^2$  functions. More details are in [BS08].



**Assumption 8.1.2.** Let  $U_x \subset \mathbb{R}^\nu$  and  $U_z \subset \mathbb{R}^{n-\nu}$  be the projections of the set  $U$  to the  $x$  subspace and the  $z$  subspace, respectively. The system  $\dot{z} = F_0(z, x)$  with  $z(0) \in U_z$  is input-state stable (ISS) with respect to any constrained input  $x(t) \in U_x$ .  $\square$

Let  $Z$  be the bounded set which contains all feasible solutions  $z(t)$  of Assumption 8.1.2.

**Assumption 8.1.3.** There are positive constants  $l_{f_0}$ ,  $l_f$ ,  $l_{ft}$ , and  $l_{gt}$  such that  $|F_0(z, x)| \leq l_{f_0}$ ,  $|F(z, x, t)| \leq l_f$ ,  $|(\partial F/\partial t)(z, x, t)| \leq l_{ft}$ , and  $|(\partial G/\partial t)| \leq g_t$ , for all  $(z, x, t) \in Z \times U_x \times \mathbb{R}_+$ . For the uncertain input gain matrix  $G(z, x, t)$ , there exist a nonsingular matrix  $K$ ,  $G^- := \text{diag}\{g_1^-, \dots, g_m^-\}$  and  $G^+ := \text{diag}\{g_1^+, \dots, g_m^+\}$  such that  $0 < G^- < G^+$  and that

$$(G(z, x, t)K\vartheta - G^-\vartheta)^T \Pi^2 (G(z, x, t)K\vartheta - G^+\vartheta) \leq 0.$$

$$\forall \vartheta \in \mathbb{R}^m, \forall (z, x, t) \in Z \times U_x \times \mathbb{R}_+$$

where  $\Pi = \text{diag}\{\pi_1, \dots, \pi_m\} := 2(G^+ + G^-)^{-1}$ . In addition, the disturbance signal  $d(t)$  is at least  $\mathcal{C}^2$ , and  $d(t)$  and  $\dot{d}(t)$  are bounded with known bounds  $l_d$  and  $l_{dt}$  such that  $|d(t)| \leq l_d$  and  $|\dot{d}(t)| \leq l_{dt}$ , respectively.  $\square$

The Q-filter, a key ingredient for the design of the disturbance observer, is given by

$$\frac{a_{i0}}{s^{\nu_i} + a_{i,\nu_i-1}s^{\nu_i-1} + \dots + a_{i0}}. \quad (8.1.4)$$

Compared to (2.1.2), we restrict the structure of Q-filter in such a form whose degrees of the numerator and denominator equal to zero and the relative degree of the plant, respectively. However, by the virtue of simple structure, a systematic design procedure of the disturbance observer can be obtained.

### 8.1.1 SISO Nonlinear Disturbance Observer with Nonlinear Nominal Model

In some applications, the systems are required to generate signals or trajectories, which cannot be generated by linear systems, with high accuracy. Therefore,

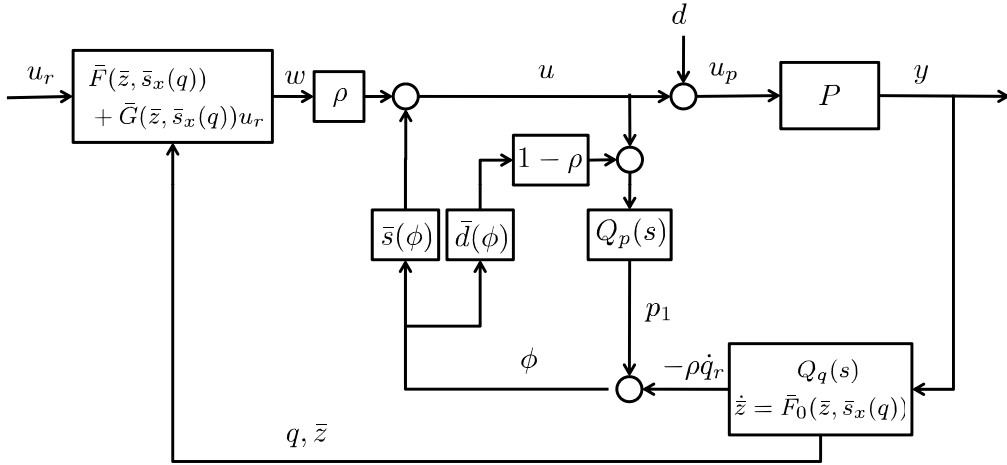


Figure 8.1: Proposed SISO nonlinear disturbance observer structure.  $P$ ,  $Q_q(s)$ , and  $Q_p(s)$  correspond to (8.1.1) and (8.1.10), respectively.

a SISO nonlinear disturbance observer with the nonlinear nominal model was proposed in [BS08]. To deal with SISO uncertain systems, it is assumed that  $m = 1$  in (8.1.1), all matrices and coefficients are appropriately defined (e.g.,  $A^1 = A$ ,  $a_{i0} = a_0$ , and so on), and positive constants  $G^-$  and  $G^+$  satisfy the inequality  $0 < G^- \leq 1 \leq G^+$ . It is always achieved by scaling the control input and disturbance.

Fig. 8.1 shows the structure of the proposed inner-loop controller where  $P$  denotes the plant (8.1.1). We begin by introducing some essential design parameters and components of the proposed controller. Let  $a = [a_0, a_1, \dots, a_{\nu-1}]$  such that all the roots of (8.1.5) and (8.1.6) shown below are in  $\mathbb{C}^-$ . (When  $\nu = 1$ , consider the equation (8.1.5) only.)

$$s^\nu + a_{\nu-1}s^{\nu-1} + \dots + a_1s + a_0 = 0, \quad (8.1.5)$$

$$s^{\nu-1} + a_{\nu-1}s^{\nu-2} + \dots + a_1 = 0. \quad (8.1.6)$$

From Lemma A. 3 in Appendix, such  $a_i$ 's always exist.

Now, choose a constant  $\rho > 0$  from the following procedure. First, let

$$H(s) := \frac{1}{s} \frac{a_0}{s^{\nu-1} + a_{\nu-1}s^{\nu-2} + \dots + a_1}. \quad (8.1.7)$$

Consider a disk  $D(\rho G^-, \rho G^+)$ , which is defined as a closed disk in the complex plane whose diameter is the line segment connecting  $-1/(\rho G^-)$  and  $-1/(\rho G^+)$ . Then, choose a sufficiently small  $\rho > 0$  such that the disk  $D$  is disjoint from the Nyquist plot and the plot does not encircle the disk.

$\bar{s}_x$  and  $\bar{s}$ , globally bounded continuous differentiable ( $\mathcal{C}^1$ ) saturation functions, are used in the scheme and satisfy the following:

$$\begin{aligned} \bar{s}_x(x) &= x, \quad \forall x \in U_x, \text{ and } \left| \frac{\partial \bar{s}_x}{\partial x}(x) \right| \leq k_0, \quad \forall x \in \mathbb{R}^\nu \\ \bar{s}(s) &= s, \quad \forall s \in S_\phi, \text{ and } 0 \leq \bar{s}' \leq 1, \quad \forall s \in \mathbb{R} \end{aligned} \quad (8.1.8)$$

where  $'$  denotes the derivative,  $k_0 > 0$  is a constant, and

$$\begin{aligned} S_\phi = \left\{ s = \left( \frac{1}{G(z, x)} - \rho \right) (\bar{F}(\bar{z}, x) + \bar{G}(\bar{z}, x)\gamma(\eta, x_1, r)) \right. \\ \left. - \frac{F(z, x)}{G(z, x)} - d : z \in Z, [\bar{z}; x; \eta] \in U, r \in S_r, |d| \leq l_d \right\}. \end{aligned}$$

The set  $S_\phi$  indicates the steady-state range of the signal  $\phi(t)$  to be defined in (8.1.10). In fact, it is enough to have the saturation levels of  $\bar{s}_x$  and  $\bar{s}$  sufficiently large so that the saturation functions are not active during the nominal transient and steady-state operation. Note that the knowledge of the bounds for  $F$  and  $G$  is used for choosing the function  $\bar{s}$ .

In addition to the saturation functions, we introduce a dead-zone function  $\bar{d}(s) := s - \bar{s}$ , which will be used shortly.

Let  $\tau > 0$  which will be chosen later and define

$$\begin{aligned} \Delta_\tau &= \text{diag} \left\{ \frac{1}{\tau^\nu}, \frac{1}{\tau^{\nu-1}}, \dots, \frac{1}{\tau} \right\}, \\ A_{a\tau} &= \begin{bmatrix} 0 & 1 & \cdots & 0 \\ \vdots & \vdots & \ddots & \vdots \\ 0 & 0 & \cdots & 1 \\ -\frac{a_0}{\tau^\nu} & -\frac{a_1}{\tau^{\nu-1}} & \cdots & -\frac{a_{\nu-1}}{\tau} \end{bmatrix}. \end{aligned} \quad (8.1.9)$$

With all the components introduced so far, we now present an inner-loop

controller given by

$$\begin{aligned}
\dot{\bar{z}} &= \bar{F}_0(\bar{z}, \bar{s}_x(q)), \\
\dot{q} &= A_{a\tau}q + \frac{a_0}{\tau^\nu}By, \\
\dot{p} &= A_{a\tau}p + \frac{a_0}{\tau^\nu}B(\phi - \rho\bar{d}(\phi) + \rho w), \\
u &= \bar{s}(\phi) + \rho w,
\end{aligned} \tag{8.1.10}$$

where  $q = [q_1, \dots, q_\nu]^T \in \mathbb{R}^\nu$ ,  $p = [p_1, \dots, p_\nu]^T \in \mathbb{R}^\nu$ , and

$$\begin{aligned}
\phi &= p_1 - \rho\dot{q}_\nu = p_1 a^T \Delta_\tau q - \rho \frac{a_0}{\tau^\nu} y, \\
w &= \bar{F}(\bar{z}, \bar{s}_x(q)) + \bar{G}(\bar{z}, \bar{s}_x(q))u_r.
\end{aligned}$$

**Theorem 8.1.1.** [BS08] Let  $S_{pq}$  be a compact set for the initial condition  $[p(0); q(0)]$ ,  $\bar{S}$  be a compact set slightly small than  $S$  (i.e.,  $\bar{S} \subset S$  and their boundaries are disjoint), and  $\bar{S}_z$  be the projection of  $\bar{S}$  into the  $z$  plane. Under Assumption 8.1.1–8.1.3, for given  $\epsilon > 0$ , there exists a  $\bar{\tau} > 0$  such that, for each  $0 < \tau \leq \bar{\tau}$ , the solution of the closed-loop system (8.1.1), (8.1.3), and (8.1.10) denoted by  $[z(t); \bar{z}(t); x(t); \eta(t)]$ , initiated at  $[z(0); \bar{z}(0); x(0); \eta(0)] \in \bar{S}_z \times \bar{S}$ , is bounded and satisfies that

$$|[z(t); x(t); \eta(t)] - [\bar{z}_N(t); \bar{x}_N(t); \eta_N(t)]| \leq \epsilon, \quad \forall t \geq 0. \tag{8.1.11}$$

where  $[\bar{z}_N(t); \bar{x}_N(t); \eta_N(t)]$  is the solution of the nominal closed-loop system, i.e., (8.1.2) and (8.1.3), with  $[\bar{z}_N(0); \bar{x}_N(0); \eta_N(0)] = [\bar{z}(0); x(0); \eta(0)]$ .  $\square$

### 8.1.2 MIMO Nonlinear Disturbance Observer with Linear Nominal Model

The result in Section 8.1.1 was extended to a class of MIMO nonlinear systems having the same number of inputs and outputs under the restriction that the nominal model is linear. But, this restriction allows a much simpler control structure than the result in Section 8.1.1. Recalling that the linear nominal models are sufficient for many applications, we may enjoy the benefit of the simpler control

structure even for SISO cases.

Now, we present the design procedure of an inner-loop controller, MIMO nonlinear disturbance observer. First, let  $a_i = [a_{i0}, a_{i1}, \dots, a_{i,\nu_i-1}]$ ,  $i = 1, \dots, m$ . For each  $i$ , choose  $a_{i1}, \dots, a_{i,\nu_i-1}$  such that

$$s^{\nu_i-1} + a_{i,\nu_i-1}s^{\nu_i-2} + \dots + a_{i1} = 0 \quad (8.1.12)$$

has all roots in  $\mathbb{C}^-$ . When  $\nu_i = 1$ , there is nothing to choose. For each  $i$ , with  $a_{i1}, \dots, a_{i,\nu_i-1}$  fixed, we choose  $a_{i0}$  as follows. Let  $\lambda_{max} = \|\Pi(G^+ - G^-)/2\|$ . Define  $D(1 - \lambda_{max}, 1 + \lambda_{max})$  by a closed disk in the complex plane whose diameter is the line segment connecting the points  $-1/(1 - \lambda_{max}) + j0$  and  $-1/(1 + \lambda_{max}) + j0$ . Let

$$H_i(s) := \frac{1}{s} \frac{a_{i0}}{s^{\nu_i-1} + a_{\nu_i-1}s^{\nu_i-2} + \dots + a_{i1}}. \quad (8.1.13)$$

and find a positive constant  $a_{i0}$  such that the Nyquist plot of  $H_i(s)$  is disjoint from the disk  $D(1 - \lambda_{max}, 1 + \lambda_{max})$  and does not encircle the disk. Such  $a_{i0}$  always exists.

Now, we define saturation functions  $\phi : \mathbb{R}^r \rightarrow \mathbb{R}^r$  and  $\Phi : \mathbb{R}^m \rightarrow \mathbb{R}^m$  as globally bounded  $\mathcal{C}^1$  functions satisfying

$$\begin{aligned} \phi(x) &= x, \quad \forall x \in U_x, \text{ and } \left| \frac{\partial \phi}{\partial x}(x) \right| \leq 1, \quad \forall x \in \mathbb{R}^r \\ \Phi(\omega) &= \omega, \quad \forall \omega \in S_\omega, \text{ and } \left| \frac{\partial \Phi}{\partial \omega}(\omega) \right| \leq 1, \quad \forall \omega \in \mathbb{R}^m \end{aligned} \quad (8.1.14)$$

where

$$\begin{aligned} S_\omega &= \left\{ \omega \in \mathbb{R}^m : \omega = (G^{-1}(z, x, t) - \Pi)\bar{G}\gamma(\eta, C^m x, r) \right. \\ &\quad \left. + G^{-1}(z, x, t)(\bar{F}[\bar{z}; x] - F(z, x, t)) - d : z \in Z, t \in \mathbb{R}_+, \right. \\ &\quad \left. [\bar{z}; x; c] \in U, r \in S_r, |d| \leq l_d \text{ for all admissible } F \text{ and } G \right\}. \end{aligned}$$

The set  $S_\omega$  indicates the steady-state range of the signal  $\omega(t)$  to be defined in (8.1.16). In fact, it is enough to have the saturation levels of  $\phi$  and  $\Phi$  sufficiently large so that the saturation functions are not active during the steady-state op-

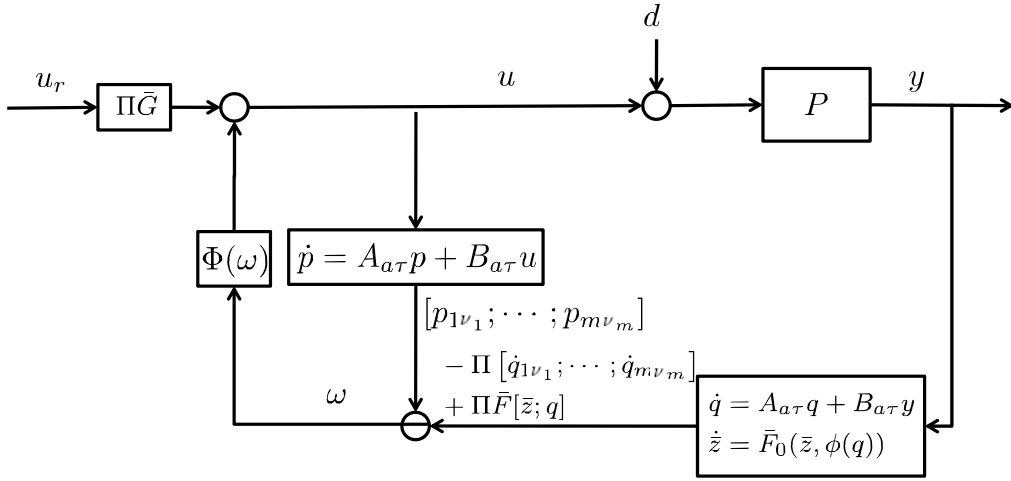


Figure 8.2: Proposed MIMO nonlinear disturbance observer structure.  $P$  corresponds to (8.1.1).

eration.

With a positive parameter  $\tau$  (to be designed), let

$$A_{ai\tau} = \begin{bmatrix} 0 & 1 & \cdots & 0 \\ \vdots & \vdots & \ddots & \vdots \\ 0 & 0 & \cdots & 1 \\ -\frac{a_{i0}}{\tau^{\nu_i}} & -\frac{a_{i1}}{\tau^{\nu_i-1}} & \cdots & -\frac{a_{i,\nu_i-1}}{\tau} \end{bmatrix}. \quad (8.1.15)$$

The proposed inner-loop controller, MIMO nonlinear disturbance observer, is given by

$$\begin{aligned} \dot{\bar{z}} &= \bar{F}_0(\bar{z}, \phi(q)), \\ \dot{q}_i &= A_{ai\tau}q_i + \frac{a_{i0}}{\tau^{\nu_i}}B_i y_i, \quad 1, \dots, m, \\ \dot{p}_i &= A_{ai\tau}p_i + \frac{a_{i0}}{\tau^{\nu_i}}B_i u_i, \quad 1, \dots, m, \\ u &= \Phi(\omega) + \Pi\bar{G}u_r, \end{aligned} \quad (8.1.16)$$

where  $q = [q_1; \dots; q_m] \in \mathbb{R}^\nu$ ,  $q_i = [q_{i1}, \dots, q_{i\nu_i}]^T \in \mathbb{R}^{\nu_i}$ ,  $p = [p_1; \dots; p_m] \in \mathbb{R}^\nu$ ,

$p_i = [p_{i1}, \dots, p_{i\nu_i}]^T \in \mathbb{R}^{\nu_i}$ ,  $\omega = [\omega_1, \dots, \omega_m]^T \in \mathbb{R}^m$ , and

$$\omega_i = p_{i1} - \pi_i \dot{q}_{i\nu_i} + \pi_i \bar{F}_i[\bar{z}; q], \quad i = 1, \dots, m.$$

Here, we write  $F_i$ ,  $G_i$ ,  $\bar{F}_i$ , and  $\bar{G}_i$  to indicate the  $i$ -th row (or component) of  $F$ ,  $G$ ,  $\bar{F}$ , and  $\bar{G}$ , respectively.

Fig. 8.2 shows the structure of the proposed inner-loop controller where  $P$  denotes the plant (8.1.1) and the matrices are  $A_{a\tau} = \text{diag}\{A_{a1\tau}, \dots, A_{am\tau}\}$  and  $B_{a\tau} = \text{diag}\{(a_{10}/\tau^{\nu_1})B_1, \dots, (a_{m0}/\tau^{\nu_m})B_m\}$ . It is noted that the structure is much simpler than that of [BS08] (i.e., SISO nonlinear disturbance observer in Section 8.1.1) since we consider the linear nominal model.

**Theorem 8.1.2.** [BS09] Let  $S_{pq}$  be a compact set for the initial condition  $[p(0); q(0)]$ ,  $\bar{S}$  be a compact set slightly small than  $S$  (i.e.,  $\bar{S} \subset S$  and their boundaries are disjoint), and  $\bar{S}_z$  be the projection of  $\bar{S}$  into the  $z$  subspace. Under Assumption 8.1.1–8.1.3, for given  $\epsilon > 0$ , there exists a  $\bar{\tau} > 0$  such that, for each  $0 < \tau \leq \bar{\tau}$ , the solution of the closed-loop system (8.1.1), (8.1.3), and (8.1.16) denoted by  $[z(t); \bar{z}(t); x(t); \eta(t)]$ , initiated at  $[z(0); \bar{z}(0); x(0); \eta(0)] \in \bar{S}_z \times \bar{S}$ , is bounded for all  $t \geq 0$ , and satisfies that

$$\|[x(t); \eta(t)] - [\bar{x}_N(t); \eta_N(t)]\| \leq \epsilon, \quad \forall t \geq 0. \quad (8.1.17)$$

where  $[\bar{x}_N(t); \eta_N(t)]$  is from the solution  $[\bar{z}_N(t); \bar{x}_N(t); \eta_N(t)]$  of the nominal closed-loop system (8.1.2) and (8.1.3), with  $[\bar{z}_N(0); \bar{x}_N(0); \eta_N(0)] = [\bar{z}(0); x(0); \eta(0)]$ .  $\square$

# Chapter 9

## Conclusions

Throughout the dissertation, we have discussed the stability and performance of the disturbance observer based control system both in the frequency and time domain. This chapter summarizes the results of the dissertation discussed so far.

In the frequency domain, we have dealt with the robust stability of the disturbance observer based on the observation about the pole locations of the closed-loop system and derived a robust stability condition. To overcome the approximate disturbance rejection property, based on the internal model principle, we proposed a method to embed the internal model into the disturbance observer structure so as to achieve asymptotic disturbance rejection in Chapter 3. In chapter 4, we have focused on the robust stability when the relative degree of the plant is unknown and proposed a universal design method for guaranteeing robust stability of the closed-loop system for the case that the relative degree of the plant is less than or equal to 4. In Chapter 5, focusing on the role of each Q-filter, we have generalized the design of disturbance observer structure and proposed a reduced order type-k disturbance observer so as to enhance the disturbance rejection performance and reduce the design complexity simultaneously.

As a counterpart of the frequency domain analysis, Chapter 6 has analyzed the disturbance observer in the state space. Based on the singular perturbation theory, not only the equivalence relation between the frequency and time domain but also the behaviour of each block of the disturbance observer structure have been clarified. It has also revealed new facts such as peaking phenomenon as well as well-known properties of disturbance observer. In addition, the robust



stability of the closed-loop system with and without unmodeled dynamics and the nominal performance recovery depending on the time constant of Q-filter have been investigated in Chapter 6 and 7. Finally, the robust transient performance recovery of the nonlinear disturbance observer with saturation functions has been discussed.

# APPENDIX

**Theorem A. 1.** [Rouché's Theorem] [Fla83]

Let  $f(s)$  and  $g(s)$  be analytic on and inside a simple closed curve  $\mathbb{C}$ , with  $\|g(s)\| < \|f(s)\|$  on  $\mathbb{C}$ . Then,  $f(s)$  and  $f(s) + g(s)$  have the same number of roots inside  $\mathbb{C}$  (counting multiplicity).  $\square$

**Lemma A. 2.** [SJ09]

Let  $p(s)$  and  $q_j(s)$ ,  $j = 1, \dots, k$ , be polynomials of complex variable  $s$ . Define  $R(s; \tau) := p(s) + \tau q_1(s) + \tau^2 q_2(s) + \dots + \tau^k q_k(s)$ . Assume that  $\deg(p) = n$  and let  $s_i^*$ ,  $i = 1, \dots, n$ , be the roots of  $R(s; 0) = 0$ . Then, for a sufficiently small  $\tau > 0$ , there exist  $n$  roots of  $R(s; \tau) = 0$ , say  $s_i(\tau)$ ,  $i = 1, \dots, n$ , such that  $\lim_{\tau \rightarrow 0} s_i(\tau) = s_i^*$  (even if  $R(s; \tau)$  may have more than  $n$  roots for  $\tau > 0$ ).  $\square$

**Lemma A. 3.** [BS08]

If a polynomial

$$s^{l-1} + a_{l-1}s^{l-2} + \dots + a_1 \tag{9.0.1}$$

is Hurwitz, then there exists  $\bar{\gamma}_0$  such that the polynomial

$$s^l + a_{l-1}s^{l-1} + \dots + a_1s + \gamma_0 \tag{9.0.2}$$

is Hurwitz for all  $\gamma_0 \in (0, \bar{\gamma}_0)$ .  $\square$

**Proof:** Indeed, let  $H(S) = 1/(s^l + a_{l-1}s^{l-1} + \dots + a_1s)$ . Then, since  $H(s)$  has one pole at the origin and all other poles in the  $\mathbb{C}^-$ , the root locus of the unity feedback system with the gain  $\gamma_0$  remains in the  $\mathbb{C}^-$  for sufficiently small  $\gamma_0 > 0$ . Take  $\bar{\gamma}_0$  such that the plot remains in the  $\mathbb{C}^-$  for all  $\gamma_0 \in (0, \bar{\gamma}_0)$ . As a result, it is proved.  $\square$

**Lemma A. 4.** [Kharitonov Theorem] [BCK95]

Consider a set of polynomials given by  $\mathcal{I} := \{\theta_\mu s^\mu + \theta_{\mu-1} s^{\mu-1} + \dots + \theta_1 s + \theta_0 : a_i \in [\underline{\theta}_i, \bar{\theta}_i], i = 0, 1, \dots, \mu\}$  where  $\underline{\theta}_i$  and  $\bar{\theta}_i$  are positive constants such that  $\underline{\theta}_i \leq \bar{\theta}_i$ . Define four extreme polynomials given by

$$\begin{aligned}
\tilde{p}_1(s) &= \bar{\theta}_\mu s^\mu + \bar{\theta}_{\mu-1} s^{\mu-1} + \underline{\theta}_{\mu-2} s^{\mu-2} + \underline{\theta}_{\mu-3} s^{\mu-3} \\
&\quad + \bar{\theta}_{\mu-4} s^{\mu-4} + \bar{\theta}_{\mu-5} s^{\mu-5} + \dots, \\
\tilde{p}_2(s) &= \bar{\theta}_\mu s^\mu + \underline{\theta}_{\mu-1} s^{\mu-1} + \underline{\theta}_{\mu-2} s^{\mu-2} + \bar{\theta}_{\mu-3} s^{\mu-3} \\
&\quad + \bar{\theta}_{\mu-4} s^{\mu-4} + \underline{\theta}_{\mu-5} s^{\mu-5} + \dots, \\
\tilde{p}_3(s) &= \underline{\theta}_\mu s^\mu + \underline{\theta}_{\mu-1} s^{\mu-1} + \bar{\theta}_{\mu-2} s^{\mu-2} + \bar{\theta}_{\mu-3} s^{\mu-3} \\
&\quad + \underline{\theta}_{\mu-4} s^{\mu-4} + \underline{\theta}_{\mu-5} s^{\mu-5} + \dots, \\
\tilde{p}_4(s) &= \underline{\theta}_\mu s^\mu + \bar{\theta}_{\mu-1} s^{\mu-1} + \bar{\theta}_{\mu-2} s^{\mu-2} + \underline{\theta}_{\mu-3} s^{\mu-3} \\
&\quad + \underline{\theta}_{\mu-4} s^{\mu-4} + \bar{\theta}_{\mu-5} s^{\mu-5} + \dots.
\end{aligned} \tag{9.0.3}$$

Then, every polynomial in  $\mathcal{I}$  is Hurwitz if and only if the polynomials  $\tilde{p}_1(s), \dots, \tilde{p}_4(s)$  are Hurwitz.  $\square$

From Lemma A. 4, we derive the following remark.

**Remark A. 5.**

For the set  $\mathcal{I}$  in Lemma A. 4, suppose that  $m$  be a positive integer such that  $m < \mu$  and that  $\underline{\theta}_i = \bar{\theta}_i = b_i$ , for  $i = m + 1, \dots, \mu$ . Then, every polynomial in  $\mathcal{I}$  is Hurwitz if and only if the following four extreme polynomials are Hurwitz:

$$\begin{aligned}
\bar{p}_1(s) &= s^\mu + b_{\mu-1} s^{\mu-1} + \dots + b_{m+1} s^{m+1} \\
&\quad + \bar{\theta}_m s^m + \bar{\theta}_{m-1} s^{m-1} + \underline{\theta}_{m-2} s^{m-2} + \underline{\theta}_{m-3} s^{m-3} + \dots, \\
\bar{p}_2(s) &= s^\mu + b_{\mu-1} s^{\mu-1} + \dots + b_{m+1} s^{m+1} \\
&\quad + \bar{\theta}_m s^m + \underline{\theta}_{m-1} s^{m-1} + \underline{\theta}_{m-2} s^{m-2} + \bar{\theta}_{m-3} s^{m-3} + \dots, \\
\bar{p}_3(s) &= s^\mu + b_{\mu-1} s^{\mu-1} + \dots + b_{m+1} s^{m+1} \\
&\quad + \underline{\theta}_m s^m + \underline{\theta}_{m-1} s^{m-1} + \bar{\theta}_{m-2} s^{m-2} + \bar{\theta}_{m-3} s^{m-3} + \dots, \\
\bar{p}_4(s) &= s^\mu + b_{\mu-1} s^{\mu-1} + \dots + b_{m+1} s^{m+1} \\
&\quad + \underline{\theta}_m s^m + \bar{\theta}_{m-1} s^{m-1} + \bar{\theta}_{m-2} s^{m-2} + \underline{\theta}_{m-3} s^{m-3} + \dots.
\end{aligned}$$

This follows easily from the fact that  $\tilde{p}_j(s)$  of (9.0.3) corresponds to  $\bar{p}_l$  with  $l = j + ((\mu - m) \bmod 4)$ .  $\square$

**Definition A. 6.** [Value Set]

Let  $Q$  be an uncertainty bounded set defined by

$$Q := \{q = [q_1, \dots, q_l] \mid q_i \in [\underline{q}_i, \bar{q}_i], i = 1, \dots, l\}$$

where  $\underline{q}_i$  and  $\bar{q}_i$  are known constants. Given a family of polynomials  $P(s, Q) := \{p(s, q) \mid q \in Q\}$ , the value set is given by

$$\mathbf{P}(j\omega, Q) = \{p(j\omega, q) \mid q \in Q, \omega \geq 0\}.$$

$\square$

**Lemma A. 7** [Zero Exclusion Theorem] [Ack02]

Given a polynomial family  $P(s, Q)$ , the set  $P(s, Q)$  is robustly stable if and only if the following two conditions are hold:

1. There exists a stable polynomial  $p(s, q) \in P(s, Q)$ ,
2.  $0 \notin \mathbf{P}(j\omega, Q)$  for all  $\omega \geq 0$ .

$\square$

**Lemma A. 8.** [Matrix Inversion Lemma] [ZD98]

Let  $A$  be a square matrix partitioned as follows:

$$A := \begin{bmatrix} A_{11} & A_{12} \\ A_{21} & A_{22} \end{bmatrix}$$

where  $A_{11}$  and  $A_{22}$  are also square matrices. If  $A$  and  $A_{11}$  are nonsingular, then

$$\begin{bmatrix} A_{11} & A_{12} \\ A_{21} & A_{22} \end{bmatrix}^{-1} = \begin{bmatrix} A_{11}^{-1} + A_{11}^{-1}A_{12}\Delta^{-1}A_{21}A_{11}^{-1} & -A_{11}^{-1}A_{12}\Delta^{-1} \\ -\Delta^{-1}A_{21}A_{11}^{-1} & \Delta^{-1} \end{bmatrix},$$

$$\Delta := A_{22} - A_{21}A_{11}^{-1}A_{12}.$$

And, if  $A$  and  $A_{22}$  are nonsingular, then

$$\begin{bmatrix} A_{11} & A_{12} \\ A_{21} & A_{22} \end{bmatrix}^{-1} = \begin{bmatrix} \hat{\Delta}^{-1} & -\hat{\Delta}^{-1}A_{12}A_{22}^{-1} \\ -A_{22}^{-1}A_{21}\hat{\Delta}^{-1} & A_{22}^{-1} + A_{22}^{-1}A_{21}\hat{\Delta}^{-1}A_{12}A_{22}^{-1} \end{bmatrix},$$
$$\hat{\Delta} := A_{11} - A_{12}A_{22}^{-1}A_{21}.$$

□

# BIBLIOGRAPHY

- [Ack02] J. Ackermann. *Robust Control: The Parameter Space Approach*. Springer, 2002.
- [AHDW94] B. Armstrong-Hélouvry, P. Dupont, and C. C. De Wit. A survey of models, analysis tools and compensation methods for the control of machines with friction. *Automatica*, 30(7):1183–1138, 1994.
- [BCK95] S. P. Bhattacharyya, H. Chapellat, and L. H. Keel. *Robust Control: The Parametric Approach*. Prentice Hall PTR, 1995.
- [BS08] J. Back and H. Shim. Adding robustness to nominal output-feedback controllers for uncertain nonlinear systems: A nonlinear version of disturbance obser. *Automatica*, 44(10):2528–2537, 2008.
- [BS09] J. Back and H. Shim. An inner-loop controller guaranteeing robust transient performance for uncertain mimo nonlinear systems. *IEEE Transactions on Automatic Control*, 54(7):1601–1607, 2009.
- [BSPS10] J. S. Bang, H. Shim, S. K. Park, and J. H. Seo. Robust tracking and vibration suppression for a two-inertia system by combining back-stepping approach with disturbance observer. *IEEE Transactions on Industrial Electronics*, 57(9):3197–3206, 2010.
- [BT99] R. Bickel and M. Tomizuka. Passivity-based versus disturbance observer based robot control: Equivalence and stability. *Journal of Dynamic Systems, Measurement, and Control*, 121(1):41–47, 1999.

- [CCY96] Y. Choi, W. K. Chung, and Y. Youm. Disturbance observer in  $h_\infty$  framework. In *Proceedings of the 1996 IEEE IECON 22nd International Conference*, volume 3, pages 1394–1400, 1996.
- [Che99] C. T. Chen. *Linear system theory and design*. Oxford University Press, 3rd edition, 1999.
- [CLP06] B. M. Chen, T. H. Lee, and K. Peng. *Hard disk drive servo systems*. Springer, 2nd edition, 2006.
- [CYC<sup>+</sup>03] Y. Choi, K. Yang, W. K. Chung, H. R. Kim, and I. H. Suh. On the robustness and performance of disturbance observers for second-order systems. *IEEE Transactions on Automatic Control*, 48(2):315–320, 2003.
- [Dav76] E. J. Davison. The robust control of a servomechanism problem for linear time-invariant multivariable systems. *IEEE Transactions on Automatic Control*, 21(1):25–34, 1976.
- [DFT92] J. C. Doyle, B. A. Francis, and A. R. Tannenbaum. *Feedback control theory*. Macmillan Publishing Company, New York, 1992.
- [DGKF89] J. C. Doyle, K. Glover, P. P. Khargonekar, and B. A. Francis. State-space solutions to standard  $h_2$  and  $h_\infty$  control problems. *IEEE Transactions on Automatic Control*, 34(8):831–847, 1989.
- [EKK<sup>+</sup>96] S. Endo, H. Kobayashi, C. J. Kempf, S. Kobayashi, M. Tomizuka, and Y. Hori. Robust digital tracking controller design for high-speed positioning systems. *Control Engineering Practice*, 4(4):527–536, 1996.
- [ESC01] K. S. Eom, I. H. Suh, and W. K. Chung. Disturbance observer based path tracking control of robot manipulator considering torque saturation. *Mechatronics*, 11:325–343, 2001.
- [Fla83] F. J. Flanigan. *Complex variables*. Dover Publications, 1983.

- [FPEN06] G. F. Franklin, J. D. Powell, and A. Emami-Naeini. *Feedback control of dynamic systems*. Prentice-Hall, 2006.
- [FW76] B. A. Francis and W. M. Wonham. The internal model principle of control theory. *Automatica*, 12(5):457–465, 1976.
- [GG01] B. A. Güvenc and L. Güvenc. Robustness of disturbance observers in the presence of structured real parametric uncertainty. In *Proceedings of the 2001 American Control Conference*, volume 6, pages 4222–4227, 2001.
- [GG02] B. A. Güvenc and L. Güvenc. Robust two degree-of-freedom add-on controller design for automatic steering. *IEEE Transactions on Control Systems Technology*, 10(1):137–148, 2002.
- [GGK09] B. A. Güvenc, L. Güvenc, and S. Karaman. Robust yaw stability controller design and hardware-in-the-loop testing for a road vehicle. *IEEE Transactions on Vehicular T*, 58(2):555–571, 2009.
- [Hah81] H. Hahn. *Higher order root-locus technique with applications in control system design*. F. Vieweg, 1981. Graduate Texts in Mathematics, vol. 207.
- [HJ85] R. A. Horn and C. R. Johnson. *Matrix Analysis*. Chmbridge University Press, 1985.
- [HKJ<sup>+</sup>13] J. Han, H. Kim, Y. Joo, N. H. Jo, and J. H. Seo. A simple noise reduction disturbance observer and q-filter design for internal stability. In *13th International Conference on Control, Automation and Systems*, pages 755–760, 2013.
- [HM98] Y. Huang and W. Messner. A novel disturbance observer design for magnetic hard drive servo with a rotary actuator. *IEEE Transactions on Magnetics*, 34(4):1892–1894, 1998.
- [Hua04] J. Huang. *Nonlinear output regulation: Theory and Applications*. SIAM, 2004.



- [IS96] P. A. Ioannou and J. Sun. *Robust adaptive control*. Prentice Hall, 1996.
- [Isi95] A. Isidori. *Nonlinear Control Systems*. Springer-Verlag, New York, New York, 3rd edition, 1995.
- [IT98] J. Ishikawa and M. Tomizuka. Pivot friction compensation using an accelerometer and a disturbance observer for hard disk drives. *IEEE/ASME Transactions on Mechatronics*, 3(3):194–201, 1998.
- [JJS11] N. H. Jo, Y. Joo, and H. Shim. Can a fast disturbance observer work under unmodeled actuators? In *11th International Conference on Control, Automation and Systems*, pages 561–566, 2011.
- [JJS14] N. H. Jo, Y. Joo, and H. Shim. A study of disturbance observers with unknown relative degree of the plant. *Automatica*, 50(6):1730–1734, 2014.
- [JJSS12] N. H. Jo, Y. Joo, H. Shim, and Y. I. Son. A note on disturbance observer with unknown relative degree of the plant. In *Proceedings of the 51th IEEE Conference on Decision and Control*, pages 943–948, 2012.
- [Joh71] C. D. Johnson. Accommodation of external disturbances in linear regulator and servomechanism problems. *IEEE Transactions on Automatic Control*, 16(6):635–644, 1971.
- [Joh86] C. D. Johnson. Disturbance-accommodating control: An overview. In *American Control Conference*, pages 526–536, 1986.
- [JPBS14] Y. Joo, G. Park, J. Back, and H. Shim. Embedding internal model in disturbance observer with robust stability. Submitted to *IEEE Transactions on Automatic Control*, 2014.
- [JS13] N. H. Jo and H. Shim. Robust stabilization via disturbance observer with noise reduction. In *2013 European Control Conference (ECC)*, pages 2861–2866, 2013.

- [JSS10] N. H. Jo, H. Shim, and Y. I. Son. Disturbance observer for non-minimum phase linear systems. *International Journal of Control, Automation, and Systems*, 8(5):994–1002, 2010.
- [JWS00] G. P. Jiang, S. P. Wang, and W. Z. Song. Design of observer with integrators for linear systems with unknown input disturbances. *Electronics Letters*, 36:1168–1169, 2000.
- [KC03a] B. K. Kim and W. K. Chung. Advanced disturbance observer design for mechanical positioning systems. *IEEE Transactions on Industrial Electronics*, 50(6):1207–1216, 2003.
- [KC03b] S. Kwon and W. K. Chung. A discrete-time design and analysis of perturbation observer for motion control applications. *IEEE Transactions on Control Systems Technology*, 11(3):399–407, 2003.
- [KCO02] B. K. Kim, W. K. Chung, and S. R. Oh. Disturbance observer based approach to the design of sliding mode controller for high performance positioning systems. In *15th IFAC World Congress on Automatic Control*, 2002.
- [Kha02] H. K. Khalil. *Nonlinear systems*. Prentice Hall, 3rd edition, 2002.
- [KIO08] S. Katsura, K. Irie, and K. Ohishi. Wideband force control by position-acceleration integrated disturbance observer. *IEEE Transactions on Industrial Electronics*, 55(4):1699–1706, 2008.
- [KK79] H. K. Khalil and P. V. Kokotovic.  $d$ -stability and multi-parameter singular perturbation. *SIAM Journal on Control and Optimization*, 17(1):56–65, 1979.
- [KK99] C. J. Kempf and S. Kobayashi. Disturbance observer and feedforward design for a high-speed direct-drive positioning table. *IEEE Transactions on Control Systems Technology*, 7(5):513–526, 1999.
- [KKO07] H. Kobayashi, S. Katsura, and K. Ohnishi. An analysis of parameter variations of disturbance observer for motion control. *IEEE Transactions on Industrial Electronics*, 54(6):3413–3421, 2007.

- [KMH00] S. Komada, N. Machii, and T. Hori. Control of redundant manipulators considering order of disturbance observer. *IEEE Transactions on Industrial Electronics*, 47(2):413–420, 2000.
- [KRK10] K. S. Kim, K. H. Rew, and S. Kim. Disturbance observer for estimating higher order disturbances in time series expansion. *IEEE Transactions on Automatic Control*, 55(8):1905–1911, 2010.
- [KT13] K. Kong and M. Tomizuka. Nominal model manipulation for enhancement of stability robustness for disturbance observer-based control systems. *International Journal of Control, Automation, and Systems*, 11(1):12–20, 2013.
- [LR85] G. S. Ladde and S. G. Rajalakshmi. Diagonalization and stability of multi-time-scale singularly perturbed linear systems. *Applied mathematics and computation*, 16(2):115–140, 1985.
- [LS83] G. S. Ladde and D. D. Siljak. Multiparameter singular perturbations of linear systems with multiple time scales. *Automatica*, 19(4):385–394, 1983.
- [LT96] H. S. Lee and M. Tomizuka. Robust motion controller design for high-accuracy positioning systems. *IEEE Transactions on Industrial Electronics*, 43(1):48–55, 1996.
- [MGB06] A. Al Mamun, G. Guo, and C. Bi. *Hard disk drive: Mechatronics and control*. CRC press, 2006.
- [MGÖ08] S. Moberg, S. Gunnarsson, and J. Öhr. A benchmark problem for robust control of a multivariable nonlinear flexible manipulator. In *Proceedings of the 17th IFAC World Congress*, pages 1206–1211, 2008.
- [MHMZ98] T. Mita, M. Hirata, K. Murata, and H. Zhang.  $h_\infty$  control versus disturbance-observer-based control. *IEEE Transactions on Industrial Electronics*, 45(3):488–495, 1998.

- [MÖ05] S. Moberg and J. Öhr. Robust control of a flexible manipulator arm: A benchmark problem. In *Proceedings of the 16th IFAC World Congress*, pages 960–966, 2005.
- [NA89] K. S. Narendra and A. M. Annaswamy. *Stable adaptive systems*. Courier Dover Publications, 1989.
- [OÅdW<sup>+</sup>98] H. Olsson, K. J. Åström, C. C. de Wit, M. Gäfvert, and P. Lischinsky. Friction models and friction compensation. *European Journal of Control*, 4(3):176–195, 1998.
- [OC99] Y. Oh and W. K. Chung. Disturbance-observer-based motion control of redundant manipulators using inertially decoupled dynamics. *IEEE/ASME Transactions on Mechatronics*, 4(2):133–146, 1999.
- [OHH08] S. Oh, N. Hata, and Y. Hori. Integrated motion control of a wheelchair in the longitudinal, lateral, and pitch directions. *IEEE Transactions on Industrial Electronics*, 55(4):1855–1862, 2008.
- [Ohn87] K. Ohnishi. A new servo method in mechatronics. *Transactions of Japanese Society of Electrical Engineers*, 107-D:83–86, 1987. in Japanese.
- [OOH10] Y. Oonishi, S. Oh, and Y. Hori. A new control method for power-assisted wheelchair based on the surface myoelectric signal. *IEEE Transactions on Industrial Electronics*, 57(9):3191–3196, 2010.
- [PJSB12] G. Park, Y. Joo, H. Shim, and J. Back. Rejection of polynomial-in-time disturbances via disturbance observer with guaranteed robust stability. In *Proceedings of the 51th IEEE Conference on Decision and Control*, pages 949–954, 2012.
- [SD02] E. Shrijver and J. V. Dijk. Disturbance observers for rigid mechanical systems: equivalence, stability, and design. *Journal of Dynamic Systems, Measurement, and Control*, 124(4):539–548, 2002.

- [SJ07] H. Shim and Y. Joo. State space analysis of disturbance observer and a robust stability condition. In *Proceedings of the 28th IEEE Conference on Decision and Control*, pages 2193–2198, 2007.
- [SJ09] H. Shim and N. H. Jo. An almost necessary and sufficient condition for robust stability of closed-loop systems with disturbance observer. *Automatica*, 45(1):296–299, 2009.
- [SK91] H. J. Sussmann and P. V. Kokotovic. The peaking phenomenon and the global stabilization of nonlinear systems. *IEEE Transactions on Automatic Control*, 36(4):424–440, 1991.
- [SK10] Y. I. Son and I. H. Kim. A robust state observer using multiple integrators for multivariable lti systems. *IEICE Transactions on Fundamentals of Electronics*, 93(5):981–984, 2010.
- [SSJH02] R. T. Stefani, B. Shahian, C. J. Savant Jr, and G. H. Hostetter. *Design of feedback control systems*. Oxford University Press, 4rd edition, 2002.
- [TLT00] A. Tesfaye, H. S. Lee, and M. Tomizuka. A sensitivity optimization approach to design of a disturbance observer in digital motion control systems. *Mechatronics*, 5(1):32–38, 2000.
- [Tom96a] M. Tomizuka. Model based prediction, preview and robust controls in motion control systems. In *Proceedings of 4th International Workshop on Advanced Motion Control*, volume 1, pages 1–6, 1996.
- [Tom96b] M. Tomizuka. Robust digital motion controllers for mechanical systems. *Robotics and autonomous systems*, 19(2):143–149, 1996.
- [UH91] T. Umeno and Y. Hori. Robust speed control of dc servomotors using modern two degrees-of-freedom controller design. *IEEE Transactions on Industrial Electronics*, 38(5):363–368, 1991.
- [UH93] T. Umeno and Y. Hori. Robust servosystem design with two degrees of freedom and its application to novel motion control of robot ma-

- nipulators. *IEEE Transactions on Industrial Electronics*, 40(5):473–485, 1993.
- [Utk92] V. I. Utkin. *Sliding modes in control and optimization*. Springer-Verlag, 1992.
- [WT04] C. Wang and M. Tomizuka. Design of robustly stable disturbance observers based on closed loop consideration using  $h_\infty$  optimization and its applications to motion control systems. In *Proceedings of the 2004 American Control Conference*, pages 3764–3769, 2004.
- [WTS00] M. T. White, M. Tomizuka, and C. Smith. Improved track following in magnetic disk drives using a disturbance observer. *IEEE/ASME Transactions on Mechatronics*, 5(1):3–11, 2000.
- [YAMT97] B. Yao, M. Al-Majed, and M. Tomizuka. High-performance robust motion control of machine tools: an adaptive robust control approach and comparative experiments. *IEEE/ASME Transactions on Mechatronics*, 2(2):63–76, 1997.
- [YCC05] K. Yang, Y. Choi, and W. K. Chung. On the tracking performance improvement of optical disk drive servo systems using error-based disturbance observer. *IEEE Transactions on Industrial Electronics*, 52(1):270–279, 2005.
- [YCS09] J. Yi, S. Chang, and Y. Shen. Disturbance-observer-based hysteresis compensation for piezoelectric actuators. *IEEE/ASME Transactions on Mechatronics*, 14(4):456–464, 2009.
- [YKIH96] K. Yamada, S. Komada, M. Ishida, and T. Hori. Characteristics of servo system using high order disturbance observer. In *Proceedings of the 35th IEEE Conference on Decision and Control*, pages 3252–3257, 1996.
- [YKIH97] K. Yamada, S. Komada, M. Ishida, and T. Hori. Analysis and classical control design of servo system using high order disturbance ob-

- server. In *in Proceedings IEEE International Conference on Industrial Electronics, Control and Instrumentation (IECON)*, pages 4–9, 1997.
- [YKMH96] K. Yamada, S. Komada, Ishida M, and T. Hori. Analysis of servo system realized by disturbance observer. In *in Proceedings of IEEE International Workshop on Advanced Motion Control*, pages 339–343, 1996.
- [YKMH99] K. Yamada, S. Komada, M.Ishida, and T. Hori. A study on higher-order disturbance observer and robust stability. *Electrical Engineering in Japan*, 128(1):37–44, 1999.
- [YT99] L. Yi and M. Tomizuka. Two-degree-of-freedom control with robust feedback control for hard disk servo systems. *IEEE/ASME Transactions on Mechatronics*, 4(1):17–24, 1999.
- [ZD98] K. Zhou and J. C. Doyle. *Essentials of robust control*. Prentice-Hall, Inc., 1998.

# 국문초록

## THEORETICAL ANALYSIS OF DISTURBANCE OBSERVER: STABILITY AND PERFORMANCE

### 외란 관측기의 이론적 해석 : 안정성 및 성능

본 논문은 외란관측기의 안정성과 성능에 대한 해석을 제공하고 강인안정성과 외란 제거 성능을 강화하기 위한 새로운 외란관측기 설계 방법을 제안한다. 실제 산업 현장에서의 다양한 적용에도 불구하고 제어 공학자들은 외란관측기 자체에 대한 이론적인 해석에 많은 관심을 기울이지 않았다. 외란관측기 구조와 특성을 명확히 분석하고 그 적용 대상을 확장하기 위하여 본 논문에서는 외란관측기를 주파수 공간과 상태 공간 모두에서 엄밀하게 이론적으로 해석한다.

주파수 공간에서 본 논문은 외란관측기의 외란 제거 성능과 강인안정성을 다룬다. 외란관측기는 뛰어난 외란 제거 성능을 가졌음에도 외란을 근사적으로만 제거한다. 이런 단점을 보완하기 위하여 본 논문에서는 외란의 내부 모델을 외란관측기 구조에 추가하는 설계 방법을 제시한다. 그러므로 제안된 외란관측기는 기존의 근사적 외란 제거 성능을 유지함과 동시에 사인파나 시간에 대한 함수 형태의 외란을 완벽하게 제거 할 수 있다. 이와 함께, 제안된 외란관측기에 대한 강인안정성 조건을 유도하며, 그 조건을 만족할 수 있는 설계 과정을 제시한다. 또 다른 중요 주제는 모델 불확실성이 존재할 때 외란관측기의 강인안정성이다. 본 논문에서는 실제 시스템의 상대 차수를 명확히 알지 못하여 외란관측기가 잘못된 정보를 바탕으로 설계되었을 때의 강인안정성에 대해 다룬다. 이에 대한 결과를 바탕으로 실제 시스템의 상대 차수가 4차 이하인 경우에 대해 항상 강인안정성을 보장할 수 있는 외란관측기 설계 방법을 제시한다. 다음으로 외란관측기 각 블록의 역할에 대한 관측을 통하여, 본 논문은 외란관측기의 설계 방법을 확장하고 이를 바탕으로 저차원  $k$ -유형 (type- $k$ ) 외란관측기를 제안한다. 저차원  $k$ -유형 외란관측기는 외란 제거 성능 향상과 간단한 설계를 동시에 달성할 수 있다.

주파수 공간 해석에 대응하여, 본 논문에서는 외란관측기의 상태 공간 해석을 제시한다. 상태 공간에서의 해석은 외란관측기 구조와 특성에 대한 더 명확한 이해를 제공하고 비선형 시스템 등으로 외란관측기의 적용 대상을 확장할 수 있게 한다. 특히 섭동 이론을 바탕으로, 이 해석은 기존에 잘 알려진 특성 뿐만 아니라



과도 상태 응답에서의 왜곡과 같은 새로운 사실들을 알려준다. 이와 함께, 본 논문의 모델링되지 않은 동역학이 실제 시스템에 존재하거나 존재하지 않을 때 모두에 대한 외란관측기 기반 제어 시스템의 강인안정성에 대해 논하고 외란관측기의 공칭 상태 회복 능력과 Q 필터의 시상수와의 명확한 관계를 제시한다. 마지막으로, 기존의 선형 외란관측기는 과도 상태에서의 성능을 보장하지 못한다. 그러므로 정상 상태 뿐만 아니라 과도 상태에서 외란관측기의 공칭 성능 회복을 보장하는 비선형 외란관측기에 대한 논의를 제시한다.

**주요어:** 외란관측기, 강인안정성, 외란 제거 성능, 내부 모델 이론, 불확실한 동역학, 공칭 성능 회복

**학 번:** 2008-30244